

Near-infrared fluorescence imaging with indocyanine green in vascular surgery

Hoven, P. van den

Citation

Hoven, P. van den. (2022, June 9). *Near-infrared fluorescence imaging with indocyanine green in vascular surgery*. Retrieved from https://hdl.handle.net/1887/3309684

Version: Publisher's Version

Licence agreement concerning inclusion of doctoral

License: thesis in the Institutional Repository of the University

of Leiden

Downloaded from: https://hdl.handle.net/1887/3309684

Note: To cite this publication please use the final published version (if applicable).



The quest for reliable quantification of tissue perfusion and potential clinical applications

Pim van den Hoven

Stellingen behorende bij het proefschrift getiteld

"Near-infrared fluorescence imaging with indocyanine green in vascular surgery"

- Kwantificatie van weefselperfusie middels nabij-infrarood fluorescentie met indocyanine groen is in staat vitaliteit van de huid te voorspellen na amputatiechirurgie – dit proefschrift.
- 2. Nabij-infrarood fluorescentie met indocyanine groen is een betrouwbare techniek om het effect van een revascularisatie op weefselperfusie in de voet te beoordelen dit proefschrift.
- 3. Normalisatie verhoogt de validiteit en betrouwbaarheid van kwantificatie van perfusie in de voet middels nabij-infrarood fluorescentie met indocyanine groen dit proefschrift.
- 4. Perifeer arterieel vaatlijden in een vergevorderd stadium leidt tot een verhoging van parameters gerelateerd aan de instroom van indocyanine groen dit proefschrift.
- 5. De zoektocht naar afkapwaarden voor adequate weefselperfusie middels nabij-infrarood fluorescentie met indocyanine groen wordt bemoeilijkt door de grote variatie aan patiënt- en camera gerelateerde factoren.
- 6. The examination of an ICG angiography is like reading in a book whose pages would be transparent (dr. Gabriel Quentel, 2000). *De dynamiek van indocyanine groen wordt beïnvloed door de weefselpenetratie.*
- 7. Een essentieel onderdeel van een betrouwbare intra-operatieve beoordeling van weefselperfusie middels nabij-infrarood fluorescentie met indocyanine groen is het geduld van de chirurg.
- 8. Je gaat het pas zien als je het doorhebt (Johan Cruijff, 1990). Over fluorescentie, promoveren, opereren, het leven en voetbal.
- 9. Livet forstås baglæns, men må leves forlæns (Søren Kierkegaard, 1843). "Het leven kan slechts achterwaarts begrepen worden, maar het moet voorwaarts worden geleefd". *Om verder te komen moet je soms niet te veel nadenken.*
- 10. In Africa there is a concept known as 'ubuntu' the profound sense that we are human only through the humanity of others; that if we are to accomplish anything in this world it will in equal measure be due to the work and achievement of others (Nelson Mandela, 1990). Alles wat we bereiken is uiteindelijk slechts mogelijk door de hulp en steun van elkaar.

Near-infrared fluorescence imaging with indocyanine green in vascular surgery

The quest for reliable quantification of tissue perfusion and potential clinical applications

© P. van den Hoven

ISBN: 978-94-6423-824-2

Design: ProefschriftMaken | www.proefschriftmaken.nl

Cover layout: Fenna Schaap, Kim de Valk, Pim van den Hoven

Financial support by the Dutch Heart Foundation for the publication of this thesis is gratefully acknowledged.

Renew Health Limited, Quest Innovations, Voetencentrum Wender, Krijnen Medical, Erbe, KARL STORZ Endoscopie Nederland B.V., Chipsoft and the Alrijne Wetenschapsfonds are also gratefully acknowledged for their financial support for the printing of this thesis.

Near-infrared fluorescence imaging with indocyanine green in vascular surgery

The quest for reliable quantification of tissue perfusion and potential clinical applications

Proefschrift

ter verkrijging van de graad van doctor aan de Universiteit Leiden, op gezag van rector magnificus prof. dr. ir. H. Bijl, volgens besluit van het college voor promoties te verdedigen op donderdag 9 juni 2022 klokke 11.15 uur

door

Pim van den Hoven Geboren te Hengelo in 1990

Promotor

Prof. dr. J.F. Hamming

Copromotoren

Dr. J.R. van der Vorst Dr. A.L. Vahrmeijer

Leden promotiecommissie

Prof. dr. P.H.A. Quax

Prof. dr. J. Burggraaf

Prof. dr. R.H. Geelkerken (Medisch Spectrum Twente, Enschede)

Dr. K.K. Yeung (Amsterdam Universitair Medisch Centrum, Amsterdam)

Voor mijn ouders Door hun grenzeloze liefde

Table of contents

| Chapter 1 | Introduction and thesis outline | Ş |
|-----------|--|-----|
| Part I | Quantification of tissue perfusion using near-infrared fluorescence imaging with indocyanine green | 17 |
| Chapter 2 | A systematic review of the use of near-infrared fluorescence imaging in patients with peripheral artery disease | 19 |
| Chapter 3 | Perfusion parameters in near-infrared fluorescence imaging with indocyanine green: a systematic review of the literature | 43 |
| Chapter 4 | Perfusion patterns in patients with chronic limb-threatening ischemia versus control patients using near-infrared fluorescence imaging with indocyanine green | 73 |
| Chapter 5 | Normalization of time-intensity curves for quantification of foot perfusion using near-infrared fluorescence imaging with indocyanine green | 87 |
| Chapter 6 | Quantification of near-infrared fluorescence imaging with indocyanine green in free flap breast reconstruction | 105 |
| Part II | Clinical translation of quantitative tissue perfusion assessment using near-infrared fluorescence imaging with indocyanine green in lower extremity arterial disease | 119 |
| Chapter 7 | Near-infrared fluorescence imaging with indocyanine green for quantification of changes in tissue perfusion following revascularization | 121 |
| Chapter 8 | Assessment of tissue viability following amputation surgery using near-infrared fluorescence imaging with indocyanine green | 135 |
| Part III | Summary, discussion and appendices | 149 |
| Chapter 9 | Summary, discussion and future perspectives | 151 |
| | | |

| Dutch summary (Nederlandse samenvatting) | 161 |
|--|---------------------------------------|
| Curriculum Vitae | 166 |
| List of publications | 167 |
| Dankwoord | 169 |
| | Curriculum Vitae List of publications |



Chapter 1

Introduction and thesis outline

Introduction

Throughout history, surgeons are trained to rely on their physical examination to guide decision making. Concerning the assessment of tissue perfusion, a surgeon relies on subjective and sometimes indirect observations, including tissue temperature, color and the presence of pulses. Although these clinical observations are of vital importance, the surgical field lacks a technique for the reliable and quantitative assessment of tissue perfusion. Within the field of vascular surgery, this becomes visible when interpreting skin circulation in patients with lower extremity arterial disease (LEAD). This disease, which is characterized by the presence of atherosclerotic disease of the lower limb, is diagnosed based on a clinical history and examination, combined with diagnostic tests providing information about the macrovascular status (1). The most utilized diagnostic tests include the ankle-brachial index, toe pressure measurement, duplex ultrasound, digital subtraction angiography, computed tomography angiography and magnetic resonance angiography. While these techniques provide valuable information about lower leg circulation, the actual perfusion on skin level remains unknown. This absence of information about skin perfusion seems the presumable cause that none of these techniques have proven predictive value in wound healing, which can be of paramount importance in patients with chronic-limb threatening ischemia (CLTI) due to ischemic wounds (2). The vulnerable patients in this latter group are at high risk of undergoing a major amputation with a substantial risk of concomitant wound healing problems (3). Besides the prediction of wound healing, adequate assessment of skin perfusion in patients with LEAD has the potential to guide revascularization strategies. Although the decision for a revascularization procedure is thoughtful, the lack of information about foot perfusion might provoke aggressive revascularization strategies with undesirable outcomes. Furthermore, adequate assessment of foot perfusion has the ability to prevent unnecessary interventions. In the search for the reliable assessment of skin perfusion, several imaging techniques have been studied (4-6). Transcutaneous oxygen pressure measurement has proven to predict healing problems following lower limb amputation to a certain extent, however, the additional benefit over clinical assessment has not been demonstrated (6). Other techniques examining the evaluation of tissue perfusion include laser-speckle imaging and dynamic volume perfusion computed tomography. For both techniques, significant differences were seen in foot perfusion when comparing results pre- and postrevascularization procedures (5, 7). However, there is still limited evidence on the validity of these techniques in determining the quality of tissue perfusion. A technique gaining popularity for tissue perfusion assessment is near-infrared (NIR) fluorescence imaging using indocyanine green (ICG). NIR fluorescence imaging is a technique to visualize fluorescence in the NIR light spectrum (780 to 1000nm). A NIR fluorescence imaging system consists of a light engine, exciting the target tissue, combined with a camera measuring the fluorescence intensity (Figure 1). The advantages

of fluorescence imaging in the NIR spectrum over visible light include the relatively deep tissue penetration of up to one centimeter and the low effect of autofluorescence (8). These features enable the system to clearly visualize a fluorophore with an excitation - and emission peak in the NIR light spectrum. The most utilized fluorophore for the assessment of tissue perfusion in near-infrared fluorescence imaging is ICG. This negatively charged, ambiphilic, water soluble tricarbocyanine was approved by the Food and Drug Administration in 1957 and has very low toxicity and side effects (9, 10). The feasibility of ICG for assessment of perfusion is explained by several properties. First of all, ICG has excellent fluorescence properties for NIR fluorescence imaging, with an excitation peak of 780nm and an emission peak of 820nm (11). Secondly, upon intravenous administration, ICG binds to plasma proteins, confining the fluorophore to the intravascular compartment (11). Furthermore, ICG has a rapid hepatic clearance, minimizing interference with the registered fluorescence intensity over time in the target tissue (12). The first reported use of this technique for assessment of vascular anatomy was in the field of ophthalmology (13). Since then, ICG in NIR fluorescence imaging has been performed in various surgical fields including gastro-intestinal surgery, cardiac surgery, and reconstructive surgery (14-19). Within the field of vascular surgery, perfusion assessment using ICG NIR fluorescence imaging has been used for various indications, including diagnosis of LEAD, quality control following revascularization and for assessment of tissue viability following amputation surgery (20-22). Following ICG NIR fluorescence imaging of the target area or so called region of interest (ROI), skin perfusion analysis is performed by either a qualitative or quantitative analysis. For qualitative analysis, this means the perfusion is interpreted based on subjective evaluations of the fluorescence intensity by the observer. For a quantitative analysis, the fluorescence intensity is most often expressed in arbitrary units (a.u.). Furthermore, the fluorescence intensity can be analyzed by creating time-intensity curves, describing the fluorescence intensity change over time. Both qualitative and quantitative analyses of ICG NIR fluorescence imaging in assessment of skin perfusion for patients with LEAD have been performed and have shown varying results (23-25). This can partially be attributed to the differences in used camera systems and used quantification software. Besides, these studies varied among design and were mostly performed in an experimental pilot setting. Furthermore, the interpretation of the fluorescence intensity can be misleading, as the signal is influenced by several factors, including camera distance and angle to the target tissue (26). In the quest towards reliable perfusion assessment with ICG NIR fluorescence imaging, these challenges have to be overcome. Therefore, this thesis aims to further assess the value of ICG NIR fluorescence imaging for perfusion assessment in vascular surgery and explore potential applications for use in clinical practice.

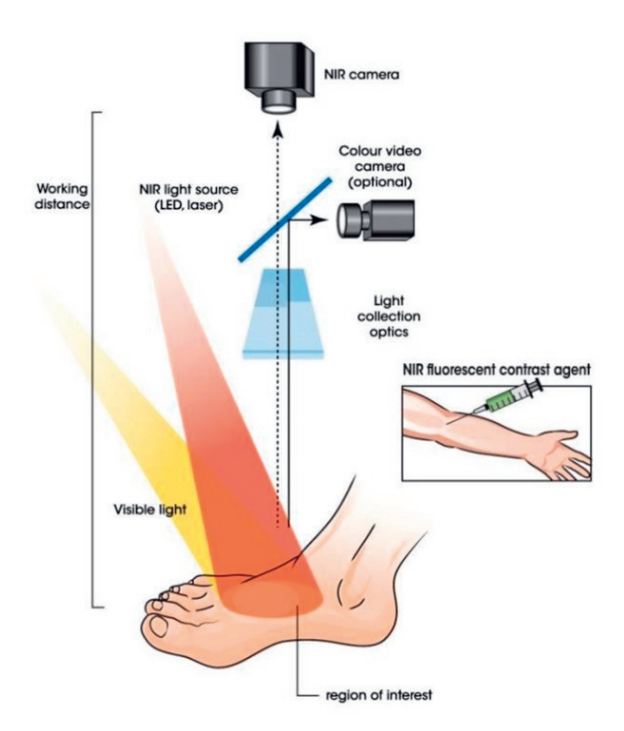


Figure 1. ICG NIR fluorescence imaging setup.

Reference list

- Aboyans V, Ricco JB, Bartelink MEL, Bjorck M, Brodmann M, Cohnert T, et al. Editor's Choice
 2017 ESC Guidelines on the Diagnosis and Treatment of Peripheral Arterial Diseases, in collaboration with the European Society for Vascular Surgery (ESVS). Eur J Vasc Endovasc Surg. 2018;55(3):305-68.
- Misra S, Shishehbor MH, Takahashi EA, Aronow HD, Brewster LP, Bunte MC, et al. Perfusion Assessment in Critical Limb Ischemia: Principles for Understanding and the Development of Evidence and Evaluation of Devices: A Scientific Statement From the American Heart Association. Circulation. 2019;140(12):e657-e72.
- 3. Mustapha JA, Katzen BT, Neville RF, Lookstein RA, Zeller T, Miller LE, et al. Disease Burden and Clinical Outcomes Following Initial Diagnosis of Critical Limb Ischemia in the Medicare Population. JACC Cardiovasc Interv. 2018;11(10):1011-2.
- 4. Benitez E, Sumpio BJ, Chin J, Sumpio BE. Contemporary assessment of foot perfusion in patients with critical limb ischemia. Semin Vasc Surg. 2014;27(1):3-15.
- Cindil E, Erbas G, Akkan K, Cerit MN, Sendur HN, Zor MH, et al. Dynamic Volume Perfusion CT of the Foot in Critical Limb Ischemia: Response to Percutaneous Revascularization. AJR Am J Roentgenol. 2020;214(6):1398-408.
- Arsenault KA, Al-Otaibi A, Devereaux PJ, Thorlund K, Tittley JG, Whitlock RP. The use of transcutaneous oximetry to predict healing complications of lower limb amputations: a systematic review and meta-analysis. Eur J Vasc Endovasc Surg. 2012;43(3):329-36.
- 7. Kikuchi S, Miyake K, Tada Y, Uchida D, Koya A, Saito Y, et al. Laser speckle flowgraphy can also be used to show dynamic changes in the blood flow of the skin of the foot after surgical revascularization. Vascular. 2019;27(3):242-51.
- 8. Frangioni JV. In vivo near-infrared fluorescence imaging. Curr Opin Chem Biol. 2003;7(5):626-34.
- 9. Fox IJ, Brooker LG, Heseltine DW, Essex HE, Wood EH. A tricarbocyanine dye for continuous recording of dilution curves in whole blood independent of variations in blood oxygen saturation. Proc Staff Meet Mayo Clin. 1957;32(18):478-84.
- 10. Obana A, Miki T, Hayashi K, Takeda M, Kawamura A, Mutoh T, et al. Survey of complications of indocyanine green angiography in Japan. Am J Ophthalmol. 1994;118(6):749-53.
- 11. Landsman ML, Kwant G, Mook GA, Zijlstra WG. Light-absorbing properties, stability, and spectral stabilization of indocyanine green. J Appl Physiol. 1976;40(4):575-83.
- 12. Alander JT, Kaartinen I, Laakso A, Patila T, Spillmann T, Tuchin VV, et al. A review of indocyanine green fluorescent imaging in surgery. Int J Biomed Imaging. 2012;2012:940585.
- 13. Kogure K, Choromokos E. Infrared absorption angiography. J Appl Physiol. 1969;26(1):154-7.
- 14. Vahrmeijer AL, Hutteman M, van der Vorst JR, van de Velde CJ, Frangioni JV. Image-guided cancer surgery using near-infrared fluorescence. Nat Rev Clin Oncol. 2013;10(9):507-18.
- 15. Schaafsma BE, Mieog JS, Hutteman M, van der Vorst JR, Kuppen PJ, Lowik CW, et al. The clinical use of indocyanine green as a near-infrared fluorescent contrast agent for image-guided oncologic surgery. J Surg Oncol. 2011;104(3):323-32.

- 16. Yamamoto M, Nishimori H, Handa T, Fukutomi T, Kihara K, Tashiro M, et al. Quantitative assessment technique of HyperEye medical system angiography for coronary artery bypass grafting. Surg Today. 2017;47(2):210-7.
- 17. Detter C, Russ D, Iffland A, Wipper S, Schurr MO, Reichenspurner H, et al. Near-infrared fluorescence coronary angiography: a new noninvasive technology for intraoperative graft patency control. Heart Surg Forum. 2002;5(4):364-9.
- 18. Munabi NC, Olorunnipa OB, Goltsman D, Rohde CH, Ascherman JA. The ability of intraoperative perfusion mapping with laser-assisted indocyanine green angiography to predict mastectomy flap necrosis in breast reconstruction: a prospective trial. J Plast Reconstr Aesthet Surg. 2014;67(4):449-55.
- 19. Driessen C, Arnardottir TH, Lorenzo AR, Mani MR. How should indocyanine green dye angiography be assessed to best predict mastectomy skin flap necrosis? A systematic review. J Plast Reconstr Aesthet Surg. 2020;73(6):1031-42.
- Terasaki H, Inoue Y, Sugano N, Jibiki M, Kudo T, Lepantalo M, et al. A quantitative method for evaluating local perfusion using indocyanine green fluorescence imaging. Ann Vasc Surg. 2013;27(8):1154-61.
- 21. Settembre N, Kauhanen P, Alback A, Spillerova K, Venermo M. Quality Control of the Foot Revascularization Using Indocyanine Green Fluorescence Imaging. World J Surg. 2017;41(7):1919-26.
- 22. Yang AE, Hartranft CA, Reiss A, Holden CR. Improving Outcomes for Lower Extremity Amputations Using Intraoperative Fluorescent Angiography to Predict Flap Viability. Vasc Endovascular Surg. 2018;52(1):16-21.
- 23. Zimmermann A, Roenneberg C, Wendorff H, Holzbach T, Giunta RE, Eckstein HH. Early postoperative detection of tissue necrosis in amputation stumps with indocyanine green fluorescence angiography. Vasc Endovascular Surg. 2010;44(4):269-73.
- 24. Igari K, Kudo T, Uchiyama H, Toyofuku T, Inoue Y. Indocyanine green angiography for the diagnosis of peripheral arterial disease with isolated infrapopliteal lesions. Ann Vasc Surg. 2014;28(6):1479-84.
- 25. Colvard B, Itoga NK, Hitchner E, Sun Q, Long B, Lee G, et al. SPY technology as an adjunctive measure for lower extremity perfusion. J Vasc Surg. 2016;64(1):195-201.
- 26. Pruimboom T, van Kuijk SMJ, Qiu SS, van den Bos J, Wieringa FP, van der Hulst R, et al. Optimizing Indocyanine Green Fluorescence Angiography in Reconstructive Flap Surgery: A Systematic Review and Ex Vivo Experiments. Surg Innov. 2020;27(1):103-19.

Thesis outline

This thesis is divided in three parts, preceded by the introduction in **Chapter 1**. **Part I** focuses on the quantification of tissue perfusion using ICG NIR fluorescence imaging. In **Part II**, the clinical applications of quantitative ICG NIR fluorescence imaging for the assessment of tissue perfusion are explored. **Part III** includes the summary, discussion and appendices of this thesis.

Part I

This section starts with a systematic review about the use of ICG NIR fluorescence imaging in patients with LEAD, displayed in **Chapter 2**. To provide an overview of the wide variety of performed quantification methods in ICG NIR fluorescence imaging, **Chapter 3** describes a systematic review about the parameters used for quantification of tissue perfusion in various surgical fields. In the three chapters following these systematic reviews, the quantification of tissue perfusion is assessed in original articles. **Chapter 4** provides an overview of the ICG NIR fluorescence perfusion patterns of CLTI patients compared to non-LEAD control patients. In **Chapter 5**, the effect of normalization on the measured fluorescence time-intensity curves is displayed. The quantification of free flap tissue perfusion using ICG NIR fluorescence during reconstructive breast surgery is demonstrated in **Chapter 6**.

Part II

This part evaluates the potential clinical applications of quantitative ICG NIR fluorescence imaging in vascular surgery. **Chapter 7** demonstrates the reliability of ICG NIR fluorescence imaging to assess changes in tissue perfusion following revascularization procedures. The predictive value of quantitative ICG NIR fluorescence imaging is shown in **Chapter 8**, which comprises the use of this technique in predicting tissue viability following amputation surgery.

Part III

The summary of the thesis and general discussion with future perspectives on the use of ICG NIR fluorescence imaging in vascular surgery as well as other surgical disciplines are pointed out in **Chapter 9**. Finally, the Dutch summary, curriculum vitae and list of publications of the author are shown in **Chapter 10**.



Part I

Quantification of tissue perfusion using near-infrared fluorescence imaging with indocyanine green



Chapter 2

A systematic review of the use of near-infrared fluorescence imaging in patients with peripheral artery disease

P. van den Hoven ¹, S. Ooms ¹, L. van Manen ¹, K.E.A. van der Bogt ¹, J. van Schaik ¹, J.F. Hamming ¹, A.L. Vahrmeijer ¹, J.R. van der Vorst ¹, J.S.D. Mieog ¹

1. Leiden University Medical Center, Leiden, The Netherlands

Published in Journal of Vascular Surgery, July 2019.

Abstract

Objective

In the diagnosis of peripheral artery disease (PAD) the ankle brachial index (ABI) plays an important role. However, results on ABI are unreliable in patients with severe media sclerosis. Near-infrared (NIR) fluorescence imaging using indocyanine green (ICG) can provide information about tissue perfusion and has already been studied in oncological, reconstructive and cardiac surgery. For patients with PAD, this technique might give insight in skin perfusion and thereby guide treatment. We performed a systematic review of the literature on the use of NIR fluorescence imaging in patients with PAD.

Methods

Pubmed, Medline, Embase and Cochrane were searched for articles and abstracts on the application of NIR fluorescence imaging using ICG as fluorescent dye in patients with PAD. Our search strategy combined the terms "fluorescence", "ICG" or synonyms and "peripheral artery disease" or synonyms. The extracted data include fluorescence parameters and test characteristics for diagnosis of PAD.

Results

Twenty-three articles were found eligible for this review, using 18 different parameters for evaluation of the fluorescence signal intensity. NIR fluorescence imaging was used for four main indications: diagnosis, quality control in revascularization, guidance in amputation surgery and to visualize vascular structures. For the diagnosis of PAD, NIR fluorescence imaging yields a sensitivity ranging from 67 to 100% and a specificity varying between 72 and 100%. Significant increases in multiple fluorescence parameters were found when comparing patients pre- and post-revascularization.

Conclusion

NIR fluorescence imaging can be used for several indications in patients with PAD. NIR fluorescence imaging seems promising in diagnosing PAD and guiding surgeons in treatment, especially in patients where current diagnostic methods are not applicable. Further standardization is needed to reliably use this modality in patients with PAD.

Introduction

Atherosclerotic disease of the lower limb or so called peripheral artery disease (PAD) is a common and potential life threatening disease. Besides clinical judgement, the anklebrachial index (ABI) plays an important role in diagnosing PAD. While ABI measurement can be highly sensitive for patients with PAD, the sensitivity varies for the asymptomatic patient and is unreliable in patients with diabetes mellitus, chronic kidney disease and those with well collateralized arterial obstructions (1-3). Novel diagnostic methods that are being studied include hyperspectral imaging, positron emission tomography (PET) and multi modal magnetic resonance imaging (4). However, these methods are relatively invasive and costly when used in routine practice. Moreover, transcutaneous oxygen pressure measurement (TcPO2) can be used to measure local skin oxygenation, although the benefit of this technique in patients with PAD remains unclear (5-7). In predicting wound complications following amputation surgery, patients with a TcPO2 of less than 40mmHg tend to have an increased risk of healing complications, however, there is insufficient evidence to determine the additional value of this technique besides clinical judgement (8).

In reliably quantifying local skin and wound perfusion and to provide insight in the distribution of perfusion, the use of Near-infrared (NIR) fluorescence imaging is promising. This technique requires a source of near infrared light, a fluorescent dye and a camera that measures the emission of near infrared light (9). It has already been used for various indications including image guidance in oncologic surgery, intra-operative perfusion measurement of bowel anastomosis to predict leakage, location of perforator vessels in reconstructive surgery and as quality control for coronary artery bypass surgery (10-19). Indocyanine green (ICG) is one of the two fluorescent dyes approved for clinical use by the food and drug administration (FDA) and is confined to vascular components making it feasible for skin perfusion assessment using either an intravenous or intraarterial route (11, 20, 21). The toxicity of ICG is low with a reported incidence of allergic reactions in 1 out of 10.000 patients (11). After administration of the fluorescent dye, the camera creates an image of the measured fluorescence intensity signals in the area recorded, i.e. the region of interest (ROI) (20). After measuring intensities over time, a time-intensity curve can be visualized, which can be derived from diverse fluorescence parameters (22). Measurement of a time-intensity curve using ICG, which has a halflife of 150 to 180 seconds, usually takes up to five minutes (11). The resulting intensity signals are influenced by several factors, including type and amount of fluorescent tracer used, excitation light delivery mode, camera distance and fluorescence light collection (9). Patient related factors influencing the intensity signals include the presence of inflammation or ulcers, edema, skin type and possibly the haemodynamic status. NIR fluorescence imaging is a relatively new technique with potential utility in vascular

surgery and might be of beneficial use in patients with PAD. The aim of this review was to outline the current research in the field of NIR fluorescence imaging in patients with PAD and to provide directions to standardize the use of this modality.

Methods

Search strategy

A literature search was performed in major databases (Pubmed, Medline, Embase and Cochrane) for articles on the application of NIR fluorescence imaging in patients with peripheral artery disease, published before March 2018. Our search strategy combined the terms "fluorescence" or "ICG" or synonyms with "peripheral artery disease" or synonyms. The full text of the search strategy is available in Appendix A. Articles were systematically screened by a two-stage method, whereby the title and abstract were screened first, which was subsequently followed by full-text screening.

Article selection

Only full text articles in English were included in this review and articles reporting use of NIR fluorescence in animals were excluded. Article selection was performed by two independent researchers (PH and SO). All articles describing the use of NIR fluorescence imaging in patients with peripheral arterial disease were included. Since this technique can be used for different applications, the results were divided in four categories, consisting of the main applications: 1. diagnosis 2. quality control following revascularization 3. amputation and 4. NIR fluorescence angiography.

Quality assessment

The quality and the risk of bias of the included articles were independently evaluated by two reviewers (PH and SO) in according to the revised quality assessment of diagnostic accuracy studies (QUADAS-2) (23). In case of discrepancies in interpretation, a third reviewer (LM) was asked to adjudicate.

Data extraction

For all articles, data extracted consisted of the relevant patient characteristics, name of fluorescence camera system and used ICG concentration, (the effect of revascularization on) measured fluorescence parameters, correlated (imaging) modalities, and the diagnostic value (sensitivity and specificity) of NIR fluorescence imaging compared to current standards. Fluorescence parameters were standardized to provide a better overview.

Results

Overview of studies

An overview of the article selection for this systematic review is reported in a flow diagram according to the PRISMA-P 2015 guidelines (Figure 1) (24). A total of 944 articles were found of which eventually 23 articles were eligible for the review. The results of the quality assessment are illustrated in Table I and Figure 2. All articles in this review used ICG as fluorescent marker. To obtain an objective assessment of the fluorescence intensity measurements, different parameters were used, as summarized in Table II. In the selected studies a total of 18 parameters were utilized. Most studies included in this review used time dependent parameters. By measuring the fluorescence intensity over time in a selected ROI, a time-intensity curve can be plotted (Figure 3) (25).

NIR fluorescence imaging was used in 9 studies as a diagnostic modality, whereas 10 studies determined its use in quality control after revascularization procedures. Six studies described the use of this perfusion measurement in patients undergoing amputation surgery. Furthermore, NIR fluorescence imaging is used in two studies for visualization of vascular structures, hereafter stated as NIR fluorescence angiography. An overview of the included studies with study characteristics, diagnostic value for detection of PAD and/or results on quality control following revascularization is provided in Table III.

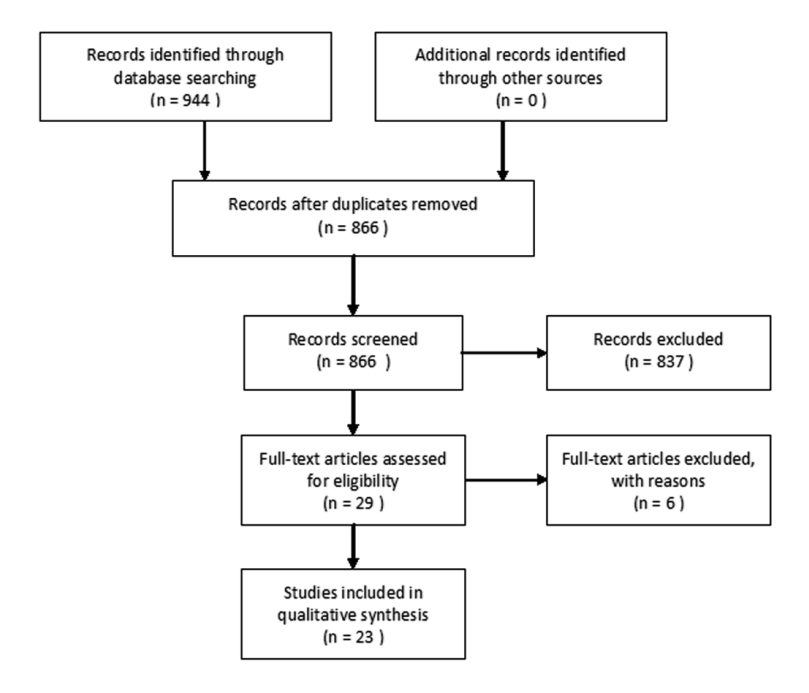


Figure 1. Prisma flowchart for selection of included studies.

Table I. Quality assessment and risk of bias according to QUADAS-2. Low risk of bias (-), high risk of bias (+), risk of bias unclear (?).

| | Risk of bias | 3 | - | | Applicabil | ity cond | erns |
|-----------------------------|--------------------|---------------|-----------------------|---|--------------------|----------|--------------------|
| Study | Patient selections | Index test | Reference standard | | Patients selection | | Reference standard |
| Igari et al. 2013 (1) | _ | + | - | - | - | - | - |
| Zimmermann et al. 2012 (6) | - | + | - | - | - | - | - |
| Yamamoto et al. 2012 (18) | - | - | - | - | - | - | - |
| Joh et al. 2016 (20) | - | + | + | ? | - | - | + |
| Igari et al. 2014 (21) | - | + | - | - | - | - | - |
| Braun et al. 2013 (22) | - | + | - | - | - | - | - |
| Igari et al. 2014 (26) | + | + | - | - | + | - | - |
| Nishizawa et al. 2016 (27) | ? | + | - | - | + | + | - |
| Kang et al. 2010 (28) | - | + | - | - | - | - | - |
| Kang et al. 2010 (29) | + | + | - | - | - | - | - |
| Terasaki et al. 2013 (30) | - | + | - | - | - | - | - |
| Venermo et al. 2016 (31) | - | + | - | - | - | - | - |
| Colvard et al. 2015 (32) | - | + | - | - | - | - | - |
| Rother et al. 2016 (33) | - | + | - | - | - | - | - |
| Settembre et al. 2017 (25) | - | + | - | - | - | - | - |
| Riess et al. 2017 (34) | - | + | - | - | - | - | - |
| Rother et al. 2018 (35) | - | + | - | - | - | - | - |
| Perry et al. 2012 (36) | + | + | ? | - | - | - | ? |
| Samies et al. 2015 (37) | + | + | ? | ? | - | - | ? |
| Zimmermann et al. 2010 (38) | - | - | ? | - | - | - | ? |
| Yang et al. 2018 (39) | - | - | ? | - | - | - | ? |
| Unno et al. 2008 (40) | - | + | - | - | - | - | - |
| Sumpio et al. 2013 (41) | ? | ? | ? | ? | ? | ? | ? |

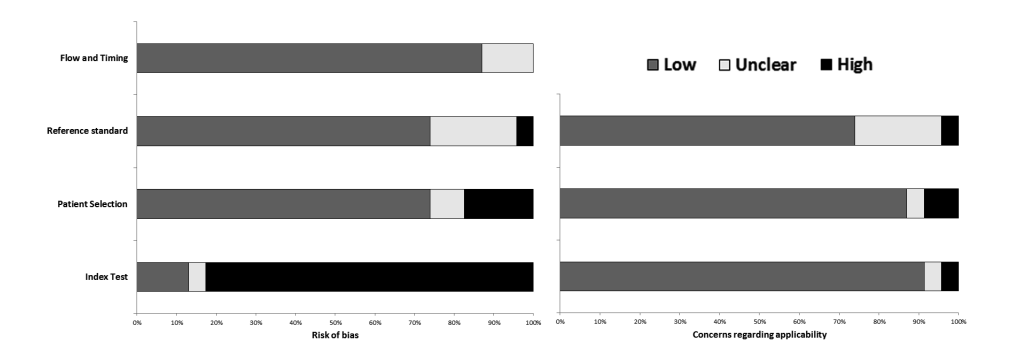


Figure 2. Proportion of studies with low, high and unclear risk of bias according to QUADAS-2.

Table II. Overview of used fluorescence parameters in current literature.

| Parameter | Definition (unit) | Equivalents | Reference(s) |
|--------------------|---|---|---------------------------------------|
| FI | Fluorescence intensity as calculated by | - | (1, 6, 10, 20-22, |
| | used software (AU) | | 25-41, 43) |
| Ingress | Magnitude of increase from baseline to peak fluorescence intensity (AU) | Imax, Maximum Peak Intensity, Maximum Intensity | (1, 6, 21, 22, 25- 27, 32, 33, 35) |
| Ingress rate | Rate of FI increase from baseline to maximum FI (AU/s) | Slope, Intensity Rate | (1, 22, 25, 32-35) |
| Egress | Magnitude of FI decrease from maximum FI to end FI (AU) | - | (22) |
| Egress rate | Rate of FI decrease from maximum FI to end FI (AU/s) | Washout Kinetics | (22, 29, 32) |
| Tmax | Time until maximum FI (s) | Time To Peak, Peak Intensity Time | (1, 10, 21, 26, 27, 29, 43) |
| T1/2 | Time until half of maximum FI (s) | - | (1, 21, 26, 27, 30, 31, 41, 43) |
| Starting FI | FI upon start ICG administration (AU) | - | (22) |
| PDE10 | FI 10 seconds following rise of FI (AU) | SPY10 | (1, 25, 30, 31, 41) |
| Perfusion | Blood exchanged per minute (%/min) | - | (28) |
| Rate | | | |
| Filling | Time following administration of ICG and first FI signal (s) | - | (29) |
| Perfusion Index | Slope of fluorescence intensity increase (%) | - | (6) |
| Curve | Area under the curve of time-intensity | - | (22) |
| Integral | curve | | |
| End Intensity | FI at end of study (AU) | - | (22) |
| Td90% | Time until 90% decrease in maximum FI (s) | - | (26, 27) |
| Td75% | Time until 75% decrease in maximum FI (s) | - | (26) |
| IR60 | Rate of FI measured 60 seconds after Tmax (AU/AU) | - | (26) |
| RPV | Percentage of maximum fluorescence intensity obtained (%) | - | (39) |

Abbreviations: FI = Fluorescence Intensity, AU = Arbitrary Units, s = seconds, PDE = PhotoDynamicEye.

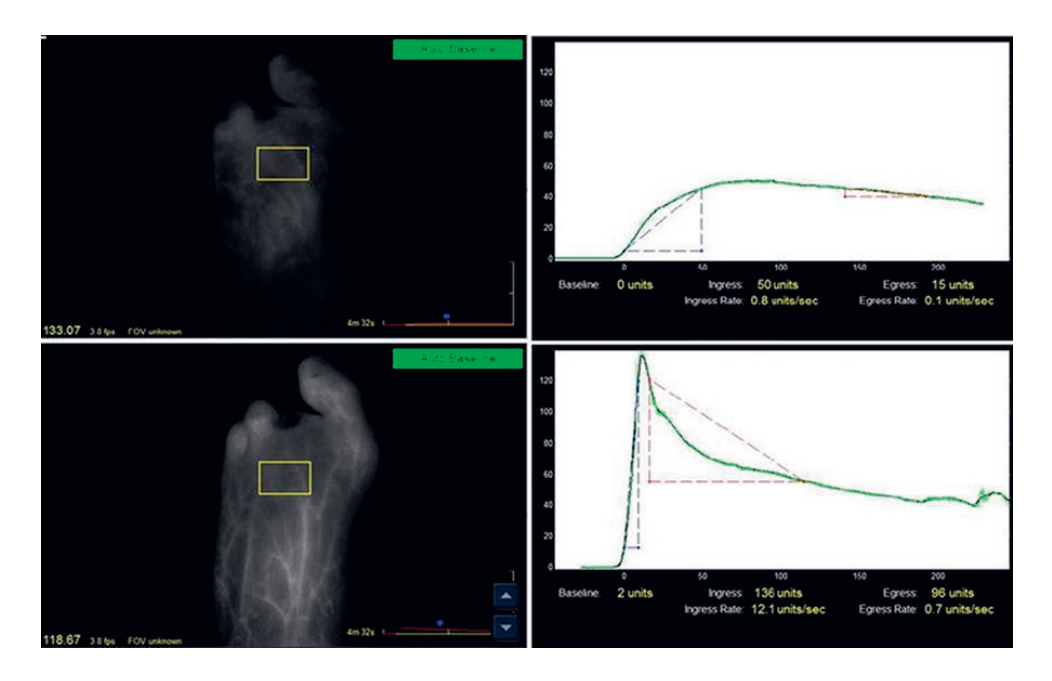


Figure 3. Fluorescence images with selected region of interest and corresponding time-intensity curves before (upper panel) and after revascularization (lower panel). Reprinted by permission from Springer Nature: World Journal of Surgery (25). © 2017.

NIR fluorescence imaging as diagnostic modality

During the past years, the role of NIR fluorescence imaging as diagnostic modality for PAD has been determined in several studies, which evaluated quantitative parameters for the diagnosis of PAD and compared these parameters with other diagnostic modalities (1, 6, 21, 26-31). Measured test accuracies for diagnosing PAD using NIR fluorescence imaging are depicted in Table III. Kang et al. first described the use of NIR fluorescence imaging in a patient with symptomatic PAD and compared these to a patient with normal results on ABI (29). The perfusion rate, defined as the percentage of blood exchanged per minute, was measured at the dorsum of both feet. A clear definition of this parameter is stated elsewhere (42). All measured outcomes, also including time to filling, time to maximum intensity and washout kinetics were worse in the patient with symptomatic PAD (data not shown in table). Two studies compared different ICG parameters in patients with - and without PAD, in which PAD was defined as a stenosis of >50% in one or more peripheral arteries (26, 28). Kang et al. showed a significantly lower perfusion rate in patients with PAD (16.6 vs 38.1 %/min) (28). In diagnosing PAD, a cut-off perfusion rate of 24.4 %/min was able to predict PAD with a sensitivity of 92%. Igari et al. found other parameters associated with PAD including Td90% and

Td75%, of which the Td90% was the most significant parameter (P=0.001) (26). A cut-off value of 25 seconds was able to predict an infrapopliteal lesion with a sensitivity of 82.6%.

NIR fluorescence imaging was also compared with currently available diagnostic modalities (ABI, TcPO2, toe pressure (TP), toe brachial index (TBI) and ankle pressure (AP) for the detection of critical limb ischemia (CLI). CLI was defined as either a Rutherford grade ≥ 4 or Fontaine stage ≥ 3 (6, 27, 30, 31). A cut-off perfusion index of 59% was able to predict CLI with a sensitivity of 100% and a specificity of 83.3% (6). Terasaki et al. compared NIR fluorescence imaging to TcPO2 measurement, showing an overall moderate correlation (R²=0.50) (30). A cut-off value of 28 arbitrary units for PDE10 predicted CLI, defined as TcPO2 <30 mm Hg, with a sensitivity of 100% and specificity of 86.6%. T1/2 showed significant difference in patients with Fontaine stage 2 and 3, however no significance was seen between Fontaine stage 2 and 4. In patients with diabetes mellitus a good reliability was found for NIR fluorescence imaging by comparing two separate measurements in patients with CLI (31). A moderate correlation between NIR fluorescence and TcPO2 was found being stronger in a subgroup of patients with diabetes mellitus. Setting 21 arbitrary units for PDE10 as cut-off, CLI was predicted with a sensitivity of 67% and a specificity of 72%. T1/2 turned out to be a good NIR fluorescence parameter after correlating to the ABI and TP. When performing NIR fluorescence imaging using an intra-arterial injection of ICG, Igari et al found the measured T1/2 was able to predict an ABI lower than 0.70 with a sensitivity of 85% and a specificity of 100% (21). In another study, they compared NIR fluorescence to TP and showed a sensitivity of 77% using a cut-off value of 20 seconds for the T1/2 to predict a toe pressure less than 50mmHg (1). In a study by Nishizawi et al. in 2015, results of NIR fluorescence imaging were compared between PAD patients with or without dialysis treatment in which results of 20 dialysis patients were compared to 42 non-dialysis patients (27). A significant difference in Td90% was found in two of the three ROIs comparing patients with and without dialysis. Tmax and Td90% showed significant differences in patients with CLI compared to patients without CLI. No comparison was made to conventional diagnostic modalities.

Conclusion

The accuracy in diagnosing PAD or CLI using NIR fluorescence imaging ranged from 67 to 100% with corresponding specificities of 72 to 100%. Time-related parameters, including T1/2, PDE10 and Td90%, showed to be the most statistically significant parameters in varying ROIs.

Table III. Overview of study characteristics and results on NIR fluorescence imaging.

| Application | Reference | Study characteristics | acteristics | | | Diagnostic value of detecting PAD and/ or $\ensuremath{\mathrm{CLI}}$ | e of detecting | g PAD and/ | Fluorescence parameters in |
|--------------------------------------|----------------------------|-----------------------|-----------------|-------------|-----------------------|---|--------------------|-----------------|--|
| | | | | | | | | | revascularization control |
| | | Patients (limbs) | Diabetes (N) | ICG dosage | Comparing modality | Fluorescence parameter | Sensitivity (%) | Specificity (%) | |
| Diagnostic modality | | | | | | | | | |
| | Kang et al. 2010 (29) | 2 | 1 | 0.16 mg/kg | 1 | 1 | 1 | 1 | 1 |
| | Kang et al. 2010 (28) | 29 (56) | 3 | 0.16 mg/kg | ABI | Perfusion rate | 0.92 | 0.90 | 1 |
| | Zimmermann et al. 2012 (6) | 30 (30) | 6 | 0.5 mg/kg | ABI | Perfusion index | 1.00 | 0.83 | 1 |
| | Terasaki et al. 2013 (30) | 34 (34) | 19 | 0.1 mg/kg | TcPO2 | PDE10 | 1.00 | 0.87 | 1 |
| | Igari et al. 2013 (1) | 21 (23) | 6 | 0.1 mg/kg | ABI, TAI, TP | T1/2 | 0.77 | 0.80 | 1 |
| | Igari et al. 2014 (21) | 16 (22) | 9 | 0.01 mg/kg | ABI, AP, TAI, TP | T1/2 | 0.85 | 1.0 | 1 |
| | Igari et al. 2014 (26) | 23 (38) | 19 | 0.1 mg/kg | ABI, TAI, TP | %06PL | 0.83 | 0.73 | 1 |
| | Venermo et al. 2016 (31) | 41 (41) | 19 | 0.1 ml/kg | ABI, TP, TcPO2 | PDE10 | 29.0 | 0.72 | 1 |
| | Nishizawa et al. 2016 (27) | 62 | 39 | 0.1 ml/kg | 1 | ı | , | 1 | 1 |
| Quality control in revascularization | | | | | | | | | |
| | Perry et al. 2012 (36) | 1 | 1 | 12.5 mg | 1 | ı | 1 | 1 | ı |
| | Braun et al. 2013 (22) | 24 (26) | 22 | 12,5 mg | ABI, TP | | | 1 | Ingress: P=0.004 Ingress rate: P= 0.015 Curve integral: P= 0.021 End intensity: P= 0.019 Egress: P= 0.004 Egress: P= 0.013 |

Table III. Continued

| Application | Reference Study | Study characteristics | ics | | Diagnostic and/or CLI | Diagnostic value of detecting PAD and/or CLI | tecting PAD | Fluore | Fluorescence parameters in revascularization control |
|--------------------|--------------------------------|-----------------------|-----|-----------|--------------------------|--|-------------|--------|--|
| | Sumpio et al. 2013 (41) | 2 | 1 | 1 | TcPO2 | 1 | 1 | 1 | 1 |
| | Igari et al. 2013 (1) | 21 (23) | 10 | 0.1 mg/kg | ABI, TBI, TP | 1 | 1 | 1 | Ingress: P<0.0001 Tmax: P=0.001 |
| | | | | | | | | | Ingress rate: P<0.0001 T1/2: P=0.005 PDE10: P=0.0001 |
| | Colvard et al. 2016 (32) | 93 | 65 | 2.5 ml | ABI | 1 | 1 | 1 | Ingress: P<0.001 Egress: P= 0.035 |
| | Joh et al. 2016 (20) | 4 | 2 | 3-5 ml | 1 | 1 | , | 1 | · , |
| | Rother et al. 2017 (33) | 33 | 13 | 0.1 ml/kg | ABI | 1 | 1 | 1 | Ingress: P<0.001 Ingress rate: P<0.001 |
| | Settembre et al. 2017 (25) | 101 (104) | 95 | 0.1 mg/kg | ABI, TP | 1 | 1 | 1 | Mean intensity: P=0.001 SPY10: P<0.001 |
| | Riess et al. 2017 (34) | 7 | 3 | 0.1 mg/kg | ABI, PPG | 1 | 1 | 1 | Ingress rate: P=0.005 |
| | Rother et al. 2018 (35) | 40 | 16 | 0.1 mg/kg | ABI | ı | 1 | 1 | Ingress: P<0.001 Ingress rate: P=0.001 |
| Amputation surgery | Ya | | | | | | | | |
| | Zimmermann et al. 2010 (38) 10 | 10 | 9 | 0.5 mg/kg | 1 | 1 | , | 1 | • |
| | Perry et al. 2012 (36) | 1 | 1 | 12.5 mg | 1 | 1 | , | 1 | 1 |
| | Sumpio et al. 2013 (41) | 2 | 1 | 1 | TcPO2 | 1 | 1 | 1 | 1 |
| | Samies et al. 2015 (37) | 2 | 2 | 1 | 1 | 1 | 1 | 1 | 1 |
| | Joh et al. 2016 (20) | 4 | 2 | 3-5 ml | 1 | 1 | 1 | 1 | 1 |
| | Yang et al. 2018 (39) | 13 (17) | 11 | 10 mg | 1 | 1 | 1 | , | 1 |

Table III. Continued

| Application R | Reference | Study c | Study characteristics | tics | | | Diagnostic value of detecting PAD and/or CLJ | ecting PAD | Fluorescer | Fluorescence parameters in revascularization control |
|----------------------|------------------------------|----------|-----------------------|------|----------------|-------|--|------------|------------|--|
| Angiography | | | | | | | | | | |
| | Unno et al. 2008 (| (40) | 6 | 1 | 1 ml | 1 | 1 | 1 | 1 | |
| | Yamamoto et al. 2017 (18) 12 | 017 (18) | 12 | 1 | 0.05 mg/kg TTF | , TTF | 1 | 1 | 1 | |

Abbreviations: ABI = Ankle Brachial Index, TAI = Toe Arm Index, TP = Toe Pressure, AP = Ankle Pressure, TcPO2= Transcutaneous oxygen pressure measurement, TTF = Transit Time Flowmetry, PPG = Photoplethysmography.

NIR fluorescence imaging as quality control in revascularization

NIR fluorescence imaging provides the possibility to measure direct effect of revascularization on regional perfusion and can be performed intra-operatively or directly following endovascular revascularization (Figure 3). Ten studies, of which were three case studies, performed NIR fluorescence imaging for evaluating the effect of endovascular and open revascularization on the fluorescence parameters in a study population varying between 1 and 101 patients (Table III).

In 2013, Braun et al. performed a cohort study in which NIR fluorescence imaging was performed within five days following revascularization in patients with PAD in Rutherford stage 5 or 6 (22). In thirteen patients, NIR fluorescence imaging was performed before and after revascularization. In these patients, there was a significant improvement in ingress, ingress rate, AUC, end intensity, egress and egress rate (all P<0.05). A significant correlation was found between ABI and ingress, ingress rate and egress rate (all P<0.05). Furthermore, in the last years, 6 studies with cohorts of 7 or more patients were performed, including endovascular as well as open revascularization (1, 25, 32-35). In these studies, improvement of outcome on several but not all fluorescence parameters was seen, in contrary to ABI, which showed significant improvement in all studies. Interestingly, when comparing pre and post interventional results on NIR fluorescence imaging in a subset of patients, who showed no clinical improvement in symptoms, no statistically significant differences (P>0.05) were found for the measured parameters (25, 32). The only study comparing pulse volume recordings pre- and postrevascularization found significant improvement in only one of two measured parameters (34). The measured ingress rate in this study showed significant improvement following revascularization (P=0.005). In a recent study the concept of angiosomes was studied by comparing NIR fluorescence parameters among four different angiosomes following single vessel outflow tibial bypass surgery. Significant improvement was seen in directly as well as indirectly revascularized angiosomes (P<0.001) (35). Interestingly, in a subset of patients with diabetes mellitus, the directly revascularized angiosomes showed tendency towards a better improvement on perfusion measurement compared to indirectly revascularized angiosomes (P=0.098).

Conclusion

Multiple NIR fluorescence parameters statistically improved upon successful revascularization, thereby showing possible benefit for use of this technique as quality control. The absence of improvement of NIR fluorescence parameters in patients without successful revascularization supports this hypothesis. Furthermore, NIR fluorescence imaging is a promising method to further investigate the relevance of angiosomes in guiding treatment.

NIR fluorescence imaging as guidance in amputation surgery

For patients with PAD, NIR fluorescence imaging might be able to predict outcome of wound healing and viability of skin flaps in amputation surgery and may therefore be useful in intra-operative determination of amputation levels. Six studies evaluated the use of NIR fluorescence imaging on predicting viability. In a case report by Perry et al., NIR fluorescence imaging was used intra-operatively to measure perfusion of the foot following tibial bypass surgery (36). NIR fluorescence intensity was measured at the foot following a femoral-tibial bypass and showed a perfusion deficit of the fourth digit and plantar side of the fourth metatarsal. Upon manual occlusion of the bypass, no signal was found in the third and fifth digit either. Amputation of the fourth digit and debridement of the plantar side of the fourth metatarsal was performed followed by primary closure of the wound. NIR fluorescence imaging as guidance for amputation surgery was also described in case series (20, 37). Measurements of fluorescence intensities all showed good intensity signals of the well-perfused parts of the foot, whereas less-perfused parts showed a well demarcated deficit in signal intensity (Figure 4) (20). After amputation of the necrotic digits, postoperatively performed NIR fluorescence intensity measurement showed good perfusion of the remaining tissue. In all case studies, no postoperative complications occurred regarding the healing of the wound.

In one cohort study of 10 patients undergoing amputation surgery, NIR fluorescence imaging was able to predict wound complications in 3 patients. Except for one patient with a thrombus in the amputation wound, no complications occurred in patients without fluorescence intensity deficit (38). Comparison of NIR fluorescence parameters with clinical judgement of necrosis was performed in a retrospective cohort of 13 patients undergoing 17 amputations (39). Absolute values for fluorescence intensity proved low sensitivity and specificity in predicting skin viability. Using relative perfusion values, a value of less than 31% was able to predict viability with a sensitivity of 100%.

Conclusion

NIR fluorescence imaging might be of use in predicting postoperative wound complications. Predicting the level of amputation could be a possible application of NIR fluorescence imaging, which has not yet been studied. The additional value of this method besides clinical judgement in predicting flap viability has yet to be identified.

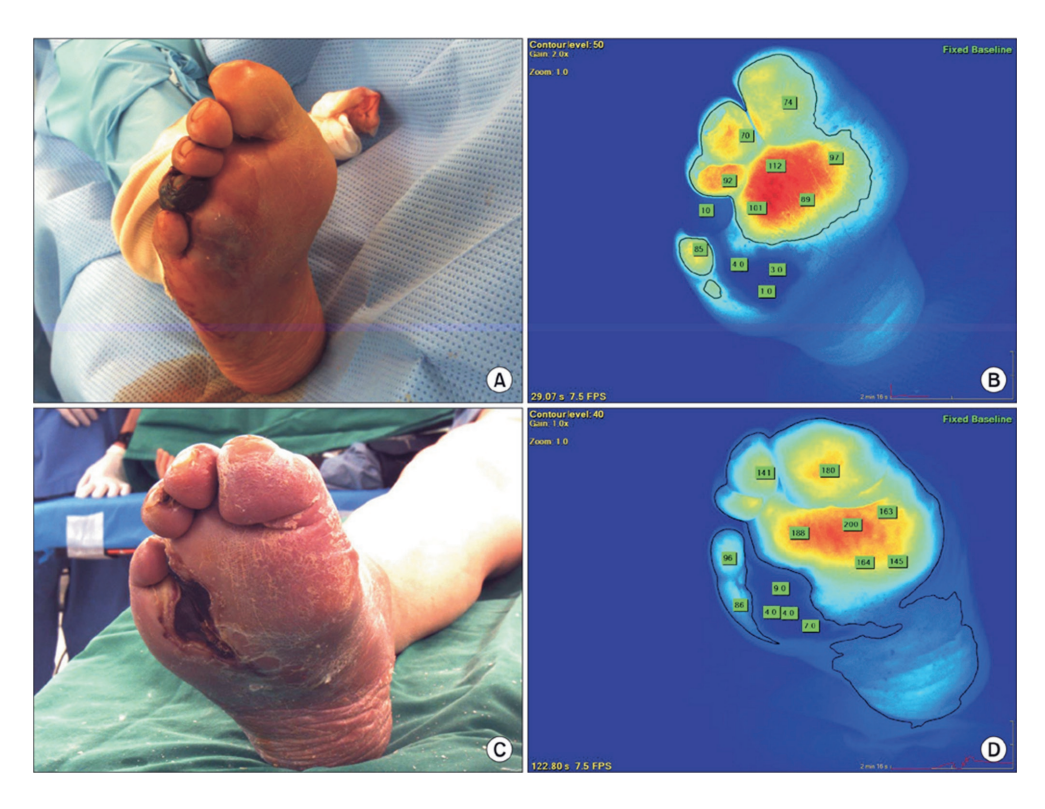


Figure 4. NIR Fluorescence intensity images. *Upper panel*: color image of right foot, showing a necrotic dig. 4 before surgical intervention (A) and the corresponding NIR fluorescence image (B). *Lower panel*: Color (C) and NIR fluorescence image (D) after amputation of dig. 4, showing viable tissue. Reprinted from Joh et al., Annals of Surgical Treatment and Research (2016) (20).

NIR fluorescence angiography

The use of NIR fluorescence imaging as modality to visualize vascular structures in patients with PAD has been described in two studies (10, 40). In these two studies, NIR fluorescence was used intra-operatively in peripheral artery bypass surgery to obtain information about the bypass. In these studies, with cohort sizes of 9 and 12 patients, NIR fluorescence imaging revealed decreased fluorescence intensity in two patients. In one patient, revision of the bypass was performed after revealing decreased intensity over the distal anastomosis. In the other patient, decreased signal was found over the outflow artery, which was confirmed by Transit Time Flowmetry (TTF).

Conclusion

NIR fluorescence angiography has been studied in a small cohort of patients. These studies have shown a possible application of this technique, e.g. to assess for bypass patency, however the added value besides clinical judgement and TTF is controversial.

Discussion

This systematic review shows the variety of indications for the use of NIR fluorescence imaging in patients with peripheral artery disease, including peripheral perfusion measurement for diagnosis, quality control in revascularization and for guidance in amputation surgery. Furthermore it is possible to visualize vascular structures. The use of NIR fluorescence imaging in diagnosing PAD yields a sensitivity up to 100% and is thereby not limited by media sclerosis as is seen in selected patients with diabetes mellitus and chronic kidney disease (6, 30). NIR fluorescence imaging can be performed in multiple ROIs and also a variety of parameters can be calculated using this technique, providing a real-time perfusion map of the imaged area. For quality control in revascularization, multiple parameters have shown to improve upon successful revascularization (1, 20, 22, 25, 32-36, 41). Furthermore, the absence of intensity signal measured by NIR fluorescence imaging is able to guide surgeons in performing targeted amputations, as was shown in five described case series (20, 36-38, 41). As stated earlier, most current diagnostic methods for patients with PAD focus on detecting morphological and anatomical deviations in the macrocirculation. Segmental pressure readings, Doppler waveforms and pulse volume recordings enhance the sensitivity of the ankle-brachial index for diagnosing PAD, however they do not provide information about regional tissue perfusion. The role of TcPO2 measurement to measure skin perfusion remains controversial and definitive cutoff values to guide physicians have yet to be stated (5, 7, 8). New modalities to measure skin perfusion include hyperspectral imaging, nuclear imaging and magnetic resonance imaging, but the benefit of these modern technologies has yet to be established (5, 34, 44).

NIR fluorescence imaging is able to assess the intensity signal that is the mere equivalent of skin perfusion and has already proven its feasibility and safety within different medical fields, e.g. oncologic surgery, reconstructive surgery and cardiac surgery. Studies included in this systematic review show significant correlations between fluorescence parameters and conventional methods such as ankle-brachial indices and toe pressures which gives tendency towards good reliability of NIR fluorescence imaging in diagnosing PAD. This technique might therefore be of adjunctive use in diagnosing PAD. Moreover, intra-operative use of this technique provides a new possibility to guide surgeons and radiologists in performing additional revascularization procedures or prevent unnecessary interventions. In amputation surgery, it is possible to measure intensity signals in the overlying skin flap and thereby provide information about healing tendencies or even guide intra-operative decision making. Besides improving patient outcome by reducing the amount of unnecessary interventions, this technique might also reduce costs. Cooperating with different medical fields where NIR fluorescence imaging has proven feasible helps justify the use of this costly system. NIR fluorescence imaging using ICG requires intravascular access, which might preclude easy use in the outpatient clinic. As is concerned for the technique of NIR fluorescence imaging, different camera systems can be used of which an overview is given in a review article by Dsouza et al. (45). For the clinical use of NIR fluorescence imaging, it is important to consider system- and patient related factors possibly influencing fluorescence signals. Since the penetration depth of NIR is limited up to 1 cm, no information can be obtained about perfusion of deeper underlying tissues (46). However, diminished blood supply will likely result in diminished perfusion of the skin and underlying subcutaneous tissue first. To improve reliability, further standardization of all possible intervening variables is necessary to provide a reliable and valid measurement of perfusion using NIR fluorescence imaging. Furthermore, this review shows the heterogeneity in ROIs that are used and variety of parameters used for quantitative assessment of perfusion. As stated by Igari et al., time-related parameters appear to have greater diagnostic accuracy than fluorescence intensity, especially since fluorescence intensity alone is influenced by multiple factors (9, 26). This statement is supported by this review, which shows highest diagnostic accuracies are found when using time-related parameters, such as T1/2, PDE10 and Td90%. Which parameter in which ROI provides the most reliable outcome in diagnosing PAD has yet to be established. Further studies should therefore focus on validating NIR fluorescence measurement by using a standardized protocol. These studies should minimize bias by incorporating subsets of patients (e.g. patients with diabetes mellitus or chronic kidney disease) and compare these results with conventional diagnostic methods. As is concerned for quality control following revascularization, further studies should compare changes in fluorescence parameters pre- and postrevascularization to conventional methods and clinical outcome. A valid and reliable measurement of perfusion using NIR fluorescence imaging can guide decision making and thereby improve patient outcome. This systematic review provides

an overview of the clinical use of NIR fluorescence imaging in patients with peripheral artery disease. The main limitation of this study is the heterogeneity of included studies, which precludes a comparative analysis. This supports the need for standardization of protocols for NIR fluorescence imaging in patients with PAD.

Conclusion

NIR fluorescence imaging can be of additional diagnostic value in patients with PAD, especially where current methods are not applicable. The intra-operative use of this technique shows promising results on predicting outcome following revascularization and might prevent unnecessary interventions. Future studies should focus on standardizing diagnostic protocols, with a focus on NIR fluorescence measurement, fluorescence parameters and ROIs.

Appendices

Appendix A. Search strategy.

(("Fluorescence" [Mesh] OR "fluorescence" [tw] OR fluorescen* [tw] OR "Indocyanine Green" [Mesh] OR "Indocyanine Green" [tw] OR "ICG" [tw] OR "Fluorescein Angiography" [Mesh] OR Fluorescein* [tw]) AND ("Peripheral Arterial Disease" [Mesh] OR "Peripheral Arterial Disease" [tw] OR "Peripheral Arterial Diseases" [tw] OR "Peripheral Artery Diseases" [tw] OR "Peripheral Artery Diseases" [tw] OR "Peripheral Vascular Diseases" [tw] OR "Peripheral Vascular Diseases" [tw] OR "Peripheral Vascular Diseases" [tw] OR "Peripheral Vessel Diseases" [tw] OR "Peripheral Vessel Diseases" [tw] OR "Imb ischaemia" [tw] OR "Imb ischaemia" [tw] OR ("Ischemia" [mesh] AND "Leg" [mesh]) OR ((ischemi* [tw] OR ischaemi* [tw]) AND ("leg" [tw] OR "legs" [tw] OR "Imbs" [tw] OR hindlimb* [tw])) OR "Arteriosclerosis Obliterans" [mesh] OR "arteriosclerosis obliterans" [tw] OR peripheral arter* [tw] OR "peripheral vascular" [tw] OR peripheral vessel* [tw] OR ("Extremities" [mesh] AND "Arterial Occlusive Diseases" [Mesh]))) NOT ("Animals" [mesh] NOT "Humans" [mesh]).

Reference list

- 1. Igari K, Kudo T, Toyofuku T, Jibiki M, Inoue Y, Kawano T. Quantitative evaluation of the outcomes of revascularization procedures for peripheral arterial disease using indocyanine green angiography. Eur J Vasc Endovasc Surg. 2013;46(4):460-5.
- 2. Herraiz-Adillo A, Cavero-Redondo I, Alvarez-Bueno C, Martinez-Vizcaino V, Pozuelo-Carrascosa DP, Notario-Pacheco B. The accuracy of an oscillometric ankle-brachial index in the diagnosis of lower limb peripheral arterial disease: A systematic review and meta-analysis. Int J Clin Pract. 2017;71(9).
- Wyman RA, Keevil JG, Busse KL, Aeschlimann SE, Korcarz CE, Stein JH. Is the ankle-brachial index a useful screening test for subclinical atherosclerosis in asymptomatic, middle-aged adults? WMJ. 2006;105(6):50-4.
- 4. Forsythe RO, Hinchliffe RJ. Assessment of foot perfusion in patients with a diabetic foot ulcer. Diabetes Metab Res Rev. 2016;32 Suppl 1:232-8.
- 5. Benitez E, Sumpio BJ, Chin J, Sumpio BE. Contemporary assessment of foot perfusion in patients with critical limb ischemia. Semin Vasc Surg. 2014;27(1):3-15.
- 6. Zimmermann A, Roenneberg C, Reeps C, Wendorff H, Holzbach T, Eckstein HH. The determination of tissue perfusion and collateralization in peripheral arterial disease with indocyanine green fluorescence angiography. Clin Hemorheol Microcirc. 2012;50(3):157-66.
- 7. de Graaff JC, Ubbink DT, Legemate DA, Tijssen JG, Jacobs MJ. Evaluation of toe pressure and transcutaneous oxygen measurements in management of chronic critical leg ischemia: a diagnostic randomized clinical trial. J Vasc Surg. 2003;38(3):528-34.
- 8. Arsenault KA, Al-Otaibi A, Devereaux PJ, Thorlund K, Tittley JG, Whitlock RP. The use of transcutaneous oximetry to predict healing complications of lower limb amputations: a systematic review and meta-analysis. Eur J Vasc Endovasc Surg. 2012;43(3):329-36.
- 9. Frangioni JV. In vivo near-infrared fluorescence imaging. Curr Opin Chem Biol. 2003;7(5):626-34.
- 10. Yamamoto M, Orihashi K, Nishimori H, Wariishi S, Fukutomi T, Kondo N, et al. Indocyanine green angiography for intra-operative assessment in vascular surgery. Eur J Vasc Endovasc Surg. 2012;43(4):426-32.
- 11. Schaafsma BE, Mieog JS, Hutteman M, van der Vorst JR, Kuppen PJ, Lowik CW, et al. The clinical use of indocyanine green as a near-infrared fluorescent contrast agent for image-guided oncologic surgery. J Surg Oncol. 2011;104(3):323-32.
- 12. Degett TH, Andersen HS, Gogenur I. Indocyanine green fluorescence angiography for intraoperative assessment of gastrointestinal anastomotic perfusion: a systematic review of clinical trials. Langenbecks Arch Surg. 2016;401(6):767-75.
- 13. Muntean MV, Muntean V, Ardelean F, Georgescu A. Dynamic perfusion assessment during perforator flap surgery: an up-to-date. Clujul Med. 2015;88(3):293-7.
- Wada H, Vargas CR, Angelo J, Faulkner-Jones B, Paul MA, Ho OA, et al. Accurate Prediction of Tissue Viability at Postoperative Day 7 Using Only Two Intraoperative Subsecond Near-Infrared Fluorescence Images. Plast Reconstr Surg. 2017;139(2):354-63.

- 15. Lee BT, Hutteman M, Gioux S, Stockdale A, Lin SJ, Ngo LH, et al. The FLARE intraoperative near-infrared fluorescence imaging system: a first-in-human clinical trial in perforator flap breast reconstruction. Plast Reconstr Surg. 2010;126(5):1472-81.
- 16. Lee BT, Matsui A, Hutteman M, Lin SJ, Winer JH, Laurence RG, et al. Intraoperative near-infrared fluorescence imaging in perforator flap reconstruction: current research and early clinical experience. J Reconstr Microsurg. 2010;26(1):59-65.
- 17. Munabi NC, Olorunnipa OB, Goltsman D, Rohde CH, Ascherman JA. The ability of intraoperative perfusion mapping with laser-assisted indocyanine green angiography to predict mastectomy flap necrosis in breast reconstruction: a prospective trial. J Plast Reconstr Aesthet Surg. 2014;67(4):449-55.
- 18. Yamamoto M, Nishimori H, Handa T, Fukutomi T, Kihara K, Tashiro M, et al. Quantitative assessment technique of HyperEye medical system angiography for coronary artery bypass grafting. Surg Today. 2017;47(2):210-7.
- 19. Detter C, Russ D, Iffland A, Wipper S, Schurr MO, Reichenspurner H, et al. Near-infrared fluorescence coronary angiography: a new noninvasive technology for intraoperative graft patency control. Heart Surg Forum. 2002;5(4):364-9.
- 20. Joh JH, Park HC, Han SA, Ahn HJ. Intraoperative indocyanine green angiography for the objective measurement of blood flow. Ann Surg Treat Res. 2016;90(5):279-86.
- 21. Igari K, Kudo T, Uchiyama H, Toyofuku T, Inoue Y. Intraarterial injection of indocyanine green for evaluation of peripheral blood circulation in patients with peripheral arterial disease. Ann Vasc Surg. 2014;28(5):1280-5.
- 22. Braun JD, Trinidad-Hernandez M, Perry D, Armstrong DG, Mills JL, Sr. Early quantitative evaluation of indocyanine green angiography in patients with critical limb ischemia. J Vasc Surg. 2013;57(5):1213-8.
- 23. Whiting PF, Rutjes AW, Westwood ME, Mallett S, Deeks JJ, Reitsma JB, et al. QUADAS-2: a revised tool for the quality assessment of diagnostic accuracy studies. Ann Intern Med. 2011;155(8):529-36.
- 24. Moher D, Shamseer L, Clarke M, Ghersi D, Liberati A, Petticrew M, et al. Preferred reporting items for systematic review and meta-analysis protocols (PRISMA-P) 2015 statement. Syst Rev. 2015;4:1.
- Settembre N, Kauhanen P, Alback A, Spillerova K, Venermo M. Quality Control of the Foot Revascularization Using Indocyanine Green Fluorescence Imaging. World J Surg. 2017;41(7):1919-26.
- Igari K, Kudo T, Uchiyama H, Toyofuku T, Inoue Y. Indocyanine green angiography for the diagnosis
 of peripheral arterial disease with isolated infrapopliteal lesions. Ann Vasc Surg. 2014;28(6):1479-84.
- Nishizawa M, Igari K, Kudo T, Toyofuku T, Inoue Y, Uetake H. A Comparison of the Regional Circulation in the Feet between Dialysis and Non-Dialysis Patients using Indocyanine Green Angiography. Scand J Surg. 2016.
- 28. Kang Y, Lee J, Kwon K, Choi C. Dynamic fluorescence imaging of indocyanine green for reliable and sensitive diagnosis of peripheral vascular insufficiency. Microvasc Res. 2010;80(3):552-5.
- 29. Kang Y, Lee J, Kwon K, Choi C. Application of novel dynamic optical imaging for evaluation of peripheral tissue perfusion. Int J Cardiol. 2010;145(3):e99-101.

- 30. Terasaki H, Inoue Y, Sugano N, Jibiki M, Kudo T, Lepantalo M, et al. A quantitative method for evaluating local perfusion using indocyanine green fluorescence imaging. Ann Vasc Surg. 2013;27(8):1154-61.
- 31. Venermo M, Settembre N, Alback A, Vikatmaa P, Aho PS, Lepantalo M, et al. Pilot Assessment of the Repeatability of Indocyanine Green Fluorescence Imaging and Correlation with Traditional Foot Perfusion Assessments. Eur J Vasc Endovasc Surg. 2016;52(4):527-33.
- 32. Colvard B, Itoga NK, Hitchner E, Sun Q, Long B, Lee G, et al. SPY technology as an adjunctive measure for lower extremity perfusion. J Vasc Surg. 2016;64(1):195-201.
- 33. Rother U, Lang W, Horch RE, Ludolph I, Meyer A, Regus S. Microcirculation Evaluated by Intraoperative Fluorescence Angiography after Tibial Bypass Surgery. Ann Vasc Surg. 2017;40:190-7.
- 34. Riess HC, Dupree A, Behrendt CA, Kolbel T, Debus ES, Larena-Avellaneda A, et al. Initial experience with a new quantitative assessment tool for fluorescent imaging in peripheral artery disease. Vasa. 2017;46(5):383-8.
- Rother U, Lang W, Horch RE, Ludolph I, Meyer A, Gefeller O, et al. Pilot Assessment of the Angiosome Concept by Intra-operative Fluorescence Angiography After Tibial Bypass Surgery. Eur J Vasc Endovasc Surg. 2018;55(2):215-21.
- 36. Perry D, Bharara M, Armstrong DG, Mills J. Intraoperative fluorescence vascular angiography: during tibial bypass. J Diabetes Sci Technol. 2012;6(1):204-8.
- 37. Samies JH, Gehling M, Serena TE, Yaakov RA. Use of a fluorescence angiography system in assessment of lower extremity ulcers in patients with peripheral arterial disease: A review and a look forward. Semin Vasc Surg. 2015;28(3-4):190-4.
- 38. Zimmermann A, Roenneberg C, Wendorff H, Holzbach T, Giunta RE, Eckstein HH. Early postoperative detection of tissue necrosis in amputation stumps with indocyanine green fluorescence angiography. Vasc Endovascular Surg. 2010;44(4):269-73.
- 39. Yang AE, Hartranft CA, Reiss A, Holden CR. Improving Outcomes for Lower Extremity Amputations Using Intraoperative Fluorescent Angiography to Predict Flap Viability. Vasc Endovascular Surg. 2018;52(1):16-21.
- 40. Unno N, Suzuki M, Yamamoto N, Inuzuka K, Sagara D, Nishiyama M, et al. Indocyanine green fluorescence angiography for intraoperative assessment of blood flow: a feasibility study. Eur J Vasc Endovasc Surg. 2008;35(2):205-7.
- 41. Sumpio BE, Forsythe RO, Ziegler KR, van Baal JG, Lepantalo MJ, Hinchliffe RJ. Clinical implications of the angiosome model in peripheral vascular disease. J Vasc Surg. 2013;58(3):814-26.
- 42. Kang Y, Choi M, Lee J, Koh GY, Kwon K, Choi C. Quantitative analysis of peripheral tissue perfusion using spatiotemporal molecular dynamics. PLoS One. 2009;4(1):e4275.
- 43. Maxwell AK, Deleyiannis FW. Utility of Indocyanine Green Angiography in Arterial Selection during Free Flap Harvest in Patients with Severe Peripheral Vascular Disease. Plast Reconstr Surg Glob Open. 2016;4(10):e1097.
- 44. Aschwanden M, Partovi S, Jacobi B, Fergus N, Schulte AC, Robbin MR, et al. Assessing the endorgan in peripheral arterial occlusive disease-from contrast-enhanced ultrasound to blood-oxygen-level-dependent MR imaging. Cardiovasc Diagn Ther. 2014;4(2):165-72.

- 45. AV DS, Lin H, Henderson ER, Samkoe KS, Pogue BW. Review of fluorescence guided surgery systems: identification of key performance capabilities beyond indocyanine green imaging. J Biomed Opt. 2016;21(8):80901.
- 46. Vahrmeijer AL, Hutteman M, van der Vorst JR, van de Velde CJ, Frangioni JV. Image-guided cancer surgery using near-infrared fluorescence. Nat Rev Clin Oncol. 2013;10(9):507-18.



Chapter 3

Perfusion parameters in near-infrared fluorescence imaging with indocyanine green: a systematic review of the literature

P. van den Hoven ^{1*}, L.N. Goncalves ^{1*}, J. van Schaik ¹, L. Leeuwenburgh ¹, C.H.F. Hendricks ¹, P.S. Verduijn ¹, K.E.A. van der Bogt ¹, C.S.P. van Rijswijk ¹, A. Schepers ¹, A.L. Vahrmeijer ¹, J.F. Hamming ¹, J.R. van der Vorst ¹

- 1. Leiden University Medical Center, Leiden, The Netherlands
 - * Authors contributed equally and share first authorship

Abstract

Introduction

Near-infrared fluorescence imaging is a technique capable of assessing tissue perfusion and has been adopted in various fields including plastic surgery, vascular surgery, coronary arterial disease, and gastrointestinal surgery. While the usefulness of this technique has been broadly explored, there is a large variety in the calculation of perfusion parameters. In this systematic review, we aim to provide a detailed overview of current perfusion parameters, and determine the perfusion parameters with the most potential for application in near-infrared fluorescence imaging.

Methods

A comprehensive search of the literature was performed in Pubmed, Embase, Medline, and Cochrane Review. We included all clinical studies referencing near-infrared perfusion parameters.

Results

A total of 1511 articles were found, of which, 113 were suitable for review, with a final selection of 59 articles. Near-infrared fluorescence imaging parameters are heterogeneous in their correlation to perfusion. Time-related parameters appear superior to absolute intensity parameters in a clinical setting.

Conclusion

This literature review demonstrates the variety of parameters selected for the quantification of perfusion in near-infrared fluorescence imaging.

Introduction

Near-infrared fluorescence (NIRF) imaging is a promising technique for visualizing tissue perfusion. The measurement of fluorescence in the near-infrared spectrum is feasible for perfusion assessment due to the low tissue auto-fluorescence in this range. This allows for visualisation of an intravenously-administered fluorophore. The most frequently used fluorescent dye in perfusion assessment is indocyanine green (ICG), which is primarily contained in the vascular system due to its selective binding with the plasma protein albumin. NIRF imaging is minimally invasive, with low risk of sideeffects. The use of NIRF imaging as a technique to assess tissue perfusion has been explored in various surgical fields. In plastic surgery this technique has been used to assess perfusion in flap surgery, nipple-sparing mastectomies, and reconstructive microsurgery (1). NIRF imaging has been applied in endocrinological surgery, assisting in the preservation of critical structures, such as the parathyroid gland, during surgical procedures. For patients with peripheral arterial disease (PAD), NIRF imaging can be used for the assessment of regional tissue perfusion. Described applications of NIRF imaging in patients with PAD include (1) diagnosis, (2) the measuring of the effect of revascularization procedures, and (3) the assessment of tissue viability following amputation surgery (2). In cardiac interventions, the use of NIRF imaging has allowed for the real-time assessment of graft patency, with applications in transplantation surgery providing a diagnostic tool for the assessment of kidney microperfusion, for example (3). NIRF imaging has furthermore been applied in neurosurgery, quantifying cerebral perfusion both intra- and postoperatively. In gastro-intestinal surgery, NIRF imaging has been used to assess anastomotic perfusion after bowel resection (4).

To date the perfusion patterns visualized with fluorescence imaging have been quantified using time-intensity curves, from which various parameters can be extracted for statistical analysis. This article will systematically review the literature on the time-intensity curve parameters following NIRF imaging in perfusion assessment, with the aim of identifying optimal perfusion parameters for standardised quantification of perfusion using NIRF imaging.

Methods

Search Strategy

An electronic search was conducted using Pubmed, Medline, Embase and Cochrane Review from inception to January 2021 to identify all relevant literature. Medical Subject Headings (MeSH) were adopted and included: "perfusion", "near-infrared fluorescence imaging", and "indocyanine green". The search strategies applied can

be found in Appendix A. A manual search of references of included articles was also performed to identify further studies of interest. Articles were systematically screened with a two-stage method, with stage one including screening of the title and abstract, followed by stage two with full-text screening. The systematic review of the literature and results conducted in this article are not part of a registered study.

Article selection

Only full-text articles in English were included. Articles reporting the use of fluorescence imaging in animal studies were excluded. Article selection was performed by two independent researchers (L.G. and P.H.). Any article discussing the analysis of tissue perfusion using near-infrared fluorescence imaging was included if fluorescence—intensity curves and perfusion parameters were mentioned. Articles reporting the qualitative use of NIRF imaging without quantitative data were excluded. NIRF perfusion imaging has been applied in numerous surgical fields. The results obtained are therefore divided by subspecialization, which included gastrointestinal, neurological, vascular, transplantation, and plastic surgery, as well as other surgical subspecializations.

Quality assessment. The quality and the risk of bias of the selected and included articles were independently evaluated by two reviewers (L.G. and P.H.) according to the revised Quality Assessment of Diagnostic Accuracy Studies (5). In instances of discrepancy in interpretation, a third independent reviewer (JV) was asked to adjudicate.

Data extraction. Data extracted from all articles reviewed for inclusion consisted of relevant patient characteristics, type of NIRF imaging camera, the ICG concentration, and the perfusion parameters selected.

Results

An overview of the article selection process for this systematic review is reported in a flow diagram in Figure 1, according to the Preferred Reporting Items for Systematic review and meta-analysis Protocols 2015 guidelines. A total of 1511 articles were found based on the search terms in Appendix A, of which 113 were suitable for review, with a final selection of 57 articles. Manual review of the references in the above selected articles lead to the inclusion of 2 further references, providing a total of 59 articles for final inclusion. The results of the quality assessment can be found in the Appendices B and C. The 59 studies selected included a total of 2336 patients. The number of patients in the studies ranged from 1 to 181. All studies in this review used ICG as a fluorescence marker. The selected studies were divided into the following fields: vascular surgery (n=18), gastrointestinal surgery (n=8), plastic surgery (n=15), neurosurgery (n=14), and

transplantation surgery (n=2). Furthermore, 1 diabetes mellitus study, 1 thyroid surgery study, and 1 study regarding the imaging of breast lesions were also included. All studies were published during the period from 2008 to 2021. An overview of the perfusion parameters mentioned in the literature is reported in Table 1.

A large selection of NIRF imaging systems were used, the most common were the SPY- Elite system (n=12), Flow 800 (n=13), and the Photodynamic eye imaging system (n=13). The reviewed articles mentioned a total of 26 perfusion parameters distilled from fluorescence-intensity curves. All of the reviewed articles selected a unique combination of the perfusion parameters mentioned in Table 1 and schematically shown in Figure 2 and 3.

NIRF-imaging was performed either pre- and post-operatively, or intraoperatively. Time- dependent parameters are described in all the included literature. Perfusion parameters are based on:

- Absolute fluorescence intensity
- Time
- Changes in intensity over time

Absolute intensity parameters

Multiple studies describe significant changes in intensity-related parameters. The maximum fluorescence intensity (Imax) is the most frequently mentioned parameter (n=29). Fluorescence intensity parameters also include ingress, egress, fluorescence intensity as a range in arbitrary units, and the fluorescence intensity at the end of the measurement period or study, as described in Table 1.

Inflow and outflow parameters

Inflow parameters could be calculated from the upslope segment of the time-intensity curve and could be correlated with tissue perfusion. These include time-specific parameters such as the Tmax, T1/2, time to peak intensity, and rise time (Figures 2 and 3). Once ICG has been intravenously administered an initial fluorescence signal can be detected (Tstart). Following detection of fluorescence intensity, the time taken to reach 50% of the maximum intensity (T1/2max) and the peak intensity (Tmax) could be calculated. Furthermore, during the upslope, the interaction between fluorescence intensity and time was also broadly explored, and includes the ingress rate, or the blood flow index, which are all ratios or rates of increase of fluorescence signal over time.

Outflow parameters are calculated to quantify the decrease in ICG intensity over time, thus providing information on vascular elimination. Time specific outflow parameters include the intrinsic transit time (ITT); the time needed for ICG to circulate from the arterial to the venous system. The downslope interaction between intensity and time was

quantified by the egress rate and IR 60, which is the intensity at 60 s after Tmax/ Fmax, for example.

Relative parameters

Relative parameters were also calculated by selecting and comparing two or more regions of interest, for example, a region with suspected ischemia being compared with another region with optimal perfusion, the reference region. The relative parameters were calculated by dividing the targeted perfusion value by the reference value.

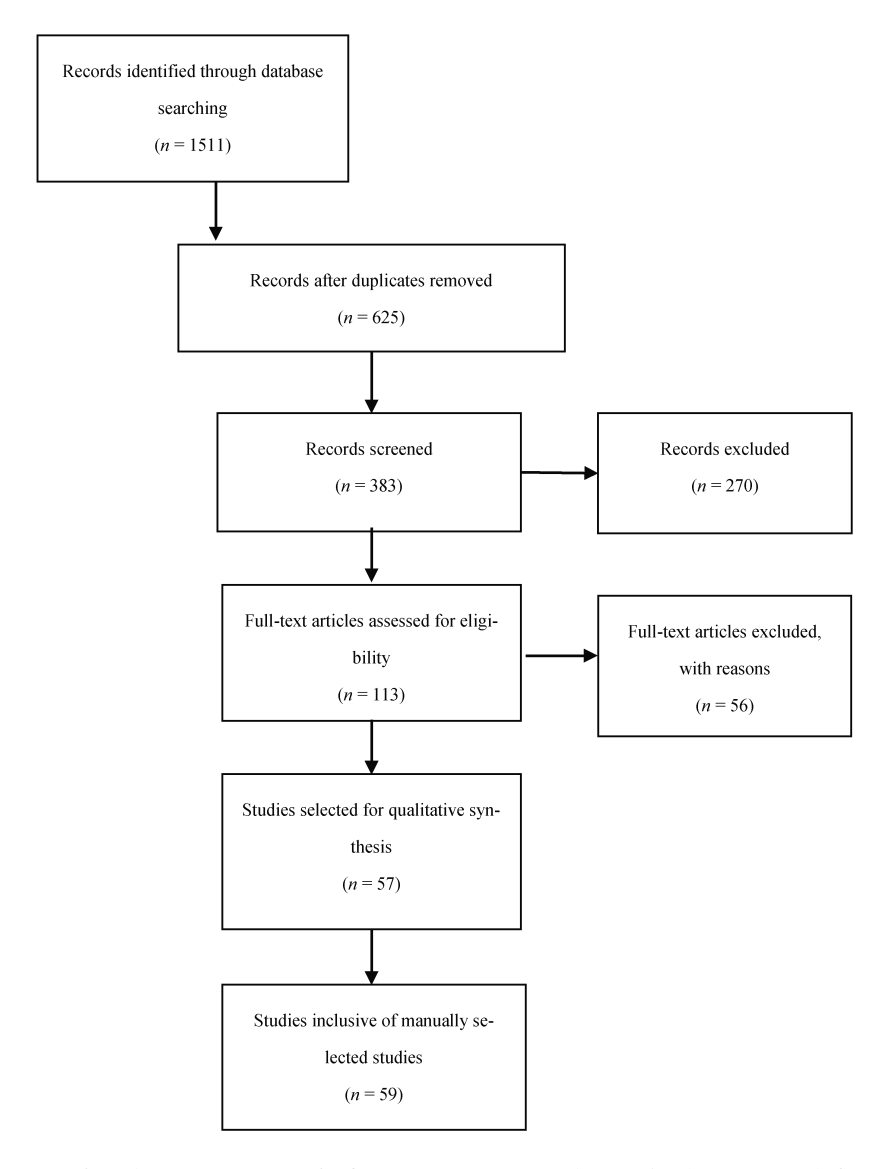


Figure 1. Preferred Reporting Items for Systematic Review and Meta-Analysis Protocols flow chart for selection of included studies.

Table 1. Overview of fluorescence perfusion parameters.

| Parameter | Definition | Equivalent | References |
|-------------------------|---|---|-------------------------------------|
| Ingress | Absolute difference between baseline | | (6-17) |
| | fluorescence and its maximum value | | |
| Ingress Rate | Rate of increase of fluorescence signal from | Wash-in rate, fluorescence | (8-19) |
| | baseline to maximum value | signal rise, blush rate | |
| Ingress AUC | Area Under the Curve from baseline to | WiAUC | (19) |
| | maximum fluorescence intensity | | |
| Egress | Absolute difference between maximum intensity | Washout | (6-9, 11, 14, 17, 18, |
| | and the final intensity | | 20) |
| Egress Rate | Rate of decrease of fluorescence signal from | | (8, 9, 11, 14, 17) |
| | maximum value to the final intensity value | | / · · |
| Fluorescence | Fluorescence intensity | | (8, 21-25) |
| ntensity | M : 0 : : | r ninc: | ((7 2/ 50) |
| max | Maximum fluorescence intensity | Fmax, Peak Perfusion, FImax, MFI, Cerebral blood volume | (6, 7, 24-50) |
| and Intensity | Eluoroscance intensity at the and of the study | | (9 33 51) |
| End Intensity Γstart | Fluorescence intensity at the end of the study Time to initial fluorescence signal | QEnd, residual FI Tl (time local), latent | (8, 33, 51) (19, 28, 43, 46, 52- |
| ı ətart | Time to initial indorescence signal | time, T0, Te, TAP | 55) |
| Гтах | Time to maximum intensity | TTP (time to peak), | (19, 20, 25-31, 33-43, |
| | 2 mile to maximum intensity | blush time | 46, 47, 49, 53, 56, 57) |
| Delta T | Time from Initial fluorescent intensity to Imax | Tmax | (26, 55) |
| Γ 1/2 | Time to half of the maximum fluorescence | Tmax1/2, delay | (25, 27-30, 32-34, 36, |
| | intensity | ,, | 38, 39, 41, 47, 48, |
| | , | | 58-60) |
| ΓR | Time ratio (T1/2 / Tmax) | | (25) |
| | | | |
| Rise Time | Time from (10-90%) OR (20-80%) of | | (19, 33-35, 41, 45, |
| | maximum fluorescence intensity | | 48, 61) |
| | OR Time from 20-80% of maximum | | |
| T. 10.00/ | fluorescence intensity | | (22, 22) |
| Γd90% | Time from Fmax to 90% of the Fmax | | (30, 39) |
| Γ d 75% | Time from the Fmax to 75% of the Fmax | | (30) |
| R 60 sec | The rate of intensity measured 60 seconds after | | (30) |
| 100 300 | the Tmax to the Fmax (Intensity at 60 sec after | | (50) |
| | Tmax/ Fmax) | | |
| Wash-in | Ratio between the WiAUC to the Rise Time | | (19) |
| erfusion index | | | (· <i>)</i> |
| Slope | Fmax/Tmax | BFI (blood flow index), | (25, 28, 29, 34, 37, |
| • | | Perfusion rate, Smax, | 40, 41, 43, 44, 46, 47, |
| | | Cerebral blood flow, | 49-52, 56, 57) |
| | | Perfusion Index | |
| BFI | Blood flow Index (Fmax/RT) | Slope | (23, 33, 35, 41, 45, |
| | OR (F90-F10)/(T90-T10) | | 48, 58, 59, 62) |
| S 1/2 | Slope of the intensity increase from baseline to | | (37) |
| | half the maximum intensity | | |
| PDE10 | The fluorescence intensity increase at 10 seconds | SPY10 | (29, 37, 44, 60) |
| TT | Intrinsic transit time – the time needed for | Transit time | (23, 27, 41, 45, 48, |
| | the fluorescent dye to circulate from arterial to | | 61) |
| | venous anastomosis | | 4-2 |
| AUC | Area Under the curve of intensity over time | Curve Integral | (8) |
| Perfusion rate | Fraction of blood exchanged per min in vascular volume (%/min) | | (20) |
| Relative | Perfusion as a percentage of a reference region | | (6, 7, 24, 50-53, 57) |
| perfusion | | | |

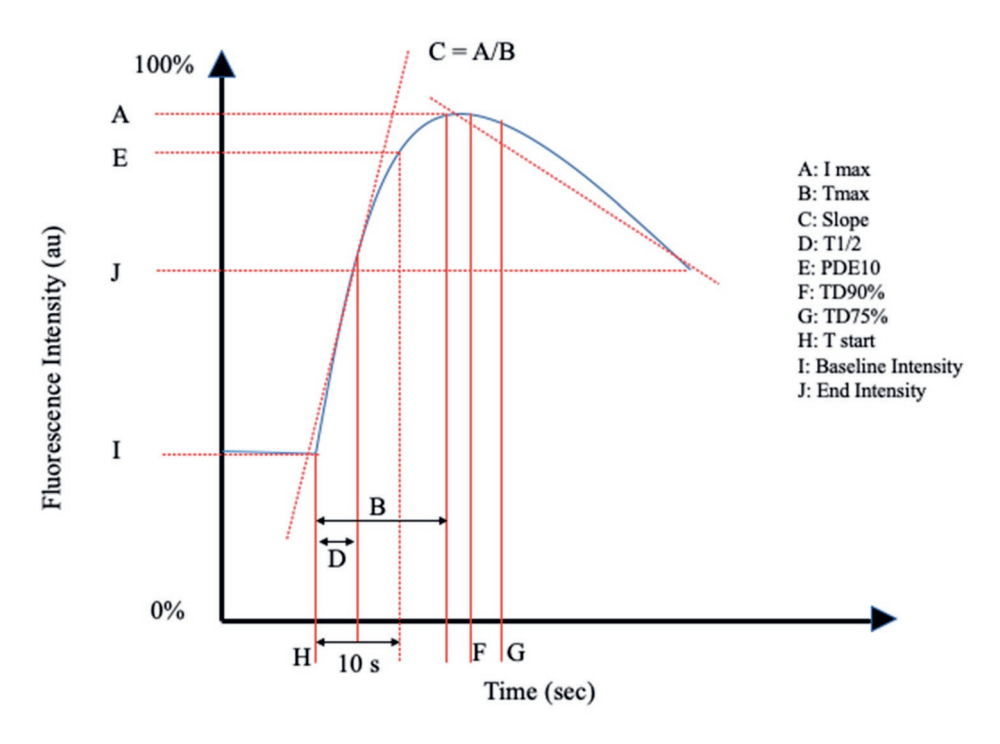


Figure 2. Schematic representation I of the perfusion parameters in Table 1.

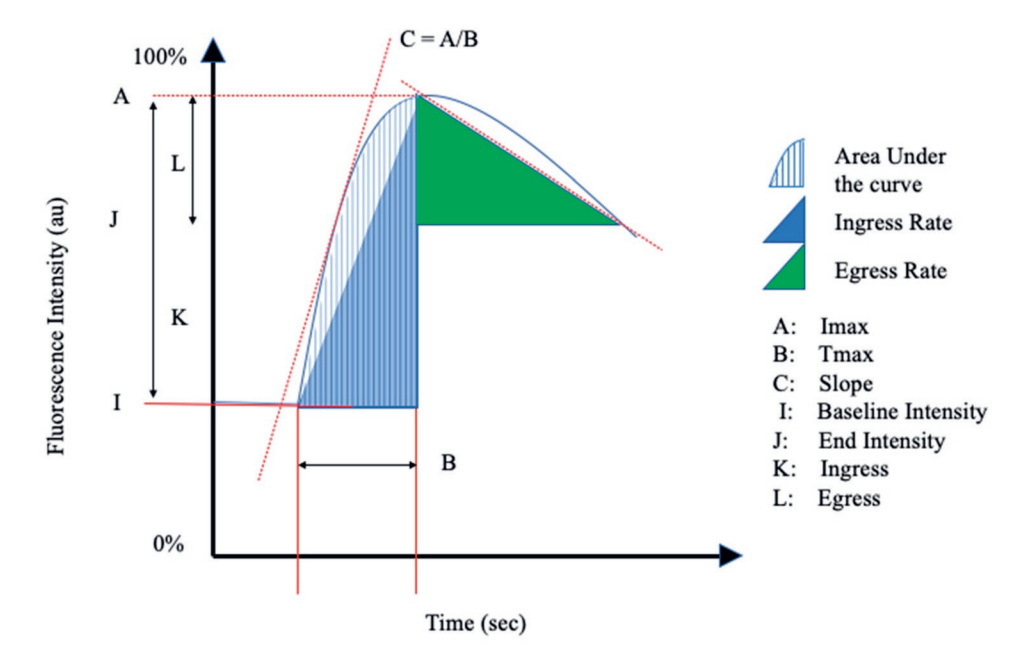


Figure 3. Schematic Representation II of the perfusion parameters in Table 1.

Gastro-intestinal Surgery

The surgical procedures discussed in this review include colorectal surgery (n=6), specifically resections followed by anastomosis, and esophagectomy (n=2). Two of the six studies on colorectal surgery performed retrospective analysis of prospective data (32, 54). Four of the eight studies on gastro-intestinal surgery included in this review administered a weight-dependent dose of ICG, as noted in Table 2 (25, 26, 54, 56).

The Fmax was researched in 6 studies (n=335) (25, 26, 28, 31, 32, 47). Four studies described no significant difference in Fmax values between groups with and without anastomotic leakage in both colorectal and oesophageal surgery (25, 26, 28, 32). Wada et al. (n=112) highlight the predictive value of Fmax for anastomotic leakage in receiver operator curve (ROC) analysis, with a sensitivity and specificity of 100% and 92% respectively at a cut-off of 52.0 units (47). The Fmax did not significantly predict early or late flatus or defecation. A study by Ishige et al. examined the application of ICG-NIRF imaging in quantifying perfusion of the gastric conduit in esophagectomy (31). A relative comparison of Fmax in a control phase, gastric tube phase, and anastomotic phase prior to intrathoracic or cervical esophago-gastronomy, was calculated and shown to be significantly different between phases, although no anastomotic leakage occurred.

Fmin was a parameter selected by Son et al. (n=86), and was described as the fluorescence intensity at the baseline (25). There was no significant difference between groups with and without anastomotic leakage.

Five studies included the Tmax as a perfusion parameter (n=245) (26, 28, 31, 47, 56). D'Urso et al. highlighted a statistically significant lengthened Tmax in both proximal and distal colorectal resection sites in the complications group in comparison to the uncomplicated cases (p=0.01) (56). Furthermore, correlation to clinical parameters such as intestinal lactate and mitochondrial efficiency showed varying significance depending on region and parameter selected (56). Amagai et al. described a significant correlation between the Tmax and anastomotic leakage in one of four selected regions of interest (p=0.015), while Hayami et al. mention no significant correlation to anastomotic leakage (26, 28). The predictive value of the Tmax in clinical outcomes such as early or late flatus or defecation is significant in 1 study (n=112) (p=0.02, p=0.01 respectively) (47). Son et al. and Amagai et al. described the Tmax as the difference between initial fluorescence intensity and maximum fluorescence intensity.(25, 26) Both studies highlighted a statistically significant difference in Tmax values between anastomotic leakage groups (Son p<0.001, Amagai p=0.015).

The inflow parameter T0, time to initial fluorescence signal, was studied by Aiba et al. and

Hayami et al. (28, 54). Both of the aforementioned studies showed T0 to significantly differ with regards to anastomotic leakage (Aiba p=0.046, Hayami, p=0.0022).

The TR, time ratio, is a parameter encompassing the ratio between T1/2 and Tmax and is shown to significantly differ between anastomotic leakage and no anastomotic leakage groups (n=86) (25). Furthermore, a ROC analysis with an area under the curve higher than 0.9 suggests that a TR of 0.6 is significantly predictive of anastomotic leakage (25).

T1/2 was adopted as an inflow parameter by 4 studies (n=246) (25, 28, 32, 47). Two studies by Kamiya et al. and Son et al. described a statistically significant difference in T1/2 in anastomotic failure or leakage groups (p<0.01, p<0.001 respectively) (25, 32). One study showed no significant difference between groups with and without anastomotic leakage (28).

The slope was investigated in two studies (n=134) (28, 47). No significant intraoperative difference or prediction of postoperative outcomes was described.

Neurosurgery

Fourteen studies (n=345) investigated the application of ICG angiography in vascular neurosurgery (27, 33-35, 41, 45, 48, 49, 58, 59, 61-64). Eight of the fourteen studies selected for dose-dependent ICG administration, with doses ranging from 0.1mg/kg to 0.3mg/kg, see Table 2 for further details. The studies analyzed the following inflow parameters: Tmax, T1/2, RT, slope, transit time and cerebral blood flow index. The rise time is heterogeneously defined as the interval between 10% and 90% of the signal, or 20% and 80% of the signal.

The Tmax parameter was examined in seven studies (n= 191) (27, 33-35, 41, 49, 63). One study found the Tmax to significantly discriminate between patients with impaired and normal cerebral perfusion in occlusive cerebral arterial disease and control groups (p=0.013).(35) Furthermore, the ratio of Tmax pre- and post-bypass procedure was significantly lower in patients with postoperative hyperperfusion syndrome than in patients without postoperative hyperperfusion syndrome (p=0.017) (35).

The T1/2 was explored in four articles (n=181) (27, 48, 58, 59). Three studies researched the application of this perfusion parameter in patients pre- and post-bypass surgery, with only one study by Prinz et al. reporting a significant decrease (p=0.001) (27, 58, 59). However, when Prinz et al. compared the ICG perfusion data to quantitative Doppler flow, there were no significant correlations between the diagnostic methods.

Four articles (n=44) selected rise time (RT) as an ICG perfusion parameter (33, 35, 45, 61). Holling et al. found RT to be significantly shorter following a bypass procedure (p=0.025), with no change between pre- and post-bypass data in control measurements (p=0.125) (61). A study by Kamp et al. exploring cortical perfusion following traumatic brain injury found the arterial RT to be significantly longer in in patients with a favourable outcome at 3 months (p=0.002).

Of the four studies (n=153) that calculated transit time as a perfusion parameter, two studies by Holling et al. and Ye et al described significant results (27, 41, 48, 61). Ye et al. highlighted a significant difference in arteriovenous transit time in a heterogenous group of patients including arteriovenous malformations, Moyamoya disease and both unruptured and ruptured cerebral aneurysms (48).

Cerebral blood flow (CBF), or slope, was the most commonly selected neurovascular perfusion parameter, mentioned in ten articles (n=246) (35, 41, 58, 63, 64). 7 studies examined the change in cerebral blood flow pre- and post-bypass procedure (35, 41, 49, 58, 59, 63, 64). A statistically significant change in CBF was noted in five of the aforementioned seven studies (35, 41, 58, 63, 64). Four studies also examined the relationship between the development of postoperative hyperperfusion and CBF, with two studies by Zhang et al. and Uchino et al. describing a significant increase in CBF in the symptomatic hyperperfusion group (p<0.001, p=0.013 respectively) (35, 49, 63, 64).

One study by Kamp et al. describes the parameter residual fluorescence intensity, as a percentage of maximum fluorescence intensity, in patients with traumatic brain injury (33). The cortical and venous residual fluorescence intensity was significantly higher in cortical and venous tissue (p=0.01, p=0.02 respectively) in patients with an unfavourable outcome. No significant difference was noted in arterial residual fluorescence intensity (p=0.05).

Absolute fluorescence intensities were calculated in nine studies (27, 33-35, 41, 45, 48, 49, 63). Five studies found a significantly different Imax value between perfusion groups (35, 45, 48, 49, 63). Kobayashi et al. noted a significant increase in Imax after STA-MCA bypass surgery (p=0.047), yet no significant difference in Imax values when comparing patients with and without postoperative hyperperfusion (35). However, Zhang et al. also investigated Imax as a perfusion parameter in the detection of postoperative hyperperfusion and described a significantly higher Imax in the symptomatic hyperperfusion group (p<0.001) (49).

Plastic Surgery

Fluorescent imaging was quantitatively reported in fifteen articles, including 515 patients (6, 7, 10, 13, 17, 19, 22, 23, 36, 37, 46, 51-53, 57). The fields of application include free-flap and DIEP flap perfusion, breast reconstruction surgery, and microvascular surgery. The SPY Elite Imaging system was most commonly selected (n= 8), see Table 2.

Flap perfusion

Flap perfusion studies examined free flap surgery, flap perfusion in maxillofacial surgery, and DIEP flap procedures. Relative perfusion was researched in three studies (6, 7, 52). Abdelwahab et al. showed the flap-to-cheek ratio to be statistically significant in predicting flap vascularisation, while Betz et al. highlight no significant difference in relative slope values in free flap surgery (6, 7, 52).

Inflow and outflow parameters were mentioned in seven (n=128) free-flap and DIEP flap studies (10, 13, 23, 36, 37, 52, 53). Two studies described no significant differences in the ingress and ingress rate (10, 13). Significant differences in inflow parameters including the slope, Tmax, PDE10, slope at T1/2, and T1/2 were seen in three studies (23, 37, 53). Hitier et al. described a significantly lower per-operative Fmax in flaps with vascular complications (p=0.008) (23). Furthermore, in flaps with a significantly lower postoperative slope (p=0.02) and Fmax (p=0.03) values returned to normal following surgical revision (23). One study examining single-pedicle versus bipedicle blood supply in flap reconstruction found no significant difference in the Imax between the aforementioned groups, with a significant difference in the Tmax, T1/2, slope, PDE10, and slope at T1/2 between the same groups (p<0.05) (37). Absolute intensity parameters were not significant in studies by Betz et al. and Miyazaki et al. (37, 53).

Breast Reconstructive surgery

Gorai et al. explored the use of relative ICG perfusion parameters in the prediction of skin necrosis following tissue expander reconstruction in breast cancer patients (57). The application of ICG imaging lead to a significant lower rate of necrosis (p<0.05), with a statistically significant difference in relative perfusion (p<0.001). Yang et al. evaluated mastectomy flap perfusion at various tissue expander volumes, with significant differences in the ingress and egress between different expander volume groups (p=0.0001, p=0.0037 respectively) (17).

Microvascular Surgery

Reconstructive surgical procedures are dependent on adequate vascular and nervous supply to the operated region. Tanaka et al. explored the use of ICG imaging to detect blood supply to the femoral cutaneous- and vastus lateralis motor nerve, allowing for the

selection of the better vascularised nerve (46). The selected inflow parameters slope and Tstart, were heterogenous statistically significant, while the Tmax showed no statistical significance in any region measured (46). Fichter et al. examined the effect of the number of osteotomies on bone perfusion in free fibula flaps (19). The study found a significant differences in the slope with additional osteotomies (p=0.034). Mothes et al. explored tissue perfusion during hand revascularisation surgery, and found intraoperative slope values to significantly differ in tissue that survived postoperatively (p<0.01) (51). Three studies (n=75) researched absolute fluorescent intensity, namely the Imax, reporting heterogenous results depending on time points or regions selected for comparison (22, 46, 51).

Vascular Surgery

Quantitative analysis of fluorescence imaging was conducted in 18 studies included in this review (n=683) (8, 11, 12, 15, 16, 18, 20, 29, 30, 38-40, 43, 44, 50, 55, 60, 65). Fifteen studies opted for dose-dependent ICG administration, with 10 studies selecting a dose of 0.1mg/kg (8, 11, 12, 15, 16, 18, 20, 29, 30, 38-40, 43, 44, 50, 55, 60, 65). SPY Elite Imaging was the fluorescence imaging system of choice in eight studies, see Table 2. The fields of application within vascular surgery include patients with PAD, patients receiving dialysis, prediction of wound healing, microperfusion following arteriovenous fistula formation in dialysis patients, and perfusion in Raynaud's phenomenon.

The Fmax was the most frequently selected parameter (7 studies; n=297) (18, 29, 30, 38-40, 50). Four studies described a significant difference in the Fmax pre- and post-revascularisation, with Nakamura et al. mentioning no significant difference in the treated limb and a significant decrease in the contralateral limb (p=0.0875, p=0.006 respectively) (18, 29, 38, 40). No significant difference in Fmax was detected between PAD patients and controls; dialysis patients and controls, Rutherford Classification categories; or critical limb ischemia patients and controls (30, 39, 50).

Six studies selected the ingress and ingress rate as a perfusion parameter (n=237) (8, 12, 15, 16, 18, 40). Five studies evaluated the Ingress in PAD patients, all describing statistically significant results pre- and post-revascularisation (8, 15, 16, 18, 40). Regus et al. highlighted a statistically significant difference in the Ingress and Ingress rate pre- and post-arteriovenous anastomotic creation in the hand and fingers of dialysis patients (p<0.001) (12). Furthermore, there was a significant difference in the intraoperative Ingress ratio and Ingress rate ratio in patients who developed hemodialysis access-induced distal ischemia (p=0.001, p=0.003 respectively) (12).

The egress and egress rate provided heterogenous results in PAD patients undergoing revascularisation procedures in two studies (8, 18). One study by Braun et al shows a significant difference in both the Egress and Egress rate pre- and post-revascularisation (p=0.004, p=0.013 respectively), while there is no significant difference in the Egress in a study by Colvard et al. (p=0.35) (8, 18).

The perfusion parameter Tmax was discussed in six studies (n=204) (29, 30, 38, 39, 55). Heterogenous results were seen in PAD patients pre- and post-revascularisation. Igari et al. described a significant difference in the Tmax in 3 regions of interest following revascularisation (29). A study by Nakamura et al. also found the Tmax to be significantly different post-revascularisation, in both the intervention limb and the contralateral limb (p=0.016, p=0.013 respectively) (38). Only one study examined the Tmax in PAD and control patients, with a significant difference between the groups (p<0.05) (30).

Six studies selected the T1/2 as a perfusion parameter (29, 30, 38, 39, 60, 65). One study by Venermo et al. showed no significant different in T1/2 between patients with and without diabetes (65). Igari et al. state no significant difference between PAD patients and controls (30). Two studies describe significant changes in the T1/2 in PAD patients pre- and post-revascularisation (29, 38).

Studies exploring the T1/2 in patients with diabetes, on dialysis and grouped according to Fontaine Classification or critical limb ischemia showed heterogenous results (39, 60, 65).

Two studies (n=51) examined the slope (29, 50). One study showed a significant change in the slope in three selected regions of interest following revascularisation in PAD patients (n=21) (29). A study by Zimmermann et al. described a significant difference in the slope in patients grouped according to the Rutherford classification; with increased extent of arterial collateralisation; and in patients with critical limb ischemia (p<0.001, p=0.005, p<0.001) (50).

The PDE10, described as the fluorescence intensity increase at 10 seconds, was examined in four studies (29, 44, 60, 65). Two studies state a statistically significant change in the PDE10 in PAD patients following a revascularisation procedure (29, 44). An ROC analysis was performed in two studies, with a cut-off PDE10 of 28 s at a transcutaneous pressure (TcPO2) of 30mmHg in a study by Terasaki et al., and a cut-off PDE10 of 21 arbitrary units at a TcPO2 of 40mmHg in a study by Venermo et al. (60, 65).

Eleven of the eighteen vascular surgery studies included in this review assessed the correlation between the aforementioned perfusion parameters and standard diagnostic

methods in this field such as the ankle-brachial index (ABI), toe pressure, TcPO2 and the toe brachial index (TBI) (8, 11, 18, 29, 30, 38, 40, 43, 44, 50, 65). Four studies found no significant correlation between ABI and ICG-NIRF perfusion parameters (11, 38, 40, 44). Significant but heterogenous correlation is seen between the ABI and a range of parameters in five studies (8, 18, 29, 30, 65).

Transplantation

Two studies (n=205) explored the application of quantitative ICG imaging in transplantation surgery (9, 14). Both studies utilised the SPY Elite Imaging System and an ICG dose of 0.02mg/kg. Inflow parameters ingress, ingress rate, egress and egress rate were assessed. Rother et al. and Gerken et al. describe the ingress and ingress rate to significantly detect differences in kidney perfusion. Gerken et al. explores the association of intraoperative ICG angiography with delayed graft function, describing a cut off ingress value of 106.23AU for the prediction of delayed graft function with a sensitivity of 78.3% and specificity of 80.8% (p<0.0001) (9). No further mention of data related to the egress or egress rate are noted by Rother et al. (14).

Other

Diabetic Wound healing

Hajhosseini et al. researched the application of ICG angiography in the prediction of diabetic wound healing following hyperbaric oxygen therapy in cases and controls (21). Absolute fluorescence intensity was selected as perfusion parameter, showing a significant improvement between pre- and post-hyperbaric oxygen therapy in the patient group (p<0.0015).

Total thyroidectomy

Parathyroid function and perfusion was intraoperatively measured by ICG angiography, assessing if the diagnostic could predict postoperative hypocalcaemia (24). Relative perfusion parameters based on absolute fluorescent intensity and average fluorescence intensity were selected, with the anterior trachea as reference region. Relative absolute fluorescence intensity was predictive of both postoperative hypocalcaemia (p=0.027), and a postoperative drop in parathyroid hormone (p<0.001). Relative average fluorescence intensity provided no significant results.

Breast imaging

Schneider et al evaluated ICG imaging in the detection and characterisation of breast

lesions, namely malignant and benign (42). Inflow parameters peak amplitude (Imax) and time to peak (Tmax) were selected. A peak time-grouped amplitude was calculated, an average of amplitudes in malignant and benign lesions at 30 time-points. A significant difference in peak amplitude was noted between the two groups (p=0.00015).

Table 2. Overview of study characteristics and results of near-infrared fluorescence imaging.

| Application | Reference | Study Ch | aracteristics | | |
|-------------------|---------------|----------|--------------------------------------|------------------------|-----------|
| • | | Patients | Camera | Software | ICG dose |
| Gastro-intestinal | Aiba(54) | 110 | OPAL1 | Not spec | 0.1mg/kg |
| Surgery | Amagai(26) | 69 | Karl Storz | ImageJ | 0.2mg/kg |
| | D'Urso(56) | 22 | D-Light P | FLER | 0.2mg/kg |
| | Hayami(28) | 22 | D-Light P | Hamamatsu Photonics | 5mg/2ml |
| | Ishige(31) | 20 | Olympus | Hamamatsu Photonics | 1.25mg |
| | Kamiya(32) | 26 | PDE Hamamatsu | Hamamatsu Photonics | 1ml |
| | Son(25) | 86 | Image1 | Tracker 4.97 | 0.25mg.kg |
| | Wada(47) | 112 | PDE Hamamatsu | Hamamatsu Photonics | 5mg |
| Neurosurgery | Goertz(27) | 54 | Carl Zeiss Co. | Flow 800 | 10mg |
| | Holling(61) | 5 | OPMI Pentero Microscope | Flow 800 | 5mg |
| | Kamp(33) | 10 | OPMI Pentero Microscope | Flow 800 | 5mg |
| | Kamp(34) | 30 | OPMI Pentero Microscope | Flow 800 | 5mg |
| | Kobayashi(35) | 10 | OPMI Pentero Microscope | Flow 800 | 7.5mg/3m |
| | Prinz(58) | 30 | OPMI Pentero Microscope | Flow 800 | 0.25mg/kg |
| | Rennert(41) | 7 | OPMI Pentero Microscope | Flow 800 | 0.2mg/kg |
| | Rennert(59) | 10 | OPMI Pentero Microscope Or Kinevo | Flow 800 | 0.2mg/kg |
| | Shi(45) | 9 | OPMI Pentero Microscope | Flow 800 | 0.1mg/kg |
| | Uchino(64) | 10 | OPMI Pentero Microscope | Flow 800 | 0.1mg/kg |
| | Uchino(63) | 7 | OPMI Pentero Microscope | Flow 800 | 0.1mg/kg |
| | Woitzik(62) | 6 | IC-View | IC Calc | 0.3mg/kg |
| | Ye(48) | 87 | Carl Zeiss Co. | Flow 800 | 0.25mg/kg |
| | Zhang(49) | 60 | Not spec | Flow 800 | Not spec |
| Plastic Surgery | Abdelwahab(6) | 71 | SPY Elite Imaging System | SPY-Q | 5mg/2ml |
| | Abdelwahab(7) | 10 | SPY Elite Imaging System | SPY-Q | 5mg/2ml |
| | Betz(52) | 11 | Karl Storz | IC Calc | 0.3mg/kg |
| | Betz(53) | 25 | ICG Pulsion | IC Calc | 0.3mg/kg |
| | Fichter(19) | 40 | Pulsion PDE | ImageJ | 0.3mg/kg |
| | Girard(10) | 40 | SPY Elite Imaging System | SPY-Q | 5mg |
| | Gorai(57) | 181 | PDE Hamamatsu | Hamamatsu Photonics | 25mg/2ml |
| | Han(22) | 32 | SPY Elite Imaging System | Not spec | 2.5mg |
| | Hitier(23) | 20 | Fluobeam | Fluobeam | 0.25mg/kg |
| | Maxwell(36) | 1 | SPY Elite Imaging System | Not spec | Not spec |
| | Miyazaki(37) | 8 | PDE Hamamatsu | Hamamatsu Photonics | 0.1mg.kg |
| | Mothes(51) | 35 | IC-View | IC Calc | 0.5mg/kg |
| | Rother(13) | 23 | SPY Elite Imaging System | SPY-Q | 0.1mg/kg |
| | Tanaka(46) | 8 | PDE Hamamatsu | Hamamatsu Photonics | 0.1mg/kg |

| | Yang(17) | 10 | SPY Elite Imaging System | SPY-Q | 3ml |
|-----------------|-----------------|-----|---------------------------------|------------------------|------------|
| Vascular | Braun(8) | 24 | SPY Elite Imaging System | Not spec | Not spec |
| | Colvard(18) | 93 | SPY Elite Imaging System | SPY-Q | 2.5ml |
| | Igari(29) | 21 | PDE Hamamtsu | Hamamatsu Photonics | 0.1mg/kg |
| | Igari(30) | 23 | PDE Hamamtsu | Hamamatsu Photonics | 0.1mg/kg |
| | Kang(55) | 2 | Vieworks | Visual C++ | 0.16mg/kg |
| | Kang(20) | 2 | VIeworks | Not spec | 0.16mg/kg |
| | Mironov(11) | 28 | SPY Elite Imaging System | SPY-Q | 5mg/250ml |
| | Nakamura(38) | 21 | PDE Hamamatsu | Hamamatsu Photonics | 0.1mg/kg |
| | Nishizawa(39) | 62 | PDE Hamamatsu | Hamamatsu Photonics | 0.1mg/kg |
| | Patel(40) | 47 | SPY Elite Imaging System | Not spec | 0.1mg/kg |
| | Regus(12) | 47 | SPY Elite Imaging System | SPY-Q | 0.002mg/kg |
| | Rother(15) | 40 | SPY Elite Imaging System | SPY-Q | 0.1mg/kg |
| | Rother(16) | 33 | SPY Elite Imaging System | SPY-Q | 0.1mg/kg |
| | Seinturier(43) | 34 | Fluobeam | Not spec | 0.05mg/kg |
| | Settembre(44) | 101 | SPY Elite Imaging System | Not spec | 0.1mg/kg |
| | Terasaki(60) | 34 | PDE Hamamatsu | Hamamatsu Photonics | 0.1mg/kg |
| | Venermo(65) | 41 | PDE Hamamatsu | Hamamatsu Photonics | 0.1mg/kg |
| | Zimmermann(50) | 30 | IC-View | IC-Calc | 0.5mg/kg |
| Transplantation | Rother(14) | 77 | SPY Elite Imaging System | SPY-Q | 0.02mg/kg |
| | Gerken(9) | 128 | SPY Elite Imaging System | SPY-Q | 0.02mg/kg |
| Thyroid Surgery | Lang(24) | 70 | SPY Elite Imaging System | Not spec | 2.5mg |
| Diabetic Foot | Hajhosseini(21) | 21 | LUNA Fluorescence Microscope | SAS | 5mg/ml |
| Breast lesions | Schneider(42) | 30 | NIRx Medical Technologies | NIRx NAVI | 2.5mg |

Discussion

This review highlights the broad selection of perfusion parameters in NIRF imaging. NIRF-imaging shows great potential as a surgical tool with applications in gastro-intestinal, plastic, vascular and neurosurgery. However, the quantification of NIRF-imaging and selection of optimal perfusion parameters faces several challenges. The studies included in this review were largely performed in a small cohort setting, randomised clinical studies have yet to be performed. Research in this field to date is heterogeneous in study design, methodology, selected perfusion parameters and endpoints. The heterogeneity in perfusion parameters selected and the large variation in significance of outcomes in the articles presented in this review highlight the need for procedure-specific parameters and protocols to allow for clinical application of this technique. Before the application of quantitative perfusion analysis in a clinical setting, comparison of perfusion parameters in cases and controls is advised for baseline values. While intensity dependent parameters are frequently discussed, they are susceptible to

intra- and interpatient variability. Intensity dependent parameters can vary with changes in the imaging setting such as light intensity or camera angulation or distance from the patient. Statistical significance is often in a relative pre- and post-intervention setting, with no correlation to standard perfusion techniques such as the ankle–brachial index. Time-related parameters such as the Tmax or T1/2max are commonly mentioned as the parameters of choice, due to a reduced influence of fluorescence intensity as mentioned above. Furthermore, time-related parameters allow for the selection and measurement of regions of interest (ROIs) with a different camera distance and angle. This is advantageous in gastrointestinal surgery for example, where perfusion pre- and post-anastomosis needs to be documented.

Relative perfusion parameters are a favourable option for a clinical setting, to a degree removing the influence of fluorescence intensity. Problems occur in a setting where the perfusion in the reference region is incorrectly assumed to be sufficient or is difficult to calculate. Peripheral arterial disease patients illustrate the pitfalls in relative parameters, with the example of a patient set to undergo an above the knee amputation. A large majority of patients also have arterial disease in the contralateral limb raising making the reference perfusion value less reliable. Furthermore, should the patient already have a below the knee amputation of the intervention limb, it would not be feasible to film comparable sections of limb with one ICG dose. Table 3 summarizes the advantages and disadvantages of the various methods of quantification in NIRF imaging, Limitations in this field concern the fluorescence angiography technique. In vascular surgery, the presence of inflammation or necrosis can impact the fluorescence signal. Inflammation leads to vasodilatation and hyperemia, falsely increasing the intensity-related parameters (43). The influence of reactive hyperperfusion following a revascularization procedure in the field of vascular surgery also requires further research, as it remains unclear if post-revascularization NIRF measurements are representative of the patient's vascular status. The influence of the circulatory status of the patient on NIRF parameters, such as Tmax or T1/2, is unclear. Theoretically, hypotension or reduced cardiac output could explain a lengthened Tmax, rather than the presence of an occlusion in neurovascular or vascular surgery. Furthermore, the impact of a patient's plasma protein level on ICG uptake, and the subsequent intensity of the ICG measured requires further research. The validity of quantified fluorescence data is further distorted by the range in ICG dose, camera selection, camera and environmental settings and quantification software. Imaging systems have different sensitivities to fluorescence signals, creating heterogenous data before factoring in the impact of environmental influences. Son et al selected an Image 1 S fluorescence imaging system and (Tracker 4.97, Douglas Brown, Open Source Physics, Boston MA, USA) quantification software, while Wada et al chose a PDEneo system and ROIs (Hamamatsu Photonics K.K.) analysis software (25, 47). The abovementioned differences between studies are explored in a recent systematic review

by Lutken et al. (66). The authors describe the diversity in perfusion parameters and methodology in the field of gastro-intestinal surgery, concluding that the application of ICG-NIRF imaging in this field requires standardisation before implementation in a clinical setting. A potential means of achieving standardization is by the process of normalization, a mathematical means of correcting for fluctuations in fluorescence intensity, as yet only described in animal studies with promising results (67-69).

Table 3. Summary of methods of quantification in NIRF imaging.

| Parameter | Advantages | Disadvantages |
|------------------------------|--|---|
| Intensity-related parameters | Broad parameter selection | Influencing factors on intensity: - Patient-related: ICG concentration, cardiac output - System-related: camera distance, camera angle, environmental light |
| Time-related parameters | No influence of measured intensity Comparison possible between ROIs with different camera distance and angle | Narrow parameter selection |
| Relative parameters | Patient vasculature provides case-control data | Reference region may not be representative of optimal perfusion Influencing factors on intensity (see above) |

Conclusion

In conclusion, quantitative analysis of fluorescence imaging has made great advances in recent years, showing potential across multiple surgical fields both intraoperatively, and in the relative pre- and postoperative evaluation of an intervention. Considering the rapidly growing application of this technique, research of the underlying quantification process is deficient. In this review we have explored the perfusion parameters currently used in various surgical specializations. While this review highlights the heterogenicity in parameter selection, time-related parameters appear superior to absolute fluorescence intensity parameters in quantifying perfusion. Before ICG-NIRF imaging can be considered as the as a gold standard of perfusion quantification, standardisation of parameter selection, and methodology with regard to ICG dose and camera type need to be explored.

Appendices

Appendix A. Search strategy.

Pubmed

("Perfusion" [Mesh] OR "perfus*" [tw] OR "reperfus*" [tw]) AND ("Indocyanine green" [Mesh] OR "indocyanin*" [tw] OR "ICG" [tiab] OR "Wofaverdin*" [tw] OR "Vophaverdin*" [tw] OR "Cardio-Green*" [tw] OR "Cardio-Green*" [tw] OR "Cardio-Green*" [tw] OR "Cardio-Green*" [tw] OR "variable" [tw] OR "variables" [tw] OR "variables" [tw] OR "perfus*" [ti] OR "reperfus*" [ti] OR "Indocyanine green" [Majr] OR "indocyanin*" [ti] OR "ICG" [ti] OR "Wofaverdin*" [ti] OR "Vophaverdin*" [ti] OR "Cardio-Green*" [ti] OR "Card

Medline

(exp Perfusion/ OR "perfus*".mp. OR "reperfus*".mp.) AND (exp Indocyanine green/ OR "indocyanin*".mp. OR "ICG".ti,ab. OR "Wofaverdin*".mp. OR "Vophaverdin*".mp. OR "Vofaverdin*".mp. OR "Cardio-Green*".mp. OR "Cardio Green*".mp. OR "Cardio Green*".mp.) AND ("paramet*".mp. OR "variable".mp. OR "variables".mp.) OR ((*exp Perfusion/ OR "perfus*".ti. OR "reperfus*".ti.) AND (exp *Indocyanine green/ OR "indocyanin*".ti. OR "ICG".ti. OR "Wofaverdin*".ti. OR "Vophaverdin*".ti. OR "Vofaverdin*".ti. OR "Cardio-Green*".ti. OR "Cardio Green*".ti. OR "Cardiogreen*".ti. OR ("cardio".ti. AND "green".ti.)))

Embase

(exp Perfusion/ OR "perfus*".mp. OR "reperfus*".mp.) AND (exp Indocyanine green/ OR "indocyanin*".mp. OR "ICG".ti,ab. OR "Wofaverdin*".mp. OR "Vophaverdin*".mp. OR "Vofaverdin*".mp. OR "Cardio-Green*".mp. OR "Cardio Green*".mp. OR "Cardio Green*".mp.) AND ("paramet*".mp. OR "variable".mp. OR "variables".mp.) OR ((*exp Perfusion/ OR "perfus*".ti. OR "reperfus*".ti.) AND (exp *Indocyanine green/ OR "indocyanin*".ti. OR "ICG".ti. OR "Wofaverdin*".ti. OR "Vophaverdin*".ti. OR "Vofaverdin*".ti. OR "Cardio-Green*".ti. OR "Cardio Green*".ti. OR "Cardiogreen*".ti. OR ("cardio".ti. AND "green".ti.)))

Cochrane

(("perfus*" OR "reperfus*") AND ("indocyanin*" OR "ICG" OR "Wofaverdin*" OR "Vophaverdin*" OR "Vofaverdin*" OR "Cardio-Green*" OR "Cardio Green*" OR "Cardio Green*"

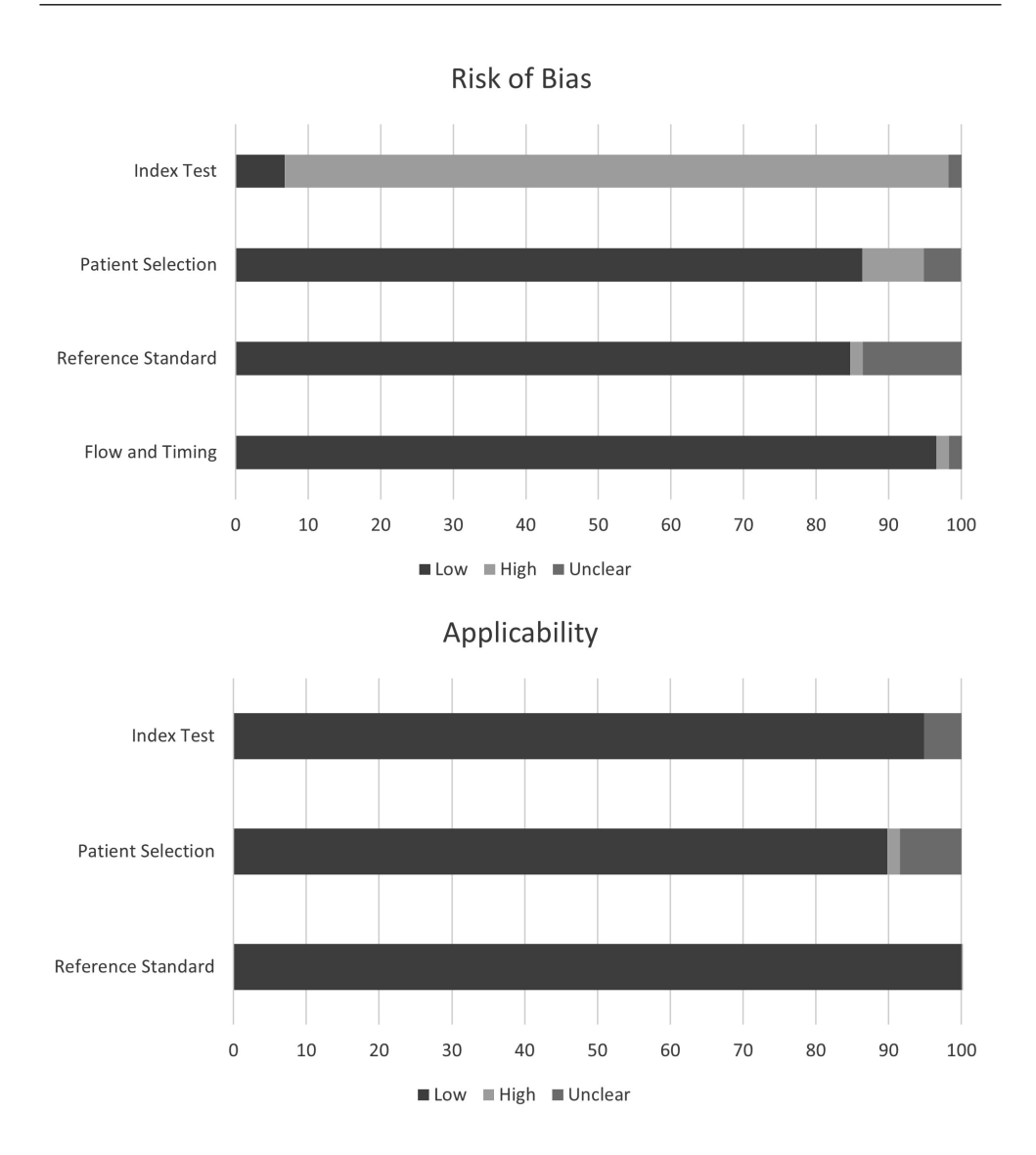


Figure S1. Proportion of studies with low, high, and unclear risk of bias according to the revised Quality Assessment of Diagnostic Accuracy Studies.

Table SL. Quality assessment and risk of bias according to the revised Quality Assessment of Diagnostic Accuracy Studies.

| | | Applica | Applicability Concerns | | | Risk of bias | |
|-----------------------|-------------------|------------|------------------------|-----------------|-------------------|--------------|--------------------|
| Study | Patient Selection | Index test | Reference Standard | Flow and Timing | Patient Selection | Index test | Reference Standard |
| Abdelwahab, 2019(6) | 1 | + | ۸. | • | 1 | 1 | , |
| Abdelwahab, 2019(7) | + | + | ۸. | 1 | 1 | 1 | 1 |
| Aiba, 2021(54) | • | + | ۸. | 1 | 1 | 1 | 1 |
| Amagai, 2020(26) | 1 | + | ì | 1 | 1 | 1 | 1 |
| Betz, 2009(52) | 1 | + | 1 | 1 | ı | ı | ı |
| Betz, 2013(53) | 1 | + | • | • | 1 | 1 | , |
| Braun, 2013(8) | 1 | + | , | , | 1 | 1 | , |
| Colvard, 2016(18) | , | + | 1 | 1 | 1 | 1 | 1 |
| D'urso, 2020(56) | 1 | + | ı | 1 | 1 | 1 | 1 |
| Fichter, 2019(19) | 1 | + | ۸. | 1 | 1 | 1 | , |
| Gerken, 2020(9) | 1 | + | , | , | 1 | , | , |
| Girard, 2019(10) | 1 | + | 1 | 1 | 1 | 1 | , |
| Goertz, 2019(27) | 1 | + | ۸. | 1 | 1 | 1 | 1 |
| Gorai, 2017(57) | 1 | + | 1 | 1 | ı | 1 | • |
| Hajhosseini, 2021(21) | 1 | + | ۸. | + | 1 | ı | • |
| Han, 2018(22) | 1 | + | 1 | 1 | 1 | 1 | • |
| Hayami, 2019(28) | 1 | + | 1 | 1 | ı | ı | 1 |
| Hitier, 2016(23) | 1 | + | 1 | 1 | 1 | 1 | • |
| Holling, 2013(61) | 1 | + | 1 | 1 | ı | ı | • |
| Igari, 2013(29) | , | + | 1 | 1 | 1 | 1 | 1 |
| Igari, 2014(30) | + | + | 1 | 1 | + | ı | 1 |
| Ishige, 2019(31) | 1 | + | ۸. | 1 | 1 | ۸. | 1 |
| Kamiya, 2015(32) | 1 | + | 1 | 1 | 1 | 1 | 1 |
| Kamp, 2017(33) | 1 | + | , | , | 1 | 1 | • |
| Kamp, 2012(34) | 1 | ۸. | , | , | 1 | ۸. | • |
| Kang, 2011(55) | + | + | , | , | ۸. | 1 | • |
| Kang 2010(20) | + | + | 1 | 1 | ۸. | ı | • |
| Kobayashi, 2014(35) | 1 | + | 1 | 1 | ı | ı | , |
| Lang, 2017(24) | 1 | + | 1 | 1 | 1 | 1 | 1 |
| Maxwell, 2016(36) | + | + | 1 | 1 | ۸. | 1 | 1 |
| Mironov, 2019(11) | ı | 1 | 1 | 1 | ı | 1 | 1 |
| Miyazaki, 2017(37) | 1 | + | ı | ı | 1 | 1 | 1 |
| | | | | | | | |

| Mothes, 2009(51) | 1 | + | 1 | 1 | 1 | 1 | 1 |
|--|---------------------------|---|----|----|----|----|---|
| Nakamura, 2017(38) | , | + | 1 | 1 | 1 | , | , |
| Nishizawa, 2017(39) | , | + | , | , | 1 | , | , |
| Patel, 2018(40) | • | + | • | 1 | 1 | • | , |
| Prinz, 2014(58) | ı | + | ۸. | ı | 1 | 1 | 1 |
| Regus, 2019(12) | 1 | + | • | ı | 1 | 1 | 1 |
| Rennert, 2018(41) | 1 | + | 1 | ı | 1 | 1 | 1 |
| Rennert, 2019(59) | 1 | + | 1 | 1 | 1 | 1 | 1 |
| Rother, 2019(14) | 1 | + | 1 | ı | 1 | 1 | 1 |
| Rother, 2018(15) | 1 | + | 1 | ı | 1 | 1 | 1 |
| Rother, 2017(16) | 1 | + | 1 | 1 | 1 | 1 | 1 |
| Rother, 2020(13) | ۸. | + | 1 | ı | 1 | 1 | 1 |
| Schneider, 2011(42) | ۸. | + | • | ı | ۸. | 1 | 1 |
| Seinturier, 2020(43) | • | + | • | ۸. | 1 | 1 | • |
| Settembre, 2017(44) | 1 | + | 1 | 1 | 1 | 1 | 1 |
| Shi, 2015(45) | 1 | + | 1 | 1 | 1 | 1 | 1 |
| Son, 2019(25) | 1 | + | 1 | ı | ı | 1 | 1 |
| Tanaka, 2015(46) | 1 | + | 1 | 1 | 1 | 1 | 1 |
| Terasaki, 2013(60) | 1 | + | 1 | ı | 1 | 1 | 1 |
| Uchino, 2014(64) | 1 | + | 1 | 1 | 1 | 1 | 1 |
| Uchino, 2013(63) | 1 | + | 1 | 1 | 1 | 1 | 1 |
| Venermo, 2016(65) | 1 | + | 1 | ı | 1 | 1 | 1 |
| Wada, 2017(47) | 1 | 1 | 1 | 1 | 1 | 1 | 1 |
| Woitzik, 2006(62) | ۸. | + | ۸. | ı | ۸. | ۸. | 1 |
| Yang, 2018(17) | 1 | + | 1 | 1 | 1 | 1 | 1 |
| Ye, 2013(48) | 1 | + | 1 | ı | ı | 1 | 1 |
| Zhang, 2020(49) | 1 | + | 1 | 1 | 1 | 1 | 1 |
| Zimmermann, 2012(50) | 1 | + | 1 | 1 | 1 | 1 | 1 |
| -, Low risk of bias; + high risk of bias | s; ? risk of bias unclear | | | | | | |

Reference List

- Cornelissen AJM, van Mulken TJM, Graupner C, Qiu SS, Keuter XHA, van der Hulst RRWJ, et al. Near-infrared fluorescence image-guidance in plastic surgery: A systematic review. Eur J Plast Surg. 2018;41(3):269-78.
- 2. al PvdHe. A systematic review of the use of near-infrared fluorescence imaging in patients with peripheral artery disease. Journal of Vascular Surgery. 2019;70(1).
- 3. Singh SKMDM, Desai NDMDP, Chikazawa GMDP, Tsuneyoshi HMDP, Vincent JB, Zagorski BMM, et al. The Graft Imaging to Improve Patency (GRIIP) clinical trial results. J Thorac Cardiovasc Surg. 2010;139(2):294-301.e1.
- 4. Mangano A, Masrur MA, Bustos R, Chen LL, Fernandes E, Giulianotti PC. Near-Infrared Indocyanine Green-Enhanced Fluorescence and Minimally Invasive Colorectal Surgery: Review of the Literature. Surg Technol Int. 2018;33:77-83.
- 5. Whiting PF, Rutjes AWS, Westwood ME, Mallett S, Deeks JJ, Reitsma JB, et al. QUADAS-2: a revised tool for the quality assessment of diagnostic accuracy studies. Ann Intern Med. 2011;155(8):529-36.
- Abdelwahab M, Kandathil CK, Most SP, Spataro EA. Utility of Indocyanine Green Angiography to Identify Clinical Factors Associated With Perfusion of Paramedian Forehead Flaps During Nasal Reconstruction Surgery. JAMA Facial Plast Surg. 2019;21(3):206-12.
- 7. Abdelwahab M, Spataro EA, Kandathil CK, Most SP. Neovascularization Perfusion of Melolabial Flaps Using Intraoperative Indocyanine Green Angiography. JAMA Facial Plast Surg. 2019;21(3):230-6.
- 8. Braun JD, Trinidad-Hernandez M, Perry D, Armstrong DG, Mills JL, Sr. Early quantitative evaluation of indocyanine green angiography in patients with critical limb ischemia. J Vasc Surg. 2013;57(5):1213-8.
- Gerken ALH, Nowak K, Meyer A, Weiss C, Kruger B, Nawroth N, et al. Quantitative Assessment of Intraoperative Laser Fluorescence Angiography with Indocyanine Green Predicts Early Graft Function after Kidney Transplantation. Annals of Surgery Publish Ahead of Print. 2020;30:30.
- 10. Girard N, Delomenie M, Malhaire C, Sebbag D, Roulot A, Sabaila A, et al. Innovative DIEP flap perfusion evaluation tool: Qualitative and quantitative analysis of indocyanine green-based fluorescence angiography with the SPY-Q proprietary software. PLoS One. 2019;14(6):e0217698.
- 11. Mironov O, Zener R, Eisenberg N, Tan KT, Roche-Nagle G. Real-Time Quantitative Measurements of Foot Perfusion in Patients With Critical Limb Ischemia. Vasc Endovascular Surg. 2019;53(4):310-5.
- 12. Regus S, Klingler F, Lang W, Meyer A, Almasi-Sperling V, May M, et al. Pilot study using intraoperative fluorescence angiography during arteriovenous hemodialysis access surgery. Journal of Vascular Access. 2019;20(2):175-83.
- 13. Rother U, Muller-Mohnssen H, Lang W, Ludolph I, Arkudas A, Horch RE, et al. Wound closure by means of free flap and arteriovenous loop: Development of flap autonomy in the long-term follow-up. International Wound Journal. 2020;17(1):107-16.

- 14. Rother U, Amann K, Adler W, Nawroth N, Karampinis I, Keese M, et al. Quantitative assessment of microperfusion by indocyanine green angiography in kidney transplantation resembles chronic morphological changes in kidney specimens. Microcirculation. 2019;26(3):e12529.
- 15. Rother U, Lang W, Horch RE, Ludolph I, Meyer A, Gefeller O, et al. Pilot Assessment of the Angiosome Concept by Intra-operative Fluorescence Angiography After Tibial Bypass Surgery. European Journal of Vascular and Endovascular Surgery. 2018;55(2):161.
- Rother U, Lang W, Horch RE, Ludolph I, Meyer A, Regus S. Microcirculation Evaluated by Intraoperative Fluorescence Angiography after Tibial Bypass Surgery. Annals of Vascular Surgery. 2017;40:190-7.
- 17. Yang CE, Chung SW, Lee DW, Lew DH, Song SY. Evaluation of the Relationship Between Flap Tension and Tissue Perfusion in Implant-Based Breast Reconstruction Using Laser-Assisted Indocyanine Green Angiography. Ann Surg Oncol. 2018;25(8):2235-40.
- 18. Colvard B, Itoga NK, Hitchner E, Sun Q, Long B, Lee G, et al. SPY technology as an adjunctive measure for lower extremity perfusion. J Vasc Surg. 2016;64(1):195-201.
- Fichter AM, Ritschl LM, Georg R, Kolk A, Kesting MR, Wolff KD, et al. Effect of Segment Length and Number of Osteotomy Sites on Cancellous Bone Perfusion in Free Fibula Flaps. Journal of Reconstructive Microsurgery. 2019;35(2):108-16.
- 20. Kang Y, Lee J, Kwon K, Choi C. Application of novel dynamic optical imaging for evaluation of peripheral tissue perfusion. International Journal of Cardiology. 2010;145(3):e99-101.
- 21. Hajhosseini B, Chiou GJ, Virk SS, Chandra V, Moshrefi S, Meyer S, et al. Hyperbaric Oxygen Therapy in Management of Diabetic Foot Ulcers: Indocyanine Green Angiography May Be Used as a Biomarker to Analyze Perfusion and Predict Response to Treatment. Plast Reconstr Surg. 2021;147(1):209-14.
- 22. Han MD, Miloro M, Markiewicz MR. Laser-Assisted Indocyanine Green Imaging for Assessment of Perioperative Maxillary Perfusion During Le Fort I Osteotomy: A Pilot Study. J Oral Maxillofac Surg. 2018;76(12):2630-7.
- 23. Hitier M, Cracowski JL, Hamou C, Righini C, Bettega G. Indocyanine green fluorescence angiography for free flap monitoring: A pilot study. J Craniomaxillofac Surg. 2016;44(11):1833-41.
- 24. Lang BHH, Wong CKH, Hung HT, Wong KP, Mak KL, Au KB. Indocyanine green fluorescence angiography for quantitative evaluation of in situ parathyroid gland perfusion and function after total thyroidectomy. Surgery (United States). 2017;161(1):87-95.
- 25. Son GM, Kwon MS, Kim Y, Kim J, Kim SH, Lee JW. Quantitative analysis of colon perfusion pattern using indocyanine green (ICG) angiography in laparoscopic colorectal surgery. Surg Endosc. 2019;33(5):1640-9.
- 26. Amagai H, Miyauchi H, Muto Y, Uesato M, Ohira G, Imanishi S, et al. Clinical utility of transanal indocyanine green near-infrared fluorescence imaging for evaluation of colorectal anastomotic perfusion. Surg Endosc. 2020;34(12):5283-93.
- Goertz L, Hof M, Timmer M, Schulte AP, Kabbasch C, Krischek B, et al. Application of Intraoperative FLOW 800 Indocyanine Green Videoangiography Color-Coded Maps for Microsurgical Clipping of Intracranial Aneurysms. World Neurosurg. 2019;131:e192-e200.

- 28. Hayami S, Matsuda K, Iwamoto H, Ueno M, Kawai M, Hirono S, et al. Visualization and quantification of anastomotic perfusion in colorectal surgery using near-infrared fluorescence. Tech Coloproctol. 2019;23(10):973-80.
- 29. Igari K, Kudo T, Toyofuku T, Jibiki M, Inoue Y, Kawano T. Quantitative Evaluation of the Outcomes of Revascularization Procedures for Peripheral Arterial Disease Using Indocyanine Green Angiography. European Journal of Vascular & Endovascular Surgery. 2013;46(4):460-5.
- Igari K, Kudo T, Uchiyama H, Toyofuku T, Inoue Y. Indocyanine Green Angiography for the Diagnosis of Peripheral Arterial Disease with Isolated Infrapopliteal Lesions. Annals of Vascular Surgery. 2014;28(6):1479-84.
- 31. Ishige F, Nabeya Y, Hoshino I, Takayama W, Chiba S, Arimitsu H, et al. Quantitative Assessment of the Blood Perfusion of the Gastric Conduit by Indocyanine Green Imaging. J Surg Res. 2019;234:303-10.
- 32. Kamiya K, Unno N, Miyazaki S, Sano M, Kikuchi H, Hiramatsu Y, et al. Quantitative assessment of the free jejunal graft perfusion. Journal of Surgical Research. 2015;194(2):394-9.
- 33. Kamp MA, Sarikaya-Seiwert S, Petridis AK, Beez T, Cornelius JF, Steiger HJ, et al. Intraoperative Indocyanine Green-Based Cortical Perfusion Assessment in Patients Suffering from Severe Traumatic Brain Injury. World Neurosurg. 2017;101:431-43.
- 34. Kamp MA, Slotty P, Turowski B, Etminan N, Steiger HJ, Hanggi D, et al. Microscope-integrated quantitative analysis of intraoperative indocyanine green fluorescence angiography for blood flow assessment: first experience in 30 patients. Neurosurgery. 2012;70(1 Suppl Operative):65-73; discussion -4.
- 35. Kobayashi S, Ishikawa T, Tanabe J, Moroi J, Suzuki A. Quantitative cerebral perfusion assessment using microscope-integrated analysis of intraoperative indocyanine green fluorescence angiography versus positron emission tomography in superficial temporal artery to middle cerebral artery anastomosis. Surg Neurol Int. 2014;5:135.
- 36. Maxwell AK, Deleyiannis FW. Utility of Indocyanine Green Angiography in Arterial Selection during Free Flap Harvest in Patients with Severe Peripheral Vascular Disease. Plast Reconstr Surg Glob Open. 2016;4(10):e1097.
- 37. Miyazaki H, Igari K, Kudo T, Iwai T, Wada Y, Takahashi Y, et al. Significance of the Lateral Thoracic Artery in Pectoralis Major Musculocutaneous Flap Reconstruction: Quantitative Assessment of Blood Circulation Using Indocyanine Green Angiography. Ann Plast Surg. 2017;79(5):498-504.
- 38. Nakamura M, Igari K, Toyofuku T, Kudo T, Inoue Y, Uetake H. The evaluation of contralateral foot circulation after unilateral revascularization procedures using indocyanine green angiography. Scientific Reports. 2017;7.
- Nishizawa M, Igari K, Kudo T, Toyofuku T, Inoue Y, Uetake H. A Comparison of the Regional Circulation in the Feet between Dialysis and Non-Dialysis Patients using Indocyanine Green Angiography. Scandinavian Journal of Surgery. 2017;106(3):249-54.
- Patel HM, Bulsara SS, Banerjee S, Sahu T, Sheorain VK, Grover T, et al. Indocyanine Green Angiography to Prognosticate Healing of Foot Ulcer in Critical Limb Ischemia: A Novel Technique. Ann Vasc Surg. 2018;51:86-94.

- 41. Rennert RC, Strickland BA, Ravina K, Bakhsheshian J, Russin JJ. Assessment of Hemodynamic Changes and Hyperperfusion Risk After Extracranial-to-Intracranial Bypass Surgery Using Intraoperative Indocyanine Green-Based Flow Analysis. World Neurosurg. 2018;114:352-60.
- 42. Schneider P, Piper S, Schmitz CH, Schreiter NF, Volkwein N, Ludemann L, et al. Fast 3D Near-infrared breast imaging using indocyanine green for detection and characterization of breast lesions. Rofo: Fortschritte auf dem Gebiete der Rontgenstrahlen und der Nuklearmedizin. 2011:183(10):956-63.
- 43. Seinturier C, Blaise S, Tiffet T, Provencher CB, Cracowski JL, Pernod G, et al. Fluorescence angiography compared to toe blood pressure in the evaluation of severe limb ischemia. Vasa. 2020;49(3):230-4.
- 44. Settembre N, Kauhanen P, Alback A, Spillerova K, Venermo M. Quality Control of the Foot Revascularization Using Indocyanine Green Fluorescence Imaging. World J Surg. 2017;41(7):1919-26.
- 45. Shi W, Qiao G, Sun Z, Shang A, Wu C, Xu B. Quantitative assessment of hemodynamic changes during spinal dural arteriovenous fistula surgery. J Clin Neurosci. 2015;22(7):1155-9.
- 46. Tanaka K, Okazaki M, Yano T, Miyashita H, Homma T, Tomita M. Quantitative evaluation of blood perfusion to nerves included in the anterolateral thigh flap using indocyanine green fluorescence angiography: a different contrast pattern between the vastus lateralis motor nerve and femoral cutaneous nerve. J Reconstr Microsurg. 2015;31(3):163-70.
- 47. Wada T, Kawada K, Takahashi R, Yoshitomi M, Hida K, Hasegawa S, et al. ICG fluorescence imaging for quantitative evaluation of colonic perfusion in laparoscopic colorectal surgery. Surg Endosc. 2017;31(10):4184-93.
- 48. Ye X, Liu XJ, Ma L, Liu LT, Wang WL, Wang S, et al. Clinical values of intraoperative indocyanine green fluorescence video angiography with Flow 800 software in cerebrovascular surgery. Chin Med J (Engl). 2013;126(22):4232-7.
- 49. Zhang X, Ni W, Feng R, Li Y, Lei Y, Xia D, et al. Evaluation of Hemodynamic Change by Indocyanine Green-FLOW 800 Videoangiography Mapping: Prediction of Hyperperfusion Syndrome in Patients with Moyamoya Disease. Oxidative Medicine and Cellular Longevity. 2020;2020 (no pagination).
- 50. Zimmermann A, Roenneberg C, Reeps C, Wendorff H, Holzbach T, Eckstein HH. The determination of tissue perfusion and collateralization in peripheral arterial disease with indocyanine green fluorescence angiography. Clin Hemorheol Microcirc. 2012;50(3):157-66.
- Mothes H, Dinkelaker T, DÖNicke T, Friedel R, Hofmann GO, Bach O. Outcome Prediction in Microsurgery by Quantitative Evaluation of Perfusion Using ICG Fluorescence Angiography. J Hand Surg Eur Vol. 2009;34(2):238-46.
- 52. Betz CS, Zhorzel S, Schachenmayr H, Stepp H, Havel M, Siedek V, et al. Endoscopic measurements of free-flap perfusion in the head and neck region using red-excited Indocyanine Green: preliminary results. J Plast Reconstr Aesthet Surg. 2009;62(12):1602-8.
- 53. Betz CS, Zhorzel S, Schachenmayr H, Stepp H, Matthias C, Hopper C, et al. Endoscopic assessment of free flap perfusion in the upper aerodigestive tract using indocyanine green: a pilot study. J Plast Reconstr Aesthet Surg. 2013;66(5):667-74.

- 54. Aiba T, Uehara K, Ogura A, Tanaka A, Yonekawa Y, Hattori N, et al. The significance of the time to arterial perfusion in intraoperative ICG angiography during colorectal surgery. Surg Endosc. 2021.
- 55. Kang Y, Lee J, An Y, Jeon J, Choi C. Segmental analysis of indocyanine green pharmacokinetics for the reliable diagnosis of functional vascular insufficiency. J Biomed Opt. 2011;16(3):030504.
- 56. D'Urso A, Agnus V, Barberio M, Seeliger B, Marchegiani F, Charles AL, et al. Computer-assisted quantification and visualization of bowel perfusion using fluorescence-based enhanced reality in left-sided colonic resections. Surgical Endoscopy. 2020.
- 57. Gorai K, Inoue K, Saegusa N, Shimamoto R, Takeishi M, Okazaki M, et al. Prediction of Skin Necrosis after Mastectomy for Breast Cancer Using Indocyanine Green Angiography Imaging. Plast Reconstr Surg Glob Open. 2017;5(4):e1321.
- 58. Prinz V, Hecht N, Kato N, Vajkoczy P. FLOW 800 allows visualization of hemodynamic changes after extracranial-to-intracranial bypass surgery but not assessment of quantitative perfusion or flow. Neurosurgery. 2014;10 Suppl 2:231-8; discussion 8-9.
- Rennert RC, Strickland BA, Ravina K, Brandel MG, Bakhsheshian J, Fredrickson V, et al. Assessment of ischemic risk following intracranial-to-intracranial and extracranial-to-intracranial bypass for complex aneurysms using intraoperative Indocyanine Green-based flow analysis. J Clin Neurosci. 2019;67:191-7.
- 60. Terasaki H, Inoue Y, Sugano N, Jibiki M, Kudo T, Lepantalo M, et al. A quantitative method for evaluating local perfusion using indocyanine green fluorescence imaging. Ann Vasc Surg. 2013;27(8):1154-61.
- 61. Holling M, Brokinkel B, Ewelt C, Fischer BR, Stummer W. Dynamic ICG fluorescence provides better intraoperative understanding of arteriovenous fistulae. Neurosurgery. 2013;73(1 Suppl Operative):ons93-8; discussion ons9.
- 62. Woitzik J, Pena-Tapia PG, Schneider UC, Vajkoczy P, Thome C. Cortical perfusion measurement by indocyanine-green videoangiography in patients undergoing hemicraniectomy for malignant stroke. Stroke. 2006;37(6):1549-51.
- 63. Uchino H, Nakamura T, Houkin K, Murata JI, Saito H, Kuroda S. Semiquantitative analysis of indocyanine green videoangiography for cortical perfusion assessment in superficial temporal artery to middle cerebral artery anastomosis. Acta Neurochirurgica. 2013;155(4):599-605.
- 64. Uchino H, Kazumata K, Ito M, Nakayama N, Kuroda S, Houkin K. Intraoperative assessment of cortical perfusion by indocyanine green videoangiography in surgical revascularization for moyamoya disease. Acta Neurochir (Wien). 2014;156(9):1753-60.
- 65. Venermo M, Settembre N, Alback A, Vikatmaa P, Aho PS, Lepantalo M, et al. Pilot Assessment of the Repeatability of Indocyanine Green Fluorescence Imaging and Correlation with Traditional Foot Perfusion Assessments. European Journal of Vascular & Endovascular Surgery. 2016;52(4):527-33.
- 66. Lutken CD, Achiam MP, Svendsen MB, Boni L, Nerup N. Optimizing quantitative fluorescence angiography for visceral perfusion assessment. Surgical Endoscopy. 2020;34(12):5223-33.
- 67. Nerup N, Andersen HS, Ambrus R, Strandby RB, Svendsen MBS, Madsen MH, et al. Quantification of fluorescence angiography in a porcine model. Langenbecks Arch Surg. 2017;402(4):655-62.

- 68. Rønn JH, Nerup N, Strandby RB, Svendsen MBS, Ambrus R, Svendsen LB, et al. Laser speckle contrast imaging and quantitative fluorescence angiography for perfusion assessment. Langenbecks Arch Surg. 2019;404(4):505-15.
- 69. Lutken CD, Achiam MP, Osterkamp J, Svendsen MB, Nerup N. Quantification of fluorescence angiography: Toward a reliable intraoperative assessment of tissue perfusion A narrative review. Langenbecks Archives of Surgery. 2020;21:21.



Chapter 4

Perfusion patterns in patients with chronic limb-threatening ischemia versus control patients using near-infrared fluorescence imaging with indocyanine green

P. van den Hoven ¹, L.N. Goncalves ¹, P.H.A. Quax ¹, C.S.P. van Rijswijk ¹, J. van Schaik ¹, A. Schepers ¹, A.L. Vahrmeijer ¹, J.F. Hamming ¹, J.R. van der Vorst ¹

1. Leiden University Medical Center, Leiden, The Netherlands

Published in Biomedicines, October 2021.

Abstract

Introduction

In assessing the severity of lower extremity arterial disease (LEAD), physicians rely on clinical judgement supported by conventional measurements of macrovascular blood flow. However, current diagnostic techniques provide no information about regional tissue perfusion and are of limited value in patients with chronic limb-threatening ischemia (CLTI). Near-infrared (NIR) fluorescence imaging using indocyanine green (ICG) has been used extensively in perfusion studies and is a possible modality for tissue perfusion measurement in patients with CLTI.

Methods

In this prospective cohort study ICG NIR fluorescence imaging was performed in patients with CLTI and control patients using the Quest Spectrum Platform®. The time-intensity curves were analyzed using the Quest Research Framework®. Fourteen parameters were extracted.

Results

Successful ICG NIR fluorescence imaging was performed in 19 patients with CLTI and 16 control patients. The time to maximum intensity was lower for CLTI patients (90.5 vs 143.3 seconds, p=0.002). For inflow parameters, the maximum slope, the normalized maximum slope and the ingress rate were all significantly higher in the CLTI group.

Conclusion

Inflow parameters observed in patients with CLTI were superior to the control group. Possible explanations for the increased inflow include damage to the regulatory mechanisms of the microcirculation, arterial stiffness and transcapillary leakage.

Introduction

Lower-extremity arterial disease (LEAD) is most often caused by atherosclerosis (1, 2). Subsequent hemodynamic alterations leading to hypoxia can trigger a cascade of events leading to macro- and microvascular changes in the affected limb (3). In the most advanced stage, chronic limb-threatening ischemia (CLTI), blood supply to the lower extremity is insufficient to meet metabolic needs (2, 4). For these patients, a common finding in physical examination of the lower extremities is the appearance of "dependent rubor" or "blanching", which is presumably caused by dysfunction of the venoarteriolar reflex (5). In assessing the severity of LEAD, physicians often rely on their clinical judgement of the extremities. The diagnosis is confirmed using conventional measurements of macrovascular blood flow including the ankle-brachial index (ABI), toe pressure measurement, computed tomography (CT) angiography, magnetic resonance angiography and digital subtraction angiography. However, these techniques provide no information about regional tissue perfusion and have shown to be of limited value in patients with CLTI (6). New emerging methods for the assessment of regional tissue perfusion include dynamic volume perfusion CT, laser speckle imaging (LSI) and near-infrared (NIR) fluorescence imaging using indocyanine green (ICG) (7-9). ICG NIR fluorescence imaging has been used in various medical fields for assessment of tissue perfusion, including cardiac and reconstructive surgery (10, 11). This imaging technique measures fluorescence in the NIR light spectrum (700-1000nm), which is characterized by low tissue autofluorescence and deep tissue penetration (12). Upon intravenous administration of ICG, which has a peak emission of 814nm, the camera measures the NIR fluorescence intensity over time. The feasibility of ICG as a fluorophore in perfusion assessment is explained by its confinement to the intravascular compartment due to the binding with plasma proteins (13). For assessment of skin perfusion, ICG NIR fluorescence imaging is currently used intraoperatively in reconstructive surgery to predict flap viability (14). For patients with LEAD, similar results were seen in predicting skin necrosis following amputation surgery (15). However, these findings rely on qualitative analyses, meaning the observer subjectively grades the visualized NIR fluorescence intensity. To quantify and grade regional tissue perfusion, better understanding of the different perfusion patterns as observed with ICG NIR fluorescence imaging is needed. Several studies have been performed to quantify ICG NIR fluorescence imaging between patients with different stages of LEAD (16-18). However, inconsistency is seen between stages and it is unclear whether advanced stages of LEAD alter the in- and outflow of ICG (16). Furthermore, there is limited information about the perfusion patterns of ICG NIR fluorescence imaging in control patients. Therefore, as a first step in the quantification of tissue perfusion using ICG NIR fluorescence imaging, the aim of this study was to analyze the perfusion patterns seen in patients with CLTI and compare these to non-LEAD control patients.

Methods

This prospective cohort study was approved by the Medical Research and Ethics Committee of the Leiden University Medical Center and registered in the Dutch Trial Register with number NL7531. Patients with CLTI as classified according to the Global Vascular Guidelines on the management of CLTI, were included (4). These were patients diagnosed with either Fontaine stage 3 or stage 4 LEAD. The control group consisted of patients who underwent intravenous ICG administration prior to liver metastasectomy. Patients were included from December 2018 until April 2021 in a single academic hospital in the Netherlands. Exclusion criteria were allergy or hypersensitivity to sodium iodide, iodide, or ICG; known hyperthyroidism or autonomous thyroid adenoma, pregnancy, kidney failure (eGFR <45) and/or severe liver failure. Informed consent was obtained in all patients. ABI and toe pressure measurements were performed in all patients. As additional measurement for patients with CLTI, duplex ultrasound measurements of the feet were performed and the highest acceleration in either the dorsalis pedis artery or posterior tibial artery was reported. These acceleration measurements are described in detail in an earlier study by Brouwers et al. and are performed to assess the severity of arterial stenosis (19), performed as routine measurements for The Ouest Spectrum Platform® (Quest Medical Imaging, Middenmeer, The Netherlands) was used to perform ICG NIR fluorescence imaging (Figure 1).

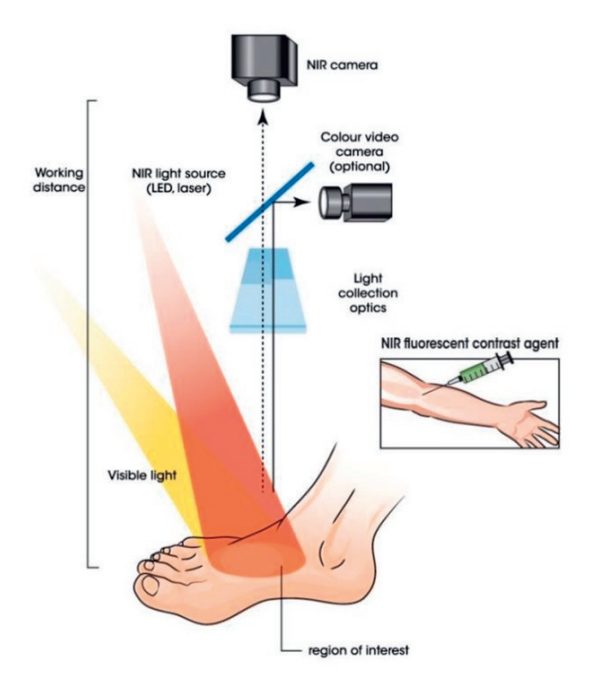


Figure 1. ICG NIR fluorescence imaging camera setup.

This imaging system is capable of measuring both visible light as well as the NIR signal of ICG. Patients with CLTI were administered an intravenous bolus injection of 0.1 mg/kg ICG (VERDYE 25 mg, Diagnostic Green GmbH, Aschheim-Dornach, Germany) using a peripheral venous line in the cubital fossa or on the dorsum of the hand. Patients in the control group were administered a bolus injection of 10mg ICG according to local hospital guidelines. Following administration of ICG, the NIR fluorescence intensity in both feet was recorded for 10 minutes (Figure 2).



Figure 2. ICG NIR fluorescence imaging in a control patient showing the visual image (left), merged image (middle) and NIR fluorescence intensity at the dorsum of both feet.

Measurements were performed on patients in a supine position following a rest period of at least 10 minutes in a room cleared of ambient light. The camera was placed perpendicular to the dorsum of both feet at a distance of 50cm. The NIR fluorescence videos were analyzed using the Quest Research Framework® (Quest Medical Imaging, Middenmeer, the Netherlands). The whole foot was selected as region of interest (ROI). Upon selection of the ROI, the software creates a time-intensity curve of the measured intensity in arbitrary units (a.u.). A tracker was used to ensure the ROI was synchronized with leg movement. Fourteen parameters were extracted from these curves, of which an explanation is given in Figure 3. The ingress rate was defined as the intensity increase per second from baseline to maximum intensity. The Tmax was measured starting at the point of 10% intensity increase upon baseline. The time-intensity curves were also analyzed after normalization for maximum intensity. The curves extracted from these curves were, in percentage per second, the maximum slope ingress and the maximum slope egress. Starting time was defined as an increase of 1 arbitrary unit for the intensity curves and 1% for the normalized curves. Statistical analyses were performed using IBM SPSS Statistics 25 (IBM Corp. Released 2017. IBM SPSS Statistics for Windows, Version 25.0. Armonk, NY, USA: IBM Corp.). Parameters were compared using the Mann-Whitney U test.

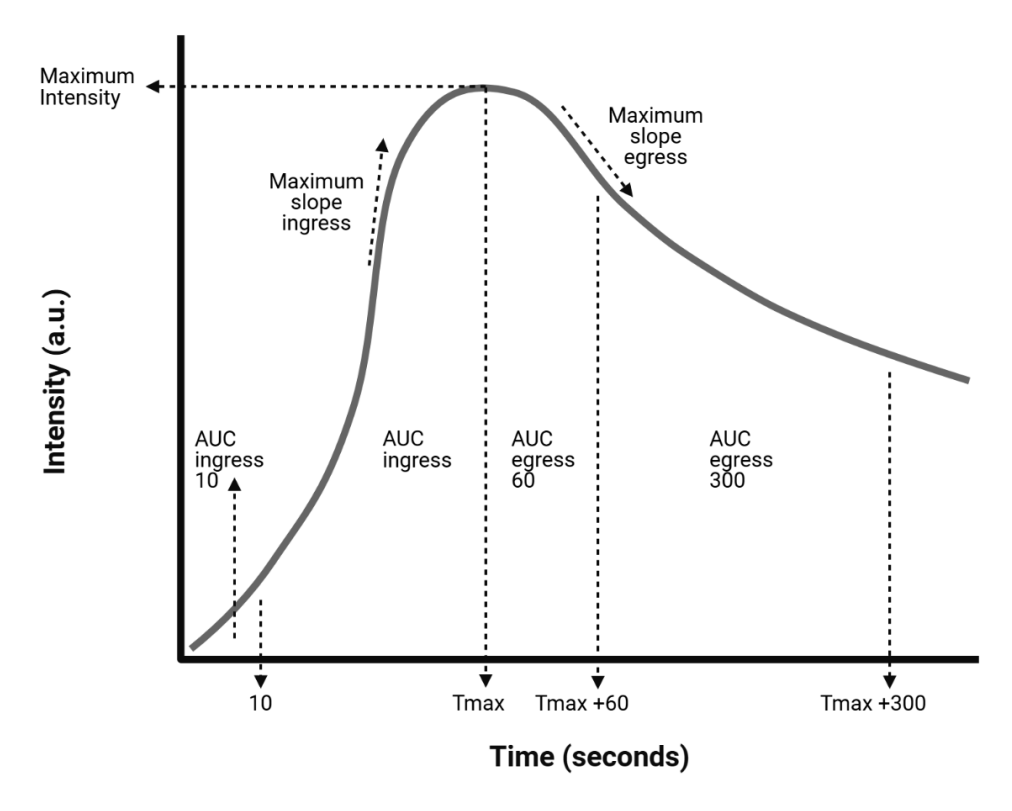


Figure 3. Time-intensity curve with extracted parameters.

Results

Successful ICG NIR fluorescence imaging measurements were performed in 35 patients. Nineteen patients presented with LEAD of whom 28 limbs were classified as CLTI. The control group consisted of 16 patients with a total of 32 limbs. The characteristics for each group are displayed in Table 1. For the CLTI group, 10 limbs were classified as Fontaine stage 4. Compared to the control group, patients in the CLTI group were more likely to present with diabetes, hypertension and smoking. The mean ABI in the CLTI group was 0.77 versus 1.11 in the control group. The ABI in the CLTI group was not measurable in 9 out of 28 limbs. The acceleration measured on duplex ultrasonography was measured in 22 CLTI limbs with a mean of 0.93 m/s².

ICG NIR fluorescence imaging parameters

The results on ICG NIR fluorescence imaging for the 14 extracted parameters are displayed in Table 2. The mean maximum intensity was significantly lower in the control group (37.9 vs 25.8 a.u., p<0.001). Furthermore, the time to maximum

intensity (i.e. Tmax) was reached earlier in the CLTI group (90.5 vs 143.3 seconds, p=0.002). When taking a closer look at the inflow parameters, the maximum slope, the normalized maximum slope and the ingress rate were all significantly higher in the CLTI group (2.0 vs 0.6 a.u./s, p<0.001; 4.2 vs 2.4 %/s, p<0.001; 1.0 vs 0.2 a.u./s, p<0.001). For outflow parameters, a significant difference was seen for the maximum slope egress, which was higher in the control group (0.5 vs 0.2 a.u./s, p=0.005). No significant difference was observed for the normalized maximum slope egress (1.0 vs 0.8 %/s, p=0.733). Comparison of the AUC for different intervals following the Tmax displayed no significant difference between the CLTI and control group.

Table 1. Patient characteristics.

| | CLTI | Control group |
|----------------------------|-------------|---------------|
| N (limbs) | 19 (28) | 16 (32) |
| Age (SD) | 70.4 (7.5) | 66.6 (12.3) |
| Diabetes Mellitus (%) | 9 (47.4) | 3 (18.8) |
| Hypertension (%) | 15 (78.9) | 7 (43.8) |
| Active smoking (%) | 5 (26.3) | 1 (6.3) |
| Fontaine stage limbs, n(%) | | |
| 3 | 18 (64.3) | - |
| 4 | 10 (35.7) | - |
| Mean ABI (SD) | 0.77 (0.34) | 1.11 (0.10) |
| Mean TP (SD) | 44 (25) | 106 (22) |
| Acceleration (SD) | 0.93 (1.23) | - |

Abbreviations: SD, standard deviation; CLTI, chronic limb-threatening ischemia; ABI, ankle-brachial index; TP, Toe Pressure).

Time-intensity curves

The time-intensity curves for the control group and CLTI group are displayed in Figure 4. Results are displayed for the intensity-related curves (above) and the normalized curves (below) for both groups. Time-intensity curves displaying the absolute intensity change over time show an overall higher absolute intensity for the CLTI group. Following a steep incline in intensity increase for the CLTI group, the outflow seems comparable with control patients. The intensity-related curves show a widespread distribution, especially in the CLTI group. In this group, the maximum slope ingress (2.0%/s) has a standard deviation of 2.5 (Table 2). For the AUC egress parameters, standard deviations between 10.0% and 13.5% are observed. When normalizing these time-intensity curves for maximum intensity, both groups display a more narrow distribution in all parameters. For the normalized maximum slope in the CLTI group (4.2%/s), a standard deviation of 3.1% was observed. When looking at AUC egress parameters, the standard deviations have a distribution of 1.8 to 6.1%.

Table 2. ICG NIR fluorescence imaging parameters.

| Parameter | CLTI | Controls | p-value |
|--------------------------------------|-------------|--------------|---------|
| Maximum intensity (SD) | 37.9 (14.4) | 25.8 (10.8) | < 0.001 |
| Maximum slope ingress (SD) | 2.0 (2.5) | 0.6 (0.4) | < 0.001 |
| Normalized maximum slope (SD) | 4.2 (3.1) | 2.4 (1.2) | < 0.001 |
| Ingress rate (SD) | 1.0 (1.7) | 0.2 (0.2) | < 0.001 |
| AUC ingress 10 (SD) | 47.4 (2.2) | 48.8 (3.3) | 0.073 |
| AUC ingress (SD) | 71.4 (6.3) | 70.6 (3.8) | 0.213 |
| Tmax (SD) | 90.5 (53.4) | 143.3 (64.5) | 0.002 |
| Maximum slope egress (SD) | 0.5 (0.7) | 0.2 (0.1) | 0.005 |
| Normalized maximum slope egress (SD) | 1.0 (0.9) | 0.8 (0.3) | 0.733 |
| AUC egress 60 (SD) | 92.8 (10.0) | 96.7 (1.8) | 0.113 |
| AUC egress 120 (SD) | 87.9 (11.9) | 92.8 (2.3) | 0.127 |
| AUC egress 180 (SD) | 82.9 (12.9) | 88.3 (4.3) | 0.164 |
| AUC egress 240 (SD) | 78.2 (13.3) | 83.8 (5.4) | 0.168 |
| AUC egress 300 (SD) | 73.7 (13.5) | 73.3 (6.0) | 0.271 |

Abbreviations: SD, standard deviation; CLTI, chronic limb-threatening ischemia; AUC, area under the curve.

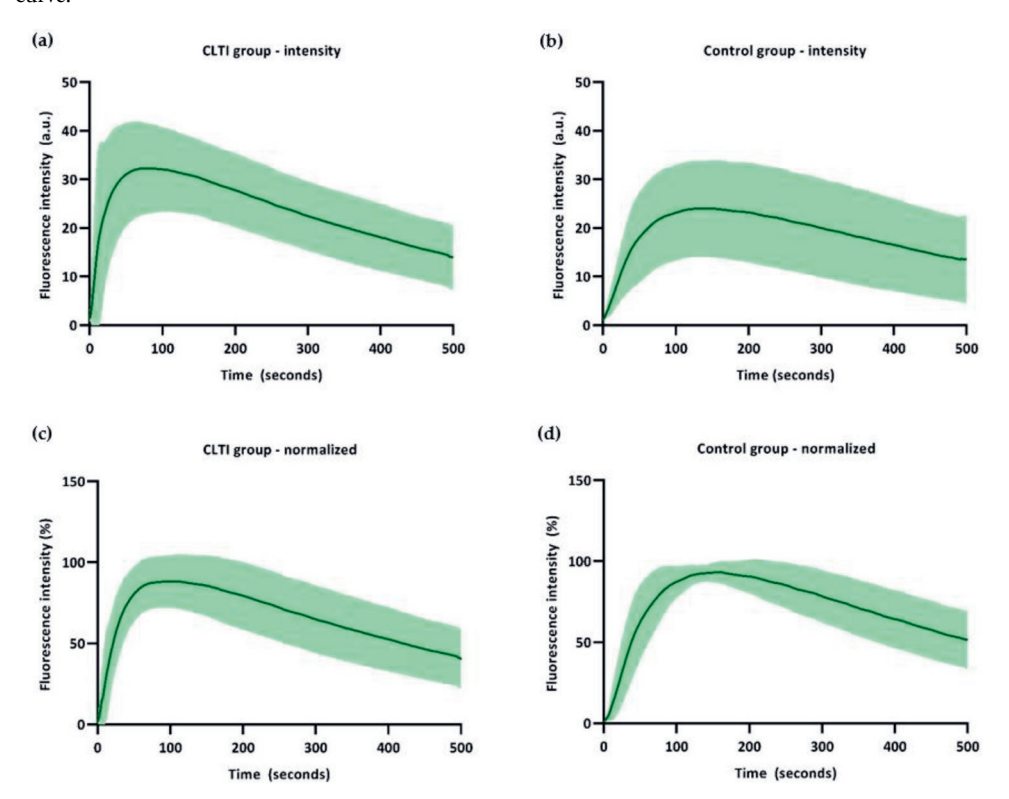


Figure 4. Absolute intensity - and normalized time-intensity curves for the CLTI group and control group: (a) Absolute time-intensity curve CLTI group, (b) Absolute time-intensity curve control group, (c) Normalized time-intensity curve CLTI group, (d) Normalized time-intensity curve control group.

Discussion

This study demonstrates the different perfusion patterns as seen on ICG NIR fluorescence imaging between patients with CLTI and control patients. Interestingly, most inflow parameters observed in patients with CLTI were higher compared to the control group. Concerning the outflow of ICG, however, no significant differences were observed. Furthermore, there is a widespread distribution of measured intensity over time in both groups. There are several earlier studies reporting the use of ICG NIR fluorescence imaging for perfusion assessment in patients with LEAD as well as control patients (7, 16, 18, 20-25). In these studies, an abundance of parameters have been examined, which have been compared to varying diagnosis measurements, including the ABI, TP and transcutaneous oxygen pressure measurements. Patterns of foot perfusion in non-LEAD control patients were analyzed in one study (18). Regarding inflow parameters, Igari et al. found a prolonged time to maximum intensity for patients with LEAD compared to control patients (18). No statistical differences were seen for the maximum intensity and T1/2 between the two groups. The differences in perfusion patterns amongst various stages of LEAD were analyzed in several studies. When comparing inflow parameters between different stages of LEAD, Terasaki et al. observed a prolonged T1/2 for Fontaine stage 3 compared to stage 2, however, this was not observed for stage 4. Regarding outflow, their study concluded that a percentage decrease of 90% in maximum measured intensity was the most accurate parameter in diagnosing LEAD. For patients with CLTI, Venermo et al. found an increase in inflow, the PDE10, to be strongly correlated to the transcutaneous oxygen pressure in patients with diabetes mellitus (23). The same parameter was moderately correlated in patients without diabetes mellitus, suggesting a difference in perfusion patterns between these groups. According to the findings in these earlier studies and the results found in this study, the hypothesis that LEAD progression leads to diminished in- and outflow of ICG is debatable. Several mechanisms might contribute to the increased inflow of ICG seen in patients with CLTI in this study. First, ICG NIR fluorescence imaging is able to penetrate tissue to a depth of several millimeters (26). Therefore, this imaging technique mainly visualizes the skin with superficial vessels and the superior part of the subcutaneous tissue, i.e. the microcirculation. Nutritional capillaries of this microcirculation in the foot account for approximately 15% of total foot blood flow, which is regulated by various mechanisms including arteriovenous (AV) shunts (27). For patients with LEAD and CLTI in particular, the diminished blood flow has led to hypoxia altering microcirculatory function and damaging these regulatory mechanisms (3, 5). The dysfunction of AV shunts might lead to a relative increase of blood flow to the skin in patients with CLTI, which also explains the "dependent rubor" seen in this group. Secondly, atherosclerosis leads to stiffness of the arterial wall which is a common finding in patients with CLTI and leading to an increased pulse wave velocity (28). In a healthy arterial system, the blood flow is gradually transmitted to the peripheral tissue due to compliance of the vessel wall (29). This might explain the more gradual perfusion pattern seen in the control group. Furthermore, damage to the microcirculation in CLTI leads to transcapillary leakage, which might further enhance the measured NIR fluorescence intensity. Although a higher dosage of ICG was administered in the majority of patients in the control group, it is unlikely that this would have influenced the perfusion pattern. Besides, an overall lower absolute intensity was seen in this group. To confirm the findings on increased inflow, a larger cohort of patients with CLTI is needed. Therefore, due to the small sample size, the conclusions in this study must be perceived as a proof of concept. Besides the small cohort size of patients with CLTI, this study is limited by the heterogenous aspect of the CLTI population. In particular for patients with diabetes mellitus, skin perfusion follows a different pattern than LEAD Fontaine stage 4 patients without diabetes mellitus. Therefore, future studies should distinguish between CLTI patients with and without diabetes mellitus. Furthermore, the control group used in the present study were patients scheduled for liver metastasectomy and therefore might not resemble healthy volunteers in terms of comorbidities. Although LEAD was excluded based on medical history and ABI measurements, there could be differences in perfusion patterns with healthy volunteers. Therefore, in future patient selection and further understanding perfusion patterns, healthy volunteers should be taken into account as well. With regards to the NIR fluorescence intensity analysis, the use of normalized time-intensity curves seems rational, since intensity-related parameters are prone to multiple influencing factors, including camera distance and ICG dosage (30, 31). This normalization minimizes the effect of these influencing factors on the measured intensity and contributes to a more narrow distribution, as can be seen in the time-intensity curves in this study. The use of this normalization might be of use in future research on quantification of tissue perfusion with ICG NIR fluorescence imaging.

Conclusion

An increase in inflow parameters was observed with ICG NIR fluorescence imaging in patients with CLTI compared to control patients. This is possibly explained by damage to the regulatory mechanisms of the microcirculation and arterial stiffness. In the search for providing cut-off values for adequate perfusion, more research in lager cohorts is needed on in- and outflow patterns for control patients and various stages of LEAD.

Reference list

- 1. Weitz JI, Byrne J, Clagett GP, Farkouh ME, Porter JM, Sackett DL, et al. Diagnosis and treatment of chronic arterial insufficiency of the lower extremities: a critical review. Circulation. 1996;94(11):3026-49.
- Aboyans V, Ricco JB, Bartelink MEL, Bjorck M, Brodmann M, Cohnert T, et al. 2017 ESC Guidelines on the Diagnosis and Treatment of Peripheral Arterial Diseases, in collaboration with the European Society for Vascular Surgery (ESVS). Rev Esp Cardiol (Engl Ed). 2018;71(2):111.
- 3. Krishna SM, Moxon JV, Golledge J. A review of the pathophysiology and potential biomarkers for peripheral artery disease. Int J Mol Sci. 2015;16(5):11294-322.
- 4. Conte MS, Bradbury AW, Kolh P, White JV, Dick F, Fitridge R, et al. Global vascular guidelines on the management of chronic limb-threatening ischemia. J Vasc Surg. 2019;69(6S):3S-125S e40.
- 5. Abularrage CJ, Sidawy AN, Aidinian G, Singh N, Weiswasser JM, Arora S. Evaluation of the microcirculation in vascular disease. J Vasc Surg. 2005;42(3):574-81.
- Misra S, Shishehbor MH, Takahashi EA, Aronow HD, Brewster LP, Bunte MC, et al. Perfusion
 Assessment in Critical Limb Ischemia: Principles for Understanding and the Development of
 Evidence and Evaluation of Devices: A Scientific Statement From the American Heart Association.
 Circulation. 2019;140(12):e657-e72.
- 7. van den Hoven P, Ooms S, van Manen L, van der Bogt KEA, van Schaik J, Hamming JF, et al. A systematic review of the use of near-infrared fluorescence imaging in patients with peripheral artery disease. J Vasc Surg. 2019;70(1):286-97 e1.
- 8. Kikuchi S, Miyake K, Tada Y, Uchida D, Koya A, Saito Y, et al. Laser speckle flowgraphy can also be used to show dynamic changes in the blood flow of the skin of the foot after surgical revascularization. Vascular. 2019;27(3):242-51.
- 9. Cindil E, Erbas G, Akkan K, Cerit MN, Sendur HN, Zor MH, et al. Dynamic Volume Perfusion CT of the Foot in Critical Limb Ischemia: Response to Percutaneous Revascularization. AJR Am J Roentgenol. 2020;214(6):1398-408.
- Driessen C, Arnardottir TH, Lorenzo AR, Mani MR. How should indocyanine green dye angiography be assessed to best predict mastectomy skin flap necrosis? A systematic review. J Plast Reconstr Aesthet Surg. 2020;73(6):1031-42.
- 11. Dupree A, Riess H, Detter C, Debus ES, Wipper SH. Utilization of indocynanine green fluorescent imaging (ICG-FI) for the assessment of microperfusion in vascular medicine. Innov Surg Sci. 2018;3(3):193-201.
- 12. Vahrmeijer AL, Hutteman M, van der Vorst JR, van de Velde CJ, Frangioni JV. Image-guided cancer surgery using near-infrared fluorescence. Nat Rev Clin Oncol. 2013;10(9):507-18.
- 13. Schaafsma BE, Mieog JS, Hutteman M, van der Vorst JR, Kuppen PJ, Lowik CW, et al. The clinical use of indocyanine green as a near-infrared fluorescent contrast agent for image-guided oncologic surgery. J Surg Oncol. 2011;104(3):323-32.
- Parmeshwar N, Sultan SM, Kim EA, Piper ML. A Systematic Review of the Utility of Indocyanine Angiography in Autologous Breast Reconstruction. Ann Plast Surg. 2020; Publish Ahead of Print.

- 15. Zimmermann A, Roenneberg C, Wendorff H, Holzbach T, Giunta RE, Eckstein HH. Early postoperative detection of tissue necrosis in amputation stumps with indocyanine green fluorescence angiography. Vasc Endovascular Surg. 2010;44(4):269-73.
- 16. Terasaki H, Inoue Y, Sugano N, Jibiki M, Kudo T, Lepantalo M, et al. A quantitative method for evaluating local perfusion using indocyanine green fluorescence imaging. Ann Vasc Surg. 2013;27(8):1154-61.
- 17. Kang Y, Lee J, Kwon K, Choi C. Application of novel dynamic optical imaging for evaluation of peripheral tissue perfusion. Int J Cardiol. 2010;145(3):e99-101.
- 18. Igari K, Kudo T, Uchiyama H, Toyofuku T, Inoue Y. Indocyanine green angiography for the diagnosis of peripheral arterial disease with isolated infrapopliteal lesions. Ann Vasc Surg. 2014;28(6):1479-84.
- Brouwers J, van Doorn LP, van Wissen RC, Putter H, Hamming JF. Using maximal systolic acceleration to diagnose and assess the severity of peripheral artery disease in a flow model study. J Vasc Surg. 2020;71(1):242-9.
- 20. Kang Y, Lee J, Kwon K, Choi C. Dynamic fluorescence imaging of indocyanine green for reliable and sensitive diagnosis of peripheral vascular insufficiency. Microvasc Res. 2010;80(3):552-5.
- 21. Zimmermann A, Roenneberg C, Reeps C, Wendorff H, Holzbach T, Eckstein HH. The determination of tissue perfusion and collateralization in peripheral arterial disease with indocyanine green fluorescence angiography. Clin Hemorheol Microcirc. 2012;50(3):157-66.
- 22. Igari K, Kudo T, Uchiyama H, Toyofuku T, Inoue Y. Quantitative evaluation of microvascular dysfunction in peripheral neuropathy with diabetes by indocyanine green angiography. Diabetes Res Clin Pract. 2014;104(1):121-5.
- 23. Venermo M, Settembre N, Alback A, Vikatmaa P, Aho PS, Lepantalo M, et al. Pilot Assessment of the Repeatability of Indocyanine Green Fluorescence Imaging and Correlation with Traditional Foot Perfusion Assessments. Eur J Vasc Endovasc Surg. 2016;52(4):527-33.
- Nishizawa M, Igari K, Kudo T, Toyofuku T, Inoue Y, Uetake H. A Comparison of the Regional Circulation in the Feet between Dialysis and Non-Dialysis Patients using Indocyanine Green Angiography. Scand J Surg. 2016.
- 25. Goncalves LN, van den Hoven P, van Schaik J, Leeuwenburgh L, Hendricks CHF, Verduijn PS, et al. Perfusion Parameters in Near-Infrared Fluorescence Imaging with Indocyanine Green: A Systematic Review of the Literature. Life (Basel). 2021;11(5).
- 26. Frangioni JV. In vivo near-infrared fluorescence imaging. Curr Opin Chem Biol. 2003;7(5):626-34.
- 27. Rossi M, Carpi A. Skin microcirculation in peripheral arterial obliterative disease. Biomed Pharmacother. 2004;58(8):427-31.
- 28. Mendes-Pinto D, Rodrigues-Machado MDG, Navarro TP, Dardik A. Association Between Critical Limb Ischemia, the Society for Vascular Surgery Wound, Ischemia and Foot Infection (WIfI) Classification System and Arterial Stiffness. Ann Vasc Surg. 2020;63:250-8 e2.
- 29. Yu S, McEniery CM. Central Versus Peripheral Artery Stiffening and Cardiovascular Risk. Arterioscler Thromb Vasc Biol. 2020;40(5):1028-33.

- 30. Pruimboom T, van Kuijk SMJ, Qiu SS, van den Bos J, Wieringa FP, van der Hulst R, et al. Optimizing Indocyanine Green Fluorescence Angiography in Reconstructive Flap Surgery: A Systematic Review and Ex Vivo Experiments. Surg Innov. 2020;27(1):103-19.
- 31. Lutken CD, Achiam MP, Svendsen MB, Boni L, Nerup N. Optimizing quantitative fluorescence angiography for visceral perfusion assessment. Surg Endosc. 2020;34(12):5223-33.



Chapter 5

Normalization of time-intensity curves for quantification of foot perfusion using near-infrared fluorescence imaging with indocyanine green

P. van den Hoven ¹, F.P. Tange ¹, J.P. van der Valk ¹, N.A. Nerup ², H. Putter ¹, C.S.P. Van Rijswijk ¹, J. van Schaik ¹, A. Schepers ¹, A.L. Vahrmeijer ¹, J.F. Hamming ¹, J.R. van der Vorst ¹

1. Leiden University Medical Center, Leiden, The Netherlands 2. Rigshospitalet, Copenhagen, Denmark

Published in Journal of Endovascular Therapy, March 2022.

Abstract

Introduction

Near-infrared (NIR) fluorescence imaging using indocyanine green (ICG) is gaining popularity for the quantification of tissue perfusion, including foot perfusion in patients with lower extremity arterial disease (LEAD). However, the absolute fluorescence intensity is influenced by patient – and system related factors limiting reliable and valid quantification. To enhance the quality of quantitative perfusion assessment using ICG NIR fluorescence imaging, normalization of the measured time-intensity curves seems useful.

Methods

In this cohort study, the effect of normalization on two aspects of ICG NIR fluorescence imaging in assessment of foot perfusion was measured: the repeatability and the region selection. Following intravenous administration of ICG, the NIR fluorescence intensity in both feet was recorded for 10 minutes using the Quest Spectrum Platform. The effect of normalization on repeatability was measured in the non-treated foot in patients undergoing unilateral revascularization pre- and postprocedural (repeatability group). The effect of normalization on region selection was performed in patients without LEAD (region selection group). Absolute and normalized time-intensity curves were compared.

Results

Successful ICG NIR fluorescence imaging was performed in 54 patients (repeatability group, n=38; region selection group, n=16). For the repeatability group, normalization of the time-intensity curves displayed a comparable inflow pattern for repeated measurements. For the region selection group, the maximum fluorescence intensity (Imax) demonstrated significant differences between the three measured regions of the foot (p=0.002). Following normalization, the time-intensity curves in both feet were comparable for all three regions.

Conclusions

This study shows the effect of normalization of time-intensity curves on both the repeatability and region selection in ICG NIR fluorescence imaging. The significant difference between absolute parameters in various regions of the foot demonstrates the limitation of absolute intensity in interpreting tissue perfusion. Therefore, normalization and standardization of camera settings are essential steps towards reliable and valid quantification of tissue perfusion using ICG NIR fluorescence imaging.

Introduction

Near-infrared (NIR) fluorescence imaging has been used as an imaging modality for various indications, including tumor visualization, identification of vital structures and assessment of tissue perfusion (1-4). For the assessment of tissue perfusion, NIR fluorescence imaging has shown potential value in various fields, including vascular -, gastrointestinal - and reconstructive surgery (2, 5, 6). However, there are several factors that influence the stability of the fluorescence intensity which compromise the reliability and validity of the technique, precluding broad application in clinical practice (3, 5). Fluorescence imaging in the NIR light spectrum (700-900nm) has the advantage of high tissue penetration and low autofluorescence, allowing for clear visualization of a fluorophore with an emission peak in the NIR spectrum (7, 8). For the assessment of tissue perfusion, the most utilized fluorophore in NIR fluorescence imaging is indocyanine green (ICG). The feasibility of ICG for assessment of tissue perfusion is explained by the binding to plasma proteins combined with a short half-life due to rapid clearance by the liver (9). Following intravenous administration of ICG, information about tissue perfusion can be obtained using either a qualitative - or quantitative interpretation of the fluorescence intensity. Applications of qualitative interpretation include the assessment of skin viability in reconstructive surgery and the evaluation of bowl perfusion in gastrointestinal surgery (10, 11). However, the qualitative and therefore subjective interpretation of the fluorescence intensity leads to different surgical outcomes and impedes comparison between studies (12). Quantitative assessment of perfusion focuses on describing the fluorescence intensity change over time in a region of interest (ROI), representing the dynamic properties of blood flow (13). Although the benefits of reliable quantitative analysis are evident, several factors influence the stability of the measured fluorescence intensity (3, 8). These factors are either related to the patient or the camera system. Patient related factors include skin type, edema, ICG concentration and the presence of ulcers (14, 15). The change in tissue properties can lead to an alteration in excitation energy and quantum yield, influencing the measured fluorescence intensity (8). Furthermore, the configuration of the camera system affects the measured intensity in several ways, including distance and angle to the target area and optical settings comprising the exposure time and gain (16, 17). This abundance of influencing factors raises questions as to whether analysis of the absolute intensity is appropriate for reliable assessment of tissue perfusion (3, 5). An emerging analyzing method for the assessment of tissue perfusion that adjusts for absolute intensity is normalization (18). Normalization sets the maximum fluorescence intensity at 100% and displays the fluorescence intensity over time as a percentual change. It is hypothesized that this method decreases the influence of beforementioned influencing factors and allows for more reliable and valid quantification. Therefore, the aim of this study was to investigate the influence of normalization on repeatability and region selection of ICG NIR fluorescence imaging for assessment of foot perfusion.

Methods

This cohort study was approved by the Medical Research and Ethics Committee of the Leiden University Medical Center and registered in the Dutch Trial Register (#NL7531). Patients undergoing unilateral successful revascularization procedures and non-LEAD control patients were included. Patients were included in a single academic hospital in the Netherlands from December 2018 until April 2021. Patients were excluded based on contra-indications to ICG: allergy or hypersensitivity to ICG or (sodium) iodide; hyperthyroidism, autonomous thyroid adenoma, pregnancy, kidney failure (eGFR <45) or severe liver failure. Informed consent was obtained from all individual participants included in the study.

ICG NIR fluorescence imaging

ICG NIR fluorescence imaging measurements were performed using the Quest Spectrum Platform® (Quest Medical Imaging, Middenmeer, The Netherlands). This system consists of a LED laser combined with a camera measuring light in the visible and NIR light spectrum (700-900nm). All patients underwent ankle-brachial index (ABI) - and toe pressure (TP) measurements prior to the ICG NIR fluorescence imaging measurement. Upon ICG (VERDYE 25 mg, Diagnostic Green GmbH, Aschheim-Dornach, Germany) administration, the camera registered the NIR fluorescence intensity change over time in both feet for 10 minutes. All measurements were performed with the patient in a supine position in a darkened room. The camera was placed at approximately 50cm of the foot, perpendicular to the dorsum of the foot. All videos were recorded using an exposure time of 145 milliseconds and a gain of 22 decibel.

Repeatability group

The effect of normalization on repeatability was measured in the non-treated foot of patients undergoing unilateral revascularization. It was hypothesized that the time-intensity curves in the non-treated contralateral foot remained unchanged. A subset of this group was described in an earlier study in which only normalized data was used (19). ICG NIR fluorescence imaging was performed before – and after the procedure (<3 days) and patients were administered an intravenous bolus injection of 0.1 mg/kg ICG. Three ROIs were analyzed: 1. The dorsum of the foot, 2. The forefoot and 3. The hallux.

Region selection group

The effect of normalization on region selection was measured in non-LEAD control patients, since this group is most likely to display a homogenous perfusion pattern in various regions of the foot. This group consisted of patients undergoing liver metastasectomy who were administered ICG intravenously 1 day before surgery. In this

group, a bolus injection of 10mg ICG was administered intravenously as part of the non-investigational treatment protocol. Three regions were selected based on differences in camera distance and angle of the surface area to the camera. These regions included: 1. The hallux, 2. The first ray of the foot and 3. The lateral foot.

Data analysis

The Quest Research Framework® (Quest Medical Imaging, Middenmeer, the Netherlands) software was used for the quantification of the measured NIR fluorescence intensity. Following manual selection of an ROI, the software creates a curve of the fluorescence intensity change over time. The measured fluorescence intensity is displayed as arbitrary units (a.u.). When normalization is applied, the software sets the maximum fluorescence intensity in the selected ROI at 100% and displays the fluorescence intensity over time as a percentual change of this maximum fluorescence. The absolute time-intensity curves and normalized time-intensity curves with the extracted parameters are displayed in Supplementary Figure 1 and Supplementary Table 1. After normalization, absolute parameters including ingress and ingress rate are depleted. The normalized slope for the ingress and egress are defined as percentage per second. A tracker was used to ensure the ROI was synchronized with foot movement and baseline subtraction was applied. Starting time of the time-intensity curves was defined as an increase of 1 arbitrary unit for the absolute time-intensity curves and 1% for the normalized time-intensity curves. Statistical analyses were performed using IBM SPSS Statistics 25 (IBM Corp. Released 2017. IBM SPSS Statistics for Windows, Version 25.0. Armonk, NY, USA: IBM Corp.). Parameters in the repeatability group were compared with the Wilcoxon rank sign test for paired analyses. Results for the region selection group were compared using the Kruskal-Wallis test.

Results

ICG NIR fluorescence imaging was successfully performed in 54 patients. The patient characteristics for both the repeatability group and region selection group are displayed in Table 1. In the repeatability group, consisting of 38 patients, the mean age was 70.9 years with a standard deviation (SD) of 7.0. The mean ABI in this group was 0.89 (SD 0.30). with a mean TP of 76 mmHg (SD 30). The 16 patients (32 limbs) in the region selection group displayed a mean age of 66.6 years (SD 12.3) with a mean ABI of 1.11 (SD 0.10) and a mean TP of 106 mmHg (SD 22).

Table 1. Patient characteristics.

| | Repeatability group (n=38) | Region selection group (n=16) |
|--------------------------|----------------------------|-------------------------------|
| Age in years (SD) | 70.9 (7.0) | 66.6 (12.3) |
| Female, n(%) | 17 (44.7) | 3 (18.8) |
| Diabetes, n(%) | 12 (31.6) | 3 (18.8) |
| Hypertension, n(%) | 29 (76.3) | 7 (43.8) |
| Active smoking, n(%) | 8 (21.1) | 1 (6.3) |
| History of smoking, n(%) | 35 (92.1) | 10 (62.5) |
| Mean baseline ABI (SD) | 0.89 (0.30) | 1.11 (0.10) |
| Mean baseline TP (SD) | 76 (30) | 106 (22) |

Abbreviations: SD, standard deviation; TP, toe pressure; ABI, ankle-brachial index.

Repeatability group

For the repeatability group, no significant differences were found for the ABI and TP preand post-procedural (ABI: 0.89 vs. 0.86, p=0.806; TP: 76 vs. 72, p=0.466). The results on repeated measurements for both the absolute and normalized time-intensity curves in the repeatability group are displayed in Figure 1. For the absolute time-intensity curves, an increase in maximum fluorescence intensity (Imax) is seen for all three ROIs for the repeated measurements. Furthermore, the absolute time-intensity curves in ROI 3 display a wider distribution compared to the other ROIs. After normalization, the timeintensity curves display a similar distribution amongst all three ROIs. Furthermore, the inflow pattern is comparable for repeated measurements. The results on quantification of the time-intensity curves for the repeatability group are depicted in Table 2. Except for the area under the curve (AUC) ingress in ROI 3, no statistical differences were found for all measured parameters in all ROIs. Although not significant, absolute parameters including the Imax, ingress rate and slope were higher for the repeated measurement. For the ingress rate in ROI 1 and 2, the repeated measurement displayed a fifty percent increase (ROI1: 0.4 vs 0.6, p=0.587, ROI 2: 0.4 vs. 0.6, p=0.404). After normalization, the slope in all ROIs were comparable (ROI 1: 3.4 vs. 3.5, p=0.983, ROI 2: 3.4 vs. 3.4, p=0.936, ROI 3: 0.8 vs 1.0, p=0.502).

Region selection group

The absolute and normalized time-intensity curves for the region selection group are visualized in Figure 2. Results for the right- and left foot are displayed separately. For the absolute time-intensity curves, there is a clear discrepancy for the measured maximum fluorescence intensity between the three ROIs. The lowest maximum intensity is seen in ROI 3, i.e. the lateral foot, which is visualized in Figure 3. Furthermore, there is a wide distribution amongst all three measured ROIs. After normalization, the patterns observed in both the right and left foot are comparable for all three ROIs. The extracted parameters for the region selection group are displayed in Table 3. For the fixed

parameters, no significant differences were found for all three ROIs in both feet. For the absolute parameters, a statistical significance was seen for the Imax, ingress rate and slope ingress in the right as well as the left foot (right: p=0.002, 0.015, 0.005; left: p=0.006, 0.011, 0.037, respectively). After normalization, a significant difference was seen for the slope egress in both feet (right: p<0.001, left: p<0.001). The normalized ingress slope was comparable for all ROIs (right: p=0.408, left p=0.921).

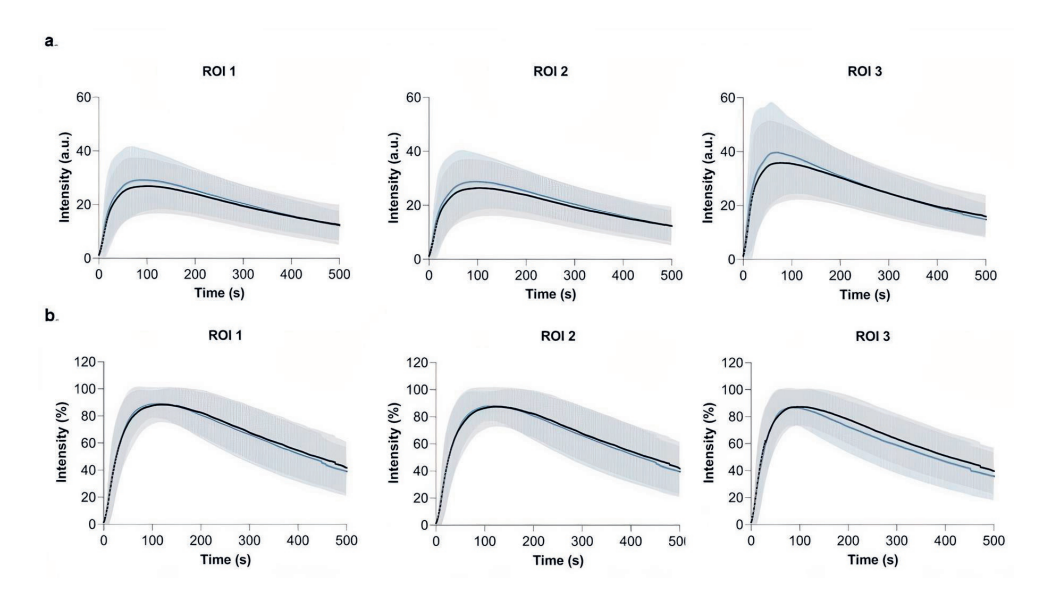


Figure 1. Repeatability group - absolute (a) and normalized (b) time-intensity curves for the three ROIs of the foot pre- (black line) and post-revascularization (blue line). Results are displayed as mean (bold line) with one standard deviation distribution.

 $\textbf{Table 2.} \ \ \textbf{Repeatability group-ICG NIR fluorescence imaging outcome.}$

| | Mean \pm SD | Mean \pm SD | | | | | | | |
|---------------------------------|------------------|------------------|-------|------------------|------------------|-------|-----------------|-----------------|-------|
| ABI | 0.89 ± 0.30 | 0.86 ± 0.33 | 908.0 | | | | | | |
| TP | 76 ± 30 | 72 ± 27 | 0.466 | | | | | | |
| | ROI 1 | | | ROI 2 | | | ROI 3 | | |
| | Pre | Post | d | Pre | Post | d | Pre | Post | d |
| ICG NIR fluorescence parameters | Mean ± SD | Mean ± SD | , | Mean ± SD | Mean ± SD | , | Mean ± SD | Mean ± SD | |
| Tmax | 111.8 ± 68.1 | 102.8 ± 61.3 | 0.346 | 115.1 ± 67.8 | 103.8 ± 60.9 | 0.218 | 90.1 ± 58.1 | 75.0 ± 48.4 | 0.177 |
| AUC10 | 47.6 ± 2.3 | 47.4 ± 1.9 | 0.733 | 47.5 ± 2.8 | 47.3 ± 2.0 | 0.538 | 47.6 ± 2.7 | 47.7 ± 4.6 | 0.922 |
| AUC ingress | 71.6 ± 4.9 | 70.6 ± 5.6 | 0.538 | 70.9 ± 5.5 | 69.5 ± 5.8 | 0.438 | 70.0 ± 5.6 | 66.5 ± 7.9 | 0.028 |
| AUC egress 60 | 95.2 ± 4.5 | 94.8 ± 4.1 | 0.879 | 95.0 ± 4.9 | 94.8 ± 4.8 | 0.567 | 93.5 ± 5.8 | 91.8 ± 7.8 | 0.331 |
| AUC egress 120 | 90.2 ± 6.8 | 89.5 ± 6.6 | 0.617 | 89.7 ± 7.5 | 89.3 ± 6.9 | 0.500 | 87.8 ± 8.5 | 85.4 ± 10.2 | 0.242 |
| AUC egress 180 | 84.9 ± 8.4 | 83.9 ± 8.3 | 0.645 | 84.3 ± 9.0 | 83.5 ± 8.5 | 0.521 | 82.4 ± 9.9 | 79.8 ± 11.5 | 0.172 |
| AUC egress 240 | 79.5 ± 9.4 | 78.5 ± 9.5 | 0.626 | 79.2 ± 10.0 | 78.4 ± 9.7 | 0.572 | 77.6 ± 10.6 | 74.4 ± 12.2 | 0.177 |
| AUC egress 300 | 74.6 ± 10.2 | 69.9 ± 12.8 | 0.623 | 73.9 ± 10.7 | 73.2 ± 10.5 | 0.578 | 72.6 ± 10.9 | 69.9 ± 12.8 | 0.172 |
| Imax | 30.0 ± 10.8 | 32.9 ± 13.5 | 0.286 | 29.7 ± 10.8 | 32.9 ± 12.6 | 0.204 | 41.2 ± 16.7 | 47.1 ± 22.2 | 0.187 |
| Ingress rate | 0.4 ± 0.5 | 0.6 ± 0.8 | 0.587 | 0.4 ± 0.5 | 0.6 ± 0.7 | 0.404 | 0.8 ± 0.9 | 1.2 ± 1.6 | 0.150 |
| Absolute slope ingress | 1.1 ± 0.9 | 1.4 ± 1.5 | 0.528 | 1.1 ± 0.8 | 1.4 ± 1.4 | 0.293 | 1.9 ± 1.8 | 2.7 ± 3.0 | 0.158 |
| Absolute slope egress | 0.3 ± 0.1 | 0.3 ± 0.2 | 0.833 | 0.2 ± 0.1 | 0.3 ± 0.1 | 0.350 | 0.3 ± 0.2 | 0.5 ± 0.5 | 0.133 |
| Normalized slope ingress | 3.4 ± 2.0 | 3.5 ± 2.4 | 0.983 | 3.4 ± 2.0 | 3.4 ± 2.3 | 0.936 | 4.1 ± 2.4 | 4.5 ± 2.9 | 0.656 |
| Normalized slope egress | 0.8 ± 0.4 | 0.8 ± 0.5 | 0.547 | 0.8 ± 0.4 | 0.7 ± 0.3 | 0.313 | 0.8 ± 0.4 | 1.0 ± 0.7 | 0.502 |

Abbreviations: SD, standard deviation; TP, toe pressure; ABI, ankle brachial index; AUC, area under the curve.

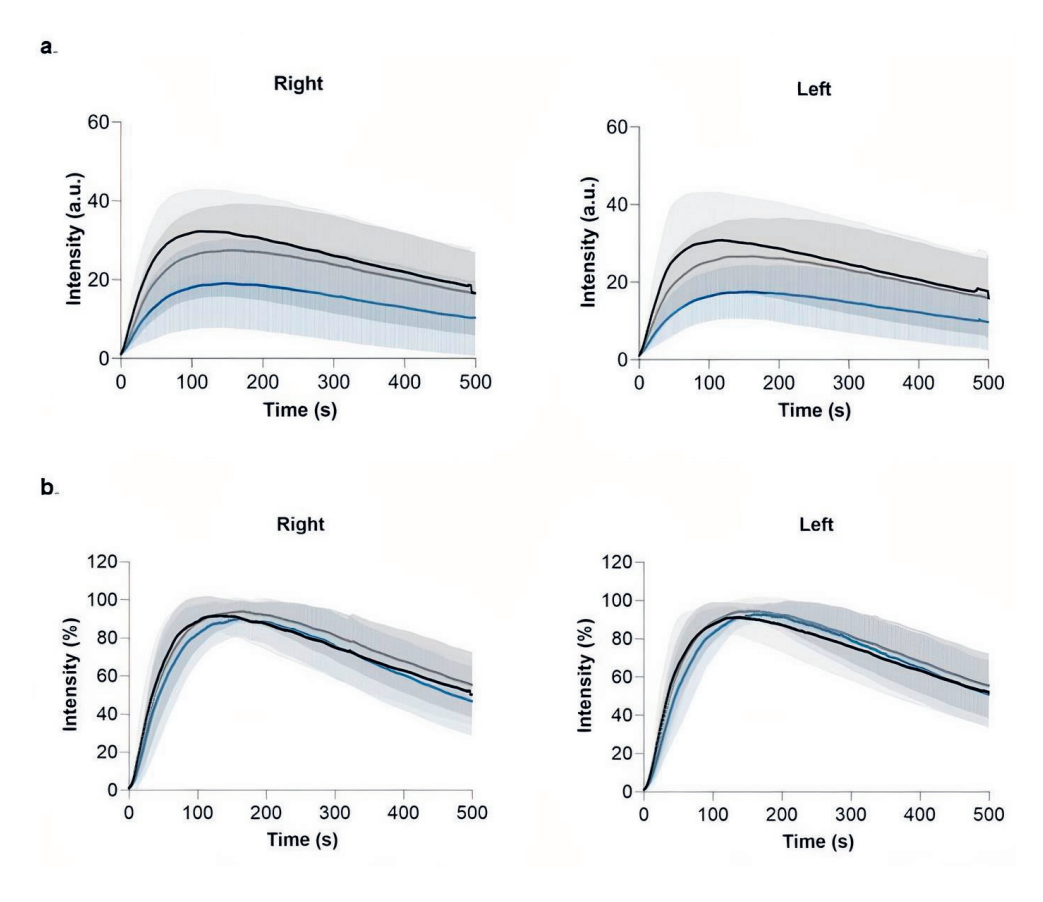


Figure 2. Region selection group - absolute (a) and normalized (b) time-intensity curves for the right and left foot displaying the hallux region (black line), first ray region (grey line) and lateral foot region (blue line). Results are displayed as mean (bold line) with one standard deviation distribution.

Table 3. Region selection group - ICG NIR fluorescence imaging outcome.

| | Right foot | | | | Left foot | | | |
|---------------------------------|------------------|------------------|------------------|--------|------------------|------------------|------------------|--------|
| | ROI 1 | ROI 2 | ROI 3 | Ь | ROI 1 | ROI 2 | ROI 3 | Ь |
| ICG NIR fluorescence parameters | Mean ± SD | Mean ± SD | Mean ± SD | | Mean ± SD | Mean ± SD | Mean ± SD | |
| Tmax | 157.7 ± 69.4 | 161.7 ± 69.8 | 126.2 ± 64.6 | 0.353 | 157.5 ± 74.9 | 153.5 ± 72.6 | 124.3 ± 73.5 | 0.341 |
| AUC10 | 50.0 ± 5.0 | 48.7 ± 4.7 | 49.8 ± 5.2 | 0.663 | 48.9 ± 6.3 | 49.3 ± 6.0 | 50.9 ± 6.4 | 0.547 |
| AUC ingress | 72.5 ± 5.3 | 68.7 ± 4.7 | 69.8 ± 5.7 | 0.147 | 72.2 ± 4.0 | 67.8 ± 5.0 | 69.5 ± 4.2 | 0.039 |
| AUC egress 60 | 96.9 ± 2.0 | 95.8 ± 1.9 | 96.2 ± 2.7 | 0.161 | 97.1 ± 1.9 | 95.0 ± 4.1 | 96.0 ± 2.8 | 0.140 |
| AUC egress 120 | 93.3 ± 3.1 | 91.9 ± 3.2 | 91.8 ± 4.7 | 0.470 | 93.6 ± 2.5 | 90.7 ± 4.9 | 91.8 ± 4.8 | 0.287 |
| AUC egress 180 | 89.1 ± 4.5 | 87.1 ± 4.6 | 87.4 ± 6.1 | 0.541 | 89.4 ± 3.5 | 85.6 ± 5.5 | 87.5 ± 6.2 | 0.169 |
| AUC egress 240 | 84.9 ± 5.6 | 81.6 ± 5.0 | 83.0 ± 7.1 | 0.270 | 85.1 ± 4.4 | 79.9 ± 5.8 | 83.3 ± 7.1 | 0.061 |
| AUC egress 300 | 80.3 ± 6.0 | 76.9 ± 5.7 | 78.2 ± 7.6 | 0.388 | 80.3 ± 5.0 | 74.7 ± 6.3 | 78.5 ± 7.4 | 0.065 |
| Imax | 28.4 ± 18.8 | 18.9 ± 7.8 | 33.7 ± 14.3 | 0.002 | 29.3 ± 12.8 | 21.1 ± 12.1 | 35.2 ± 11.8 | 900.0 |
| Ingress rate | 0.2 ± 0.1 | 0.1 ± 0.1 | 0.4 ± 0.4 | 0.015 | 0.2 ± 0.1 | 0.2 ± 0.1 | 0.4 ± 0.3 | 0.011 |
| Absolute slope ingress | 0.7 ± 0.4 | 0.4 ± 0.2 | 1.0 ± 0.7 | 0.005 | 0.7 ± 0.4 | 0.6 ± 0.4 | 1.0 ± 0.7 | 0.037 |
| Absolute slope egress | 0.2 ± 0.1 | 0.2 ± 0.1 | 0.2 ± 0.1 | 0.288 | 0.2 ± 0.1 | 0.2 ± 0.1 | 0.2 ± 0.1 | 0.104 |
| Normalized slope ingress | 2.4 ± 0.8 | 2.2 ± 0.6 | 2.8 ± 1.3 | 0.408 | 2.4 ± 0.8 | 2.7 ± 1.5 | 2.9 ± 1.9 | 0.921 |
| Normalized slope egress | 0.7 ± 0.3 | 1.2 ± 0.5 | 0.6 ± 0.2 | <0.001 | 0.6 ± 0.3 | 1.2 ± 0.5 | 0.6 ± 0.2 | <0.001 |

Abbreviations: SD, standard deviation; AUC, area under the curve.

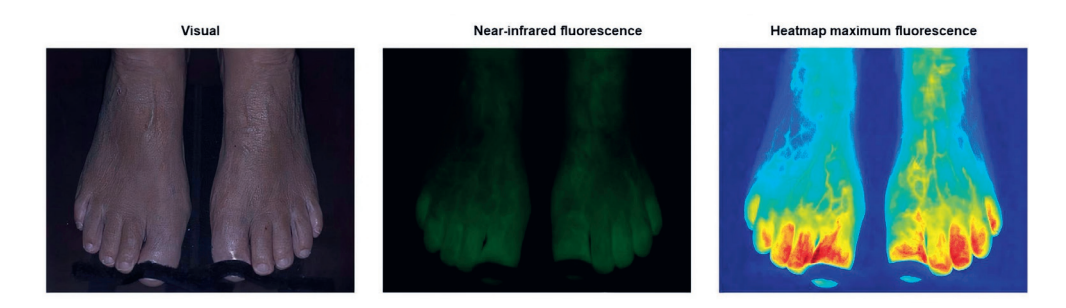


Figure 3. Output of the Quest Research Framework® showing the visual light (left), near-infrared fluorescence (middle) and heatmap of the maximum fluorescence intensity (right) of a 70-year old female control patient. The heatmap illustrates the diminished observed maximum fluorescence intensity found on the lateral side of the foot.

Discussion

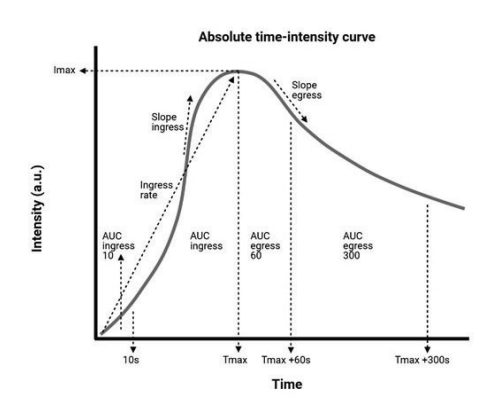
This study demonstrates the effect of normalization of time-intensity curves on both the repeatability and region selection in the quantification of tissue perfusion using ICG NIR fluorescence imaging. Concerning repeatability, time-intensity curves display a more similar pattern following normalization. Although not significant, absolute parameters including ingress rate and slope varied between measurements and displayed a wider distribution. These findings suggest that absolute parameters are less reliable and more susceptive to fluctuations on repeated measurements. The repeatability of ICG NIR fluorescence imaging for assessment of tissue perfusion in patients with LEAD was described in one earlier study (20). This study found time-intensity curves to be repeatable and focused on time- as well as absolute parameters. However, repeated measurements were performed in the same setting by the same investigator, thus reducing the impact of influencing factors of measurement setup on the NIR signal. Regarding the region selection, absolute inflow parameters in the present study were all significantly different between various areas of the foot. After normalization, the slope ingress was comparable. For the interpretation of tissue perfusion with ICG NIR fluorescence imaging, these are important findings, since absolute parameters can thus lead to an incorrect interpretation of actual tissue perfusion. In the search for reliable quantification of tissue perfusion with ICG NIR fluorescence imaging, an abundance of parameters have been studied in various target tissues (13). For the quantification of skin perfusion in patients with LEAD for example, time-related and normalized parameters appear to be superior to measurements of maximum intensity (21, 22). In reconstructive surgery, a commonly performed analyzing method for tissue quantification is the use of relative parameters (6). However, this method does not take into account the camera angle and distance, leading to a misperception of actual

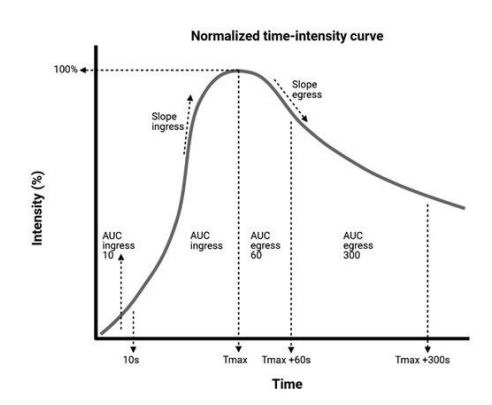
perfusion. In gastro-intestinal surgery, the effect of normalization on quantification of bowl perfusion was measured in several studies (3, 18, 23). In a series of studies by Nerup et al. on gastrointestinal perfusion in porcine models, the normalized slope ingress was significantly correlated with regional blood flow and local lactate levels (18, 23). Although reliable quantification of tissue perfusion seems to tend towards the use of normalized parameters, several items have to be discussed. First of all, normalization of the time-intensity curves leads to alteration of data, which precludes the use of absolute parameters that can be useful in the prediction of tissue necrosis (24). Furthermore, normalization can be unreliable when the measured fluorescence intensity levels are below a certain threshold. Magnification of the signal can then lead to high fluctuations in the percentual change, which is the presumable cause of the significant increase in normalized egress slope in the region selection group in this study. In addressing the effect of normalization on region selection, the cohort in this study consisted of patients without known LEAD who were administered ICG as part of the treatment protocol for liver metastasectomy. By selecting this group of patients, this study avoided the exposure of healthy volunteers to ICG. However, due to comorbidities, there might have been changes in regional circulation of the foot that could have influenced the measured fluorescence intensity. Therefore, future studies on ICG NIR fluorescence imaging for foot perfusion assessment should ideally be performed in a control group that has a significantly lower risk of possible unknown underlying LEAD. Concerning the repeatability group, this study is limited by the small sample size. Besides, measurements were performed on different days post-procedural, which might have led to inter-patient variability. Furthermore, changes in hemodynamic status, including blood pressure and pulse could have influenced the measured fluorescence intensity (25). Despite these limitations, the present study describes a new perspective on assessment of tissue perfusion in the foot using ICG NIR fluorescence imaging. Improving reliability and validity of ICG NIR fluorescence imaging in quantification of tissue perfusion using normalization can promote comparability between studies. To compare standardized quantification methods between studies, it is also of paramount importance to report on the used camera system and - settings, including exposure time and gain. Addressing these aspects in future studies on perfusion assessment using ICG NIR fluorescence imaging is an essential step towards reliable quantification. Whether this quantification will lead to a better understanding of actual in- and outflow of foot perfusion has yet to be determined. However, reliable quantification will be a crucial factor in the value of future studies on perfusion assessment with ICG NIR fluorescence imaging. Therefore, normalization should be a standard procedure in the analysis of the measured fluorescence intensity in these studies. The valid and reliable assessment of tissue perfusion using ICG NIR fluorescence imaging could then potentially aid in the prediction of clinical outcome following revascularization or in assessing the probability of wound healing.

Conclusion

This study shows the effect of normalization of time-intensity curves on both the repeatability and region selection for the quantification of foot perfusion using ICG NIR fluorescence imaging. The significant difference between absolute parameters in various regions of the foot demonstrates the limitation of absolute intensity in interpreting tissue perfusion. Therefore, normalization and standardization of camera settings are essential steps towards reliable and valid quantification of tissue perfusion using ICG NIR fluorescence imaging.

Appendices





Supplementary Figure 1. Absolute (left) and normalized (right) time-intensity curves with extracted parameters.

Supplementary Table 1. ICG NIR fluorescence imaging parameters.

| Fixed parameters | Absolute parameters | Normalized parameters |
|--------------------|------------------------|-----------------------|
| Tmax (s) | Imax (a.u.) | Slope ingress (%/s) |
| AUC10 (%) | Ingress rate (a.u./s) | Slope egress (%/s) |
| AUC ingress (%) | Slope ingress (a.u./s) | |
| AUC egress 60 (%) | Slope egress (a.u./s) | |
| AUC egress 120 (%) | | |
| AUC egress 180 (%) | | |
| AUC egress 240 (%) | | |
| AUC egress 300 (%) | | |

Abbreviations: s, seconds; AUC, area under the curve; a.u., arbitrary unit(s).

Reference list

- de Valk KS, Handgraaf HJ, Deken MM, Sibinga Mulder BG, Valentijn AR, Terwisscha van Scheltinga AG, et al. A zwitterionic near-infrared fluorophore for real-time ureter identification during laparoscopic abdominopelvic surgery. Nat Commun. 2019;10(1):3118.
- van den Hoven P, Ooms S, van Manen L, van der Bogt KEA, van Schaik J, Hamming JF, et al. A
 systematic review of the use of near-infrared fluorescence imaging in patients with peripheral artery
 disease. J Vasc Surg. 2019;70(1):286-97 e1.
- 3. Lutken CD, Achiam MP, Svendsen MB, Boni L, Nerup N. Optimizing quantitative fluorescence angiography for visceral perfusion assessment. Surg Endosc. 2020;34(12):5223-33.
- 4. Schaafsma BE, Mieog JS, Hutteman M, van der Vorst JR, Kuppen PJ, Lowik CW, et al. The clinical use of indocyanine green as a near-infrared fluorescent contrast agent for image-guided oncologic surgery. J Surg Oncol. 2011;104(3):323-32.
- 5. Slooter MD, Mansvelders MSE, Bloemen PR, Gisbertz SS, Bemelman WA, Tanis PJ, et al. Defining indocyanine green fluorescence to assess anastomotic perfusion during gastrointestinal surgery: systematic review. BJS Open. 2021;5(2).
- 6. Driessen C, Arnardottir TH, Lorenzo AR, Mani MR. How should indocyanine green dye angiography be assessed to best predict mastectomy skin flap necrosis? A systematic review. J Plast Reconstr Aesthet Surg. 2020;73(6):1031-42.
- 7. Vahrmeijer AL, Hutteman M, van der Vorst JR, van de Velde CJ, Frangioni JV. Image-guided cancer surgery using near-infrared fluorescence. Nat Rev Clin Oncol. 2013;10(9):507-18.
- 8. Frangioni JV. In vivo near-infrared fluorescence imaging. Curr Opin Chem Biol. 2003;7(5):626-34.
- 9. Desmettre T, Devoisselle JM, Mordon S. Fluorescence properties and metabolic features of indocyanine green (ICG) as related to angiography. Surv Ophthalmol. 2000;45(1):15-27.
- Johnson AC, Colakoglu S, Chong TW, Mathes DW. Indocyanine Green Angiography in Breast Reconstruction: Utility, Limitations, and Search for Standardization. Plast Reconstr Surg Glob Open. 2020;8(3):e2694.
- 11. Blanco-Colino R, Espin-Basany E. Intraoperative use of ICG fluorescence imaging to reduce the risk of anastomotic leakage in colorectal surgery: a systematic review and meta-analysis. Tech Coloproctol. 2018;22(1):15-23.
- 12. Achterberg FB, Deken MM, Meijer RPJ, Mieog JSD, Burggraaf J, van de Velde CJH, et al. Clinical translation and implementation of optical imaging agents for precision image-guided cancer surgery. Eur J Nucl Med Mol Imaging. 2021;48(2):332-9.
- Goncalves LN, van den Hoven P, van Schaik J, Leeuwenburgh L, Hendricks CHF, Verduijn PS, et al. Perfusion Parameters in Near-Infrared Fluorescence Imaging with Indocyanine Green: A Systematic Review of the Literature. Life (Basel). 2021;11(5).
- 14. Dupree A, Riess H, Detter C, Debus ES, Wipper SH. Utilization of indocynanine green fluorescent imaging (ICG-FI) for the assessment of microperfusion in vascular medicine. Innov Surg Sci. 2018;3(3):193-201.

- 15. van der Vorst JR, Schaafsma BE, Verbeek FP, Swijnenburg RJ, Hutteman M, Liefers GJ, et al. Dose optimization for near-infrared fluorescence sentinel lymph node mapping in patients with melanoma. Br J Dermatol. 2013;168(1):93-8.
- 16. Pruimboom T, van Kuijk SMJ, Qiu SS, van den Bos J, Wieringa FP, van der Hulst R, et al. Optimizing Indocyanine Green Fluorescence Angiography in Reconstructive Flap Surgery: A Systematic Review and Ex Vivo Experiments. Surg Innov. 2020;27(1):103-19.
- 17. Gioux S, Choi HS, Frangioni JV. Image-guided surgery using invisible near-infrared light: fundamentals of clinical translation. Mol Imaging. 2010;9(5):237-55.
- 18. Nerup N, Andersen HS, Ambrus R, Strandby RB, Svendsen MBS, Madsen MH, et al. Quantification of fluorescence angiography in a porcine model. Langenbecks Arch Surg. 2017;402(4):655-62.
- 19. Van den Hoven P, F SW, Van De Bent M, Goncalves LN, Ruig M, S DVDB, et al. Near-infrared fluorescence imaging with indocyanine green for quantification of changes in tissue perfusion following revascularization. Vascular. 2021:17085381211032826.
- Venermo M, Settembre N, Alback A, Vikatmaa P, Aho PS, Lepantalo M, et al. Pilot Assessment of the Repeatability of Indocyanine Green Fluorescence Imaging and Correlation with Traditional Foot Perfusion Assessments. Eur J Vasc Endovasc Surg. 2016;52(4):527-33.
- 21. Igari K, Kudo T, Uchiyama H, Toyofuku T, Inoue Y. Indocyanine green angiography for the diagnosis of peripheral arterial disease with isolated infrapopliteal lesions. Ann Vasc Surg. 2014;28(6):1479-84.
- 22. Nakamura M, Igari K, Toyofuku T, Kudo T, Inoue Y, Uetake H. The evaluation of contralateral foot circulation after unilateral revascularization procedures using indocyanine green angiography. Sci Rep. 2017;7(1):16171.
- 23. Ronn JH, Nerup N, Strandby RB, Svendsen MBS, Ambrus R, Svendsen LB, et al. Laser speckle contrast imaging and quantitative fluorescence angiography for perfusion assessment. Langenbecks Arch Surg. 2019;404(4):505-15.
- 24. Van Den Hoven P, Van Den Berg SD, Van Der Valk JP, Van Der Krogt H, Van Doorn LP, Van De Bogt KEA, et al. Assessment of Tissue Viability Following Amputation Surgery Using Near-Infrared Fluorescence Imaging With Indocyanine Green. Ann Vasc Surg. 2021.
- 25. Osterkamp J, Strandby R, Nerup N, Svendsen M, Svendsen L, Achiam M. Quantitative fluorescence angiography detects dynamic changes in gastric perfusion. Surg Endosc. 2020.



Chapter 6

Quantification of near-infrared fluorescence imaging with indocyanine green in free flap breast reconstruction

P. van den Hoven ^{1*}, P.S. Verduijn ^{1*}, L. van Capelle ¹, F.P. Tange ¹, M. Michi ¹, L.U.M. Corion ¹, B.G. Sibinga Mulder ¹, M.A.M. Mureau ², A.L. Vahrmeijer ¹, J.R. van der Vorst ¹

- Leiden University Medical Center, Leiden, The Netherlands
 Erasmus Medical Center, Rotterdam, The Netherlands
 - * Authors contributed equally and share first authorship

Published in Journal of Plastic, Reconstructive and Aesthetic Surgery, January 2022.

Abstract

Introduction

One of the complications of free flap breast reconstruction is the occurrence of skin - and fat necrosis. Intra-operative use of near-infrared (NIR) fluorescence imaging with indocyanine green (ICG) has the potential to predict these complications. In this study, quantification of the fluorescence intensity measured in free flap breast reconstruction was performed to gain insight in the perfusion patterns observed with ICG NIR fluorescence imaging.

Methods

ICG NIR fluorescence imaging was performed in patients undergoing free flap breast reconstruction following mastectomy. After completion of the arterial and venous anastomosis, 7.5mg ICG was administered intravenously. The fluorescence intensity over time was recorded using the Quest Spectrum platform. Four regions of interest (ROI) were selected based on location and interpretation of the NIR fluorescence signal: 1. The perforator, 2. Normal perfusion, 3. Questionable perfusion and 4. Low perfusion. Time-intensity curves were analyzed and two parameters were extracted: Tmax and Tmax slope.

Results

Successful ICG NIR fluorescence imaging was performed in 13 patients undergoing 17 free flap procedures. Region selection included 16 perforator -, 17 normal perfusion -, 8 questionable perfusion - and 5 low perfusion ROIs. Time-intensity curves of the perforator ROIs were comparable to the ROIs of normal perfusion and demonstrated a fast inflow. No outflow was observed for the ROIs with questionable and low perfusion.

Conclusion

This study provides insight in the perfusion patterns observed with ICG NIR fluorescence imaging in free flap breast reconstruction. Future studies should correlate quantitative parameters with clinical perfusion assessment and outcome.

Introduction

Breast cancer accounts for 30 percent of newly diagnosed malignancies in female patients and it is the leading cause of death among middle-aged women (1). The surgical treatment of breast cancer is performed either with breast-conserving surgery or mastectomy. For reconstructive surgery following mastectomy, the use of autologous tissue is gaining popularity (2). Commonly performed autologous breast reconstruction procedures include deep inferior epigastric artery perforator (DIEP) -, superficial inferior epigastric artery (SIEA) - and profunda artery perforator (PAP) flap reconstructions (3, 4). The advantages of successful autologous breast reconstruction, including long-term beneficial outcome, are evident. However, free flap surgery following mastectomy is also associated with complications including skin – and fat necrosis (5, 6). In the assessment of tissue perfusion during free flap surgery, the surgeon relies on subjective observations including skin color, capillary refill and the occurrence of bleeding. Possible techniques to aid the surgeon while assessing tissue perfusion include laser doppler and near-infrared (NIR) fluorescence imaging with indocyanine green (ICG) (7). ICG NIR fluorescence imaging is a technique that measures fluorescence in the NIR light spectrum (700-900nm), which is characterized by deep tissue penetration and low autofluorescence (8). Following intravenous administration of ICG, a fluorophore with an absorption and excitation peak in the NIR light spectrum, a time-intensity curve of the measured fluorescence intensity can be generated. The feasibility of ICG in perfusion assessment is explained by its confinement to the vascular component due to binding with serum proteins including albumin (9). For patients undergoing breast (reconstructive) surgery, the intra-operative use of ICG NIR fluorescence imaging was demonstrated to aid surgeons in their assessment of skin viability, thereby reducing the occurrence of skin necrosis in several studies (10, 11). This reduction in necrosis can be explained by the intra-operative removal of tissue with diminished fluorescence intensity observed with ICG NIR fluorescence imaging. The localization of areas with diminished perfusion is based on subjective evaluation of the measured fluorescence intensity by the surgeon (12). However, to objectively assess tissue perfusion and enhance the reliability of this technique, quantification of the fluorescence intensity is of paramount importance. Quantification studies on the use of ICG NIR fluorescence imaging in reconstructive surgery mainly have focused on absolute and relative fluorescence intensity parameters (10, 13, 14). However, there is no consensus on which parameter is most accurate for the assessment of tissue perfusion. In the search for determining cut-off values for tissue perfusion, more information is needed about the perfusion patterns observed with ICG NIR fluorescence imaging. Therefore, the aim of this study was to gain insight in these perfusion patterns by performing quantitative assessment of the ICG NIR fluorescence imaging used in free flap breast reconstruction.

Methods

This pilot cohort study was approved by the Medical Research and Ethics Committee of the Leiden University Medical Center and was conducted in accordance with the Declaration of Helsinki. Patients undergoing autologous breast reconstruction between February - and September 2019 in a single tertiary hospital in the Netherlands were included. Exclusion criteria were allergy to ICG, iodine or shellfish and impaired renal function. This study adhered to the STROBE statement on the report of cohort studies (15).

ICG NIR fluorescence imaging measurement

Intra-operative ICG NIR fluorescence imaging was performed using the Quest Spectrum Platform® (Quest Medical Imaging, Middenmeer, The Netherlands). This camera system consists of a laser with a camera that measures light in the visible and NIR light spectrum (700-830nm). Directly following an intravenous bolus injection of 7.5 mg ICG (VERDYE 25 mg, Diagnostic Green GmbH, Aschheim-Dornach, Germany), the fluorescence intensity of the anastomosed free flap was recorded for 3 minutes according to protocol. The perforator, including artery and vein, was marked with a staple. Measurements were performed with the camera placed perpendicular to the flap surface at a distance of approximately 50 centimeters. The operating room was cleared of ambient light throughout the measurement.

Data analysis

Postoperatively, a reconstructive surgeon (PV) evaluated the fluorescence intensity videos and, if observed, selected four regions of interest (ROI): 1. Perforator, 2. Normal perfusion, 3. Questionable perfusion (possible resection) and 4. Low perfusion (resection). The selected ROIs were analyzed using the Quest Research Framework® (Quest Medical Imaging, Middenmeer, the Netherlands). For the selected ROIs, the software creates a time-intensity curve of the measured intensity in arbitrary units (a.u.). Videos were analyzed for 3 minutes following start of intensity increase. Two parameters were extracted (Figure 1): time to maximum intensity (Tmax) and time to maximum slope (Tmax slope). Baseline subtraction was applied to all time-intensity curves. A tracker synchronized the ROI with movement. Videos without data on camera settings were excluded. Statistical analyses were performed using IBM SPSS Statistics 25 (IBM Corp. Released 2017. IBM SPSS Statistics for Windows, Version 25.0. Armonk, NY, USA: IBM Corp.). Results for the four ROIs were compared using the Kruskal-Wallis test.

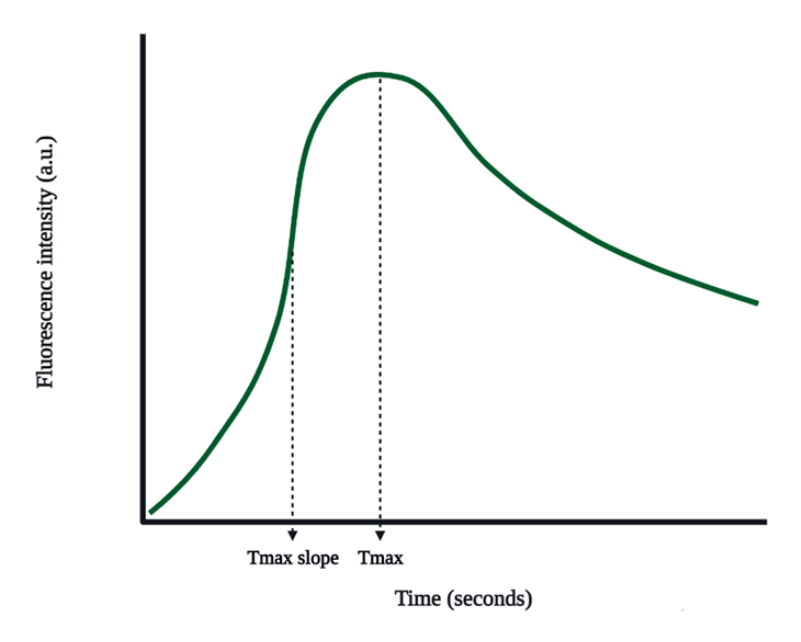


Figure 1. Time-intensity curve with extracted parameters.

Results

Successful ICG NIR fluorescence imaging was performed in 13 patients undergoing 13 DIEP -. 3 PAP - and 1 SIEA flap reconstruction(s). Four patients underwent a bilateral free flap reconstruction. The patient characteristics are displayed in Table I. An example of a normal perfusion pattern is shown in Figure 2 and Video 1 (available online via JPRAS), in which the fluorescence intensity change over time in a 65-year old patient undergoing a DIEP flap reconstruction is displayed. The video is accelerated elevenfold and demonstrates the NIR fluorescence intensity change during the measurement of 3 minutes. An example of a normal and questionably perfused ROI in a 55-year old patient following DIEP flap surgery is shown in Figure 3. The ROI selection included 16 perforator -, 17 normal perfusion -, 8 questionable perfusion - and 5 low perfusion areas. In one patient undergoing a DIEP flap reconstruction, 2 perforators were used.

Table I. Patient characteristics.

| Characteristics | Number of patients (n=13) |
|-----------------------------|---------------------------|
| Age (years, SD) | 50.4 (10.6) |
| Diabetes | 0 |
| Hypertension | 2 |
| Active smoking | 1 |
| Type reconstructive surgery | |
| DIEP | 10 |
| PAP | 2 |
| SIEAP | 1 |

Abbreviations: SD, standard deviation; DIEP, deep inferior epigastric perforator; PAP, profunda artery perforator; SIEAP, superficial inferior epigastric artery perforator.

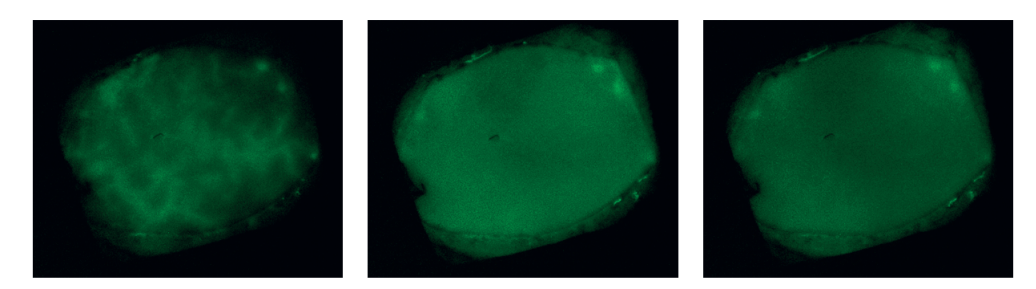


Figure 2. NIR fluorescence intensity change over time in a patient undergoing a DIEP flap reconstruction.

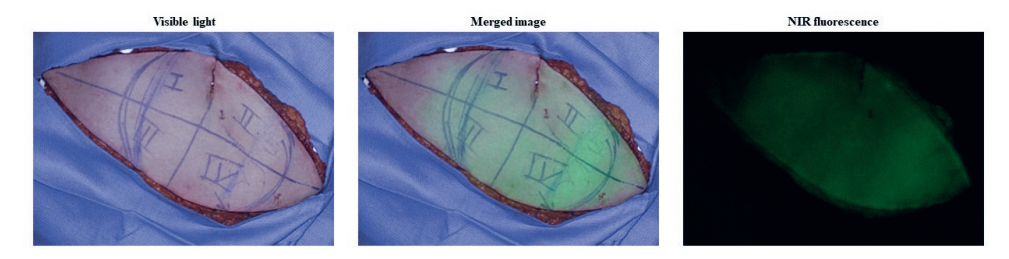


Figure 3. ICG NIR fluorescence imaging in a patient undergoing a DIEP flap reconstruction showing the visible (left), merged (middle) and NIR fluorescence (right) output.

Time-intensity curves

The time-intensity curves for the four selected ROIs are shown in Figure 4. For the perforator ROI, the majority of curves display a steep ingress followed by a steep egress. The egress phase is reached within 180 seconds for all time-intensity curves in this ROI. For the time-intensity curves in the ROIs marked as normal perfusion, an inflow pattern similar to the perforator ROI can be observed. Furthermore, comparable to

the perforator ROI, the egress phase is reached within 180 seconds in the majority of ROIs with normal perfusion. For both ROIs, there is a widespread distribution among measured maximum fluorescence intensity between curves. For the ROIs with questionable and low perfusion, a clearly lower maximum fluorescence intensity is demonstrated compared to the perforator and normal perfusion ROIs. Moreover, the curves for questionable and low perfusion ROIs are characterized by a prolonged inflow and the egress phase is not reached for all time-intensity curves in these ROIs.

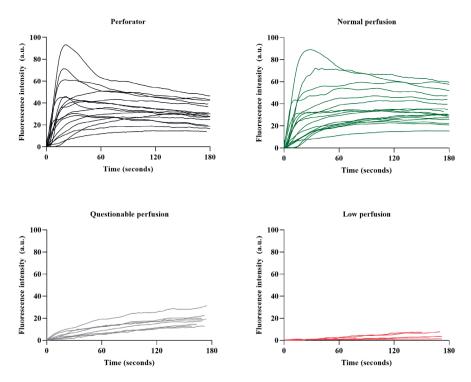


Figure 4. Time-intensity curves for the four measured ROIs.

Quantitative analysis

The results on quantitative analysis of the time-intensity curves for the four ROIs are depicted in Table II and Figure 5. The Tmax was reached earliest in the perforator ROI (63.9 seconds, standard deviation 47.8). For the Tmax slope, results between the perforator – and normal perfusion ROIs were similar 7.2 and 6.8 seconds). Tmax and Tmax slope were prolonged in the ROI with low perfusion (164.9 and 99.1 seconds respectively). Differences between the ROIs were statistically significant for both parameters (Tmax: p<0.001, Tmax slope: p=0.006).

Table II. Quantitative analysis of the time-intensity curves displaying the Tmax and Tmax slope for each ROI

| | Perforator artery | Normal perfusion | Questionable perfusion | Low perfusion |
|--------------------------|----------------------|---------------------|------------------------|---------------|
| Tmax, seconds (SD) | 68.6 (49.5) | 111.3 (42.2) | 159.9 (12.7) | 164.9 (30.4) |
| Tmax slope, seconds (SD) | 5.6 (3.8) | 4.7 (3.1) | 20.2 (27.4) | 83.9 (18.1) |

Abbreviations: SD, standard deviation.

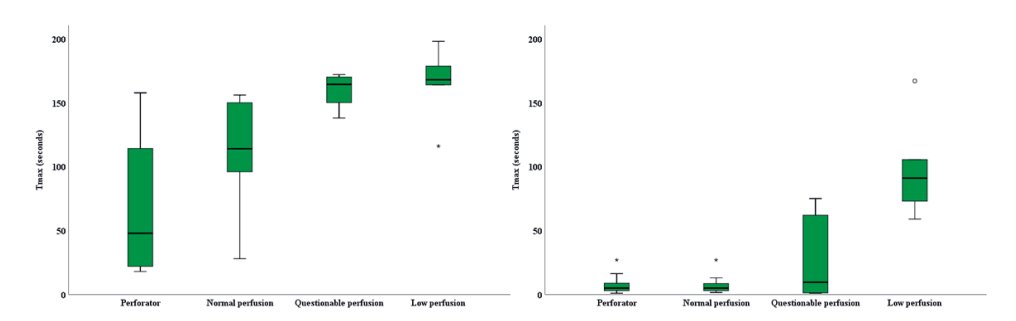


Figure 5. Quantitative analysis of the four ROIs showing the Tmax (left) and Tmax slope (right).

Clinical outcome and follow-up

Flap loss occurred in one patient undergoing a bilateral DIEP flap reconstruction. In this 44-year old female, the DIEP flap on the right side had to be removed, after a failed salvage procedure, on the fourth day postoperatively due to venous congestion. No low - or questionable perfusion ROIs were observed with ICG NIR fluorescence imaging intra-operatively.

Discussion

This study on the quantitative evaluation of ICG NIR fluorescence imaging in free flap breast reconstruction provides insight in the perfusion patterns of free flaps as observed by the surgeon. Interestingly, time-intensity curves for the perforator region were comparable to the regions classified as normal perfusion. Furthermore, these are the only observed regions in which outflow was observed. Current use of ICG NIR fluorescence imaging in free flap breast reconstruction relies on the qualitative and therefore subjective judgement of the NIR signal by the surgeon. However, to aid in decision making and enhance the reliability of ICG NIR fluorescence imaging in these patients, quantitative analysis is required. For quantitative assessment of tissue

perfusion in breast surgery, studies on mastectomy skin flap necrosis have shown relative perfusion deficits to be predictive of tissue necrosis (16-18). Relative parameters are described as a percentage of the measured maximum intensity in the target area. For patients undergoing autologous breast reconstruction, relative parameters were used as a cut-off value by Alstrup et al. to guide intra-operative decision-making on the excision of poorly perfused tissue (19). However, this study found no significant differences regarding skin necrosis between patients with - and without the use of ICG NIR fluorescence imaging. Relative parameters are influenced by the measured fluorescence intensity and therefore subjective to various influencing factors including camera angle, camera distance and ICG dosage (13, 20). Moreover, relative intensity parameters provide no data about intensity change over time. For assessment of perfusion in free flaps following microvascular anastomosis, it seems reasonable time-related parameters are more appropriate in predicting in- and outflow. This was observed in a study on the perfusion of fibular free flaps for reconstruction of hemimandibulectomy defects, in which an increased postoperative slope was found following surgical revision due to venous thrombosis (21). Concerning the quantitative analysis of ICG NIR fluorescence imaging in free flap breast reconstruction, one study assessed various perfusion patterns in DIEP flap surgery and found an increased fluorescence intensity as well as the fluorescence intensity inflow rate for perforator regions compared to more distal regions of the flap (22). These results are similar to the findings in this study, in which an increased inflow was observed for the perforator and normal perfusion ROIs. However, in exploring the value of inflow parameters in assessment of perfusion and prediction of clinical outcome, a larger cohort is needed, which is a limitation of this study. Furthermore, only one event of flap loss occurred in this study, precluding evaluation of the predictive value of quantitative assessment of ICG NIR fluorescence imaging for this outcome. Correlating quantitative parameters with clinical assessment and outcome can identify cut-off values for reliable tissue perfusion. Moreover, in this search towards valid an reliable use of ICG NIR fluorescence imaging for perfusion assessment, it is of paramount importance that comparability studies are performed between different camera systems. As shown in a review by Dsouza et al., commercially available ICG NIR fluorescence imaging systems differ in settings, including the excitation source and light sensors (23). Therefore, comparing the perfusion patterns in free flaps measured with various camera systems will provide insight in the applicability of this technique. Despite these limitations, the present study provides insight in the observed perfusion patterns for various regions which is a step towards the quantification of tissue perfusion in free flap surgery. Future studies should focus on the standardization of ICG NIR fluorescence imaging in free flap surgery and correlate quantitative parameters with clinical perfusion assessment and clinical outcome, including fat necrosis and flap viability. When performed in large cohorts, these studies can identify perfusion patterns correlated with these clinical outcomes.

Thise possible early stage prediction of fat necrosis and skin flap viability using ICG NIR fluorescence imaging will have a significant impact on patient outcome.

Conclusion

This study provides insight in the perfusion patterns observed with ICG NIR fluorescence imaging in free flap breast reconstruction. Future studies with this technique in free flap surgery should focus on the correlation of quantitative parameters with clinical perfusion assessment and outcome.

Reference list

- 1. Siegel RL, Miller KD, Fuchs HE, Jemal A. Cancer Statistics, 2021. CA Cancer J Clin. 2021;71(1):7-33.
- 2. Nahabedian MY, Patel K. Autologous flap breast reconstruction: Surgical algorithm and patient selection. J Surg Oncol. 2016;113(8):865-74.
- 3. Rose J, Puckett Y. Breast Reconstruction Free Flaps. StatPearls. Treasure Island (FL)2021.
- Qian B, Xiong L, Li J, Sun Y, Sun J, Guo N, et al. A Systematic Review and Meta-Analysis on Microsurgical Safety and Efficacy of Profunda Artery Perforator Flap in Breast Reconstruction. J Oncol. 2019;2019;9506720.
- Bhullar H, Hunter-Smith DJ, Rozen WM. Fat Necrosis After DIEP Flap Breast Reconstruction: A Review of Perfusion-Related Causes. Aesthetic Plast Surg. 2020;44(5):1454-61.
- 6. Wilkins EG, Hamill JB, Kim HM, Kim JY, Greco RJ, Qi J, et al. Complications in Postmastectomy Breast Reconstruction: One-year Outcomes of the Mastectomy Reconstruction Outcomes Consortium (MROC) Study. Ann Surg. 2018;267(1):164-70.
- 7. Smit JM, Negenborn VL, Jansen SM, Jaspers MEH, de Vries R, Heymans MW, et al. Intraoperative evaluation of perfusion in free flap surgery: A systematic review and meta-analysis. Microsurgery. 2018;38(7):804-18.
- 8. Frangioni JV. In vivo near-infrared fluorescence imaging. Curr Opin Chem Biol. 2003;7(5):626-34.
- 9. Landsman ML, Kwant G, Mook GA, Zijlstra WG. Light-absorbing properties, stability, and spectral stabilization of indocyanine green. J Appl Physiol. 1976;40(4):575-83.
- 10. Driessen C, Arnardottir TH, Lorenzo AR, Mani MR. How should indocyanine green dye angiography be assessed to best predict mastectomy skin flap necrosis? A systematic review. J Plast Reconstr Aesthet Surg. 2020;73(6):1031-42.
- Lauritzen E, Damsgaard TE. Use of Indocyanine Green Angiography decreases the risk of complications in autologous- and implant-based breast reconstruction: A systematic review and meta-analysis. J Plast Reconstr Aesthet Surg. 2021.
- 12. Komorowska-Timek E, Gurtner GC. Intraoperative perfusion mapping with laser-assisted indocyanine green imaging can predict and prevent complications in immediate breast reconstruction. Plast Reconstr Surg. 2010;125(4):1065-73.
- 13. Goncalves LN, van den Hoven P, van Schaik J, Leeuwenburgh L, Hendricks CHF, Verduijn PS, et al. Perfusion Parameters in Near-Infrared Fluorescence Imaging with Indocyanine Green: A Systematic Review of the Literature. Life (Basel). 2021;11(5).
- 14. Munabi NC, Olorunnipa OB, Goltsman D, Rohde CH, Ascherman JA. The ability of intraoperative perfusion mapping with laser-assisted indocyanine green angiography to predict mastectomy flap necrosis in breast reconstruction: a prospective trial. J Plast Reconstr Aesthet Surg. 2014;67(4):449-55.
- von Elm E, Altman DG, Egger M, Pocock SJ, Gotzsche PC, Vandenbroucke JP, et al. The Strengthening the Reporting of Observational Studies in Epidemiology (STROBE) statement: guidelines for reporting observational studies. Lancet. 2007;370(9596):1453-7.

- 16. Moyer HR, Losken A. Predicting mastectomy skin flap necrosis with indocyanine green angiography: the gray area defined. Plast Reconstr Surg. 2012;129(5):1043-8.
- Johnson AC, Colakoglu S, Chong TW, Mathes DW. Indocyanine Green Angiography in Breast Reconstruction: Utility, Limitations, and Search for Standardization. Plast Reconstr Surg Glob Open. 2020;8(3):e2694.
- 18. Newman MI, Samson MC, Tamburrino JF, Swartz KA. Intraoperative laser-assisted indocyanine green angiography for the evaluation of mastectomy flaps in immediate breast reconstruction. J Reconstr Microsurg. 2010;26(7):487-92.
- Alstrup T, Christensen BO, Damsgaard TE. ICG angiography in immediate and delayed autologous breast reconstructions: peroperative evaluation and postoperative outcomes. J Plast Surg Hand Surg. 2018;52(5):307-11.
- 20. Lutken CD, Achiam MP, Svendsen MB, Boni L, Nerup N. Optimizing quantitative fluorescence angiography for visceral perfusion assessment. Surg Endosc. 2020;34(12):5223-33.
- 21. Hitier M, Cracowski JL, Hamou C, Righini C, Bettega G. Indocyanine green fluorescence angiography for free flap monitoring: A pilot study. J Craniomaxillofac Surg. 2016;44(11):1833-41.
- 22. Girard N, Delomenie M, Malhaire C, Sebbag D, Roulot A, Sabaila A, et al. Innovative DIEP flap perfusion evaluation tool: Qualitative and quantitative analysis of indocyanine green-based fluorescence angiography with the SPY-Q proprietary software. PLoS One. 2019;14(6):e0217698.
- AV DS, Lin H, Henderson ER, Samkoe KS, Pogue BW. Review of fluorescence guided surgery systems: identification of key performance capabilities beyond indocyanine green imaging. J Biomed Opt. 2016;21(8):80901.



Part II

Clinical translation of quantitative tissue perfusion assessment using near-infrared fluorescence imaging with indocyanine green in lower extremity arterial disease



Chapter 7

Near-infrared fluorescence imaging with indocyanine green for quantification of changes in tissue perfusion following revascularization

P. van den Hoven ¹, F.S. Weller ¹, M. van de Bent ¹, L.N. Goncalves ¹, M. Ruig ¹, S.D. van den Berg ¹, S. Ooms ¹, J.S.D. Mieog ¹, K.E.A. van der Bogt ¹, J. van Schaik ¹, A. Schepers ¹, A.L. Vahrmeijer ¹, J.F. Hamming ¹, J.R. van der Vorst ¹

1. Leiden University Medical Center, Leiden, The Netherlands

Abstract

Introduction

Current diagnostic modalities for patients with peripheral artery disease (PAD) mainly focus on the macrovascular level. For assessment of tissue perfusion, near-infrared (NIR) fluorescence imaging using indocyanine green (ICG) seems promising. In this prospective cohort study, ICG NIR fluorescence imaging was performed pre- and post-revascularization to assess changes in foot perfusion.

Methods

ICG NIR fluorescence imaging was performed in 36 patients with PAD pre- and postintervention. After intravenous bolus injection of 0.1mg/kg ICG, the camera registered the NIR fluorescence intensity over time on the dorsum of the feet for 15 minutes using the Quest Spectrum Platform*. Time-intensity curves were plotted for 3 regions of interest (ROIs): 1. The dorsum of the foot, 2. The forefoot and 3. The hallux. Time-intensity curves were normalized for maximum fluorescence intensity. Extracted parameters were the maximum slope, area under the curve (AUC) for the ingress and the AUC for the egress. The non-treated contralateral leg was used as a control group.

Results

Successful revascularization was performed in 32 patients. There was a significant increase for the maximum slope and AUC egress in all three ROIs. The most significant difference was seen for the maximum slope in ROI 3 (3.7 %/s to 6.6 %/s, p<0.001). In the control group, no significant differences were seen for the maximum slope and AUC egress in all ROIs

Conclusions

This study shows the potential of ICG NIR fluorescence imaging in assessing the effect of revascularization procedures on foot perfusion. Future studies should focus on the use of this technique in predicting favourable outcome of revascularization procedures.

Introduction

Peripheral artery disease (PAD) is amongst the most frequent vascular diseases worldwide and most often involves atherosclerotic disease of the lower extremities, so called lower extremity arterial disease (LEAD) (1). In diagnosing LEAD, the ankle-brachial systolic pressure index (ABI) is a valuable tool (2). However, the use of this technique is limited in patients with severe media calcinosis or previous amputation (3). Furthermore, the ABI as well as other diagnostic methods including toe pressure measurement (TP), computed tomography angiography (CTA) and digital subtraction angiography (DSA) focus on macrovascular aspects of lower extremity circulation. Especially in patients with chronic limb-threatening ischemia (CLTI), reliable information about tissue perfusion in the area of interest can be of paramount importance in guiding revascularization procedures (3). In assessing the effect of revascularization procedures, physicians focus on clinical judgement of the foot, thereby supported by changes in ABI, TP, and macrovascular changes as seen on DSA. Objective assessment of the changes in tissue perfusion remains unknown. Several imaging techniques have been examined for quantification of tissue perfusion in patients with LEAD, including Single Photon Emission Computed Tomography and Hyperspectral Imaging (4, 5). In a recent systematic review, the use of near-infrared (NIR) fluorescence imaging with indocyanine green (ICG) to measure tissue perfusion in patients with PAD was reviewed (6). This imaging modality has already been used extensively in other medical fields for imaging and perfusion assessment, including oncologic, cardiac and reconstructive surgery (7, 8). In reconstructive surgery, perfusion assessment with ICG NIR fluorescence imaging shows promising results in predicting tissue viability (9). Measurement of tissue perfusion using NIR involves a camera that measures light in the NIR spectrum, allowing the visualization of a specific intravascular administered fluorophore: ICG. This fluorophore is confined to vascular components and therefore feasible to assess tissue perfusion. The use of this technique in patients with LEAD seems promising, especially for quality control following revascularization (6, 10-12). In a recent study by Settembre et al., 101 patients underwent NIR fluorescence imaging pre- and post-revascularization (10). A significant improvement in ingress rate (i.e. rate of fluorescence intensity increase) was seen for patients undergoing technically successful revascularization. The effect of revascularization on the contralateral non-treated leg was described in one study with 21 patients undergoing unilateral revascularization (13). In this study, ICG NIR fluorescence imaging showed a significant decrease in NIR fluorescence intensity and inflow time on the non-treated side. Whether these findings can be explained by an actual decrease in contralateral foot circulation has yet to be identified. Providing physicians with an instrument to objectively assess the effect of revascularization on tissue perfusion can guide treatment strategies and possibly predict favorable outcomes following revascularization. This requires the use of a standardized protocol for ICG NIR fluorescence imaging with the use of standardized parameters. This prospective cohort study incorporated the use of beforementioned standardized protocol in patients beforeand after revascularization. Furthermore, a recommendation is given for the standardized analyses of measured NIR fluorescence intensities in future studies.

Methods

This prospective cohort study was approved by the Medical Research and Ethics Committee of the Leiden University Medical Center and registered in the Dutch Trial Register with number NL7531. Patients undergoing revascularization procedures for LEAD from December 2018 until January 2021 were included in a single, academic hospital in the Netherlands. Informed consent was obtained in all patients. ICG NIR fluorescence imaging was performed pre- and post-revascularization. All post measurements were performed within 7 days of the initial procedure. ABI and TP were measured in all patients. Exclusion criteria, based on contra-indications for ICG, were: allergy to iodine or ICG, hyperthyroidism or thyroidal adenoma, pregnancy, kidney failure (eGFR <45) and liver failure.

NIR fluorescence imaging measurement

The Quest Spectrum Platform® (Quest Medical Imaging, Middenmeer, The Netherlands) was used to perform ICG NIR fluorescence imaging. This system is capable of measuring both visible light as well as the NIR signal of ICG. A dose of 0.1 mg/kg of ICG was administered intravenously and subsequently, the NIR fluorescence intensity was measured in both feet. Upon intravenous administration of ICG, the camera, targeted to the area of interest, measured the fluorescence intensity over time (Figure 1). The protocol used for ICG NIR fluorescence imaging in this study is displayed in Figure 2.

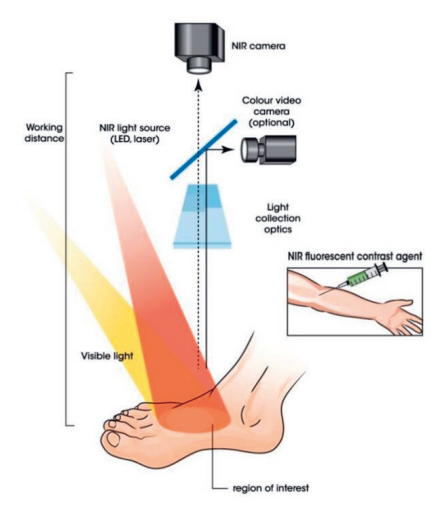


Figure 1. Near-infrared fluorescence imaging with indocyanine green setup.

| Protocol near-infrared fluorescence imaging with indocyanine green |
|---|
| 1. Confirm in- and exclusion criteria. |
| 2. Patient in supine position with room temperature of 20-25 degrees Celsius. |
| 3. Measure blood pressure, ankle-arm index and toe pressure. |
| 4. Position feet of patients against a dark background board. |
| 5. Position camera at 50 cm distance perpendicular to dorsum of feet. |
| 5. Clear room of visible light. |
| 6. Administer 0.1mg/kg indocyanine green intravenously with a minimum of 2.5mg. |
| 7. Record near-infrared fluorescence for 15 minutes. |

Figure 2. Protocol near-infrared fluorescence imaging with indocvanine green.

Data analyses

The Quest Research Framework® (Quest Medical Imaging, Middenmeer, The Netherlands) was used to create and analyse the time-intensity curves. Time-intensity curves were normalized for maximum fluorescence intensity. The extracted parameters were measured in three ROIs (i.e. the dorsum of the foot, the forefoot and the hallux) and included: maximum slope (%/s), area under the curve (AUC) for the ingress (%), and the AUC for the egress after 180 seconds (%) (Figure 3). Improvement of perfusion was defined as an increase of inflow parameters (slope and AUC ingress) and an improvement in egress time (AUC egress). Data was analysed using IBM SPSS Statistics 25 (IBM Corp. Released 2017. IBM SPSS Statistics for Windows, Version 25.0. Armonk, NY, USA). Pre- and post-intervention results were compared using the Wilcoxon Rank Sign test.

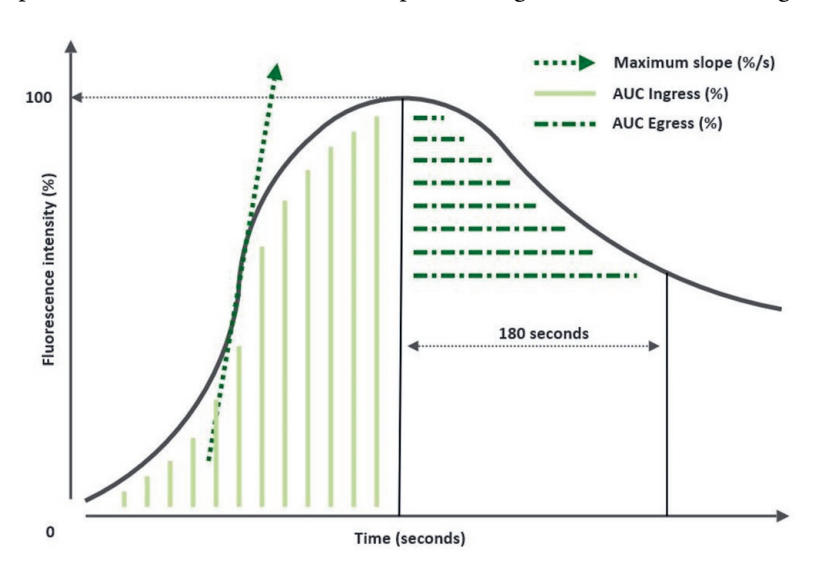


Figure 3. Normalized time-intensity curve with extracted parameters.

Results

During the study period, successful ICG NIR fluorescence imaging was performed in 36 patients pre- and post-intervention. Patient characteristics are depicted in Table 1. Revascularization was successful in 32 patients. Of the 36 patients, 21 patients underwent an endovascular revascularization. For the patients undergoing successful revascularization, there was a significant increase in ABI post-revascularization from 0.71 (±0.30) to 0.92 (±0.35) (p<0.001) and a significant increase in TP from 59 (±27) to 77 (±18) (p=0.018). No significant differences were found in ABI and TP in the control group pre- and post-revascularization (ABI: p=0.918, TP: p=0.137). No significant changes were seen for the ABI and TP in the four patients in whom revascularization was unsuccessful (ABI: p=0.895, TP: p=0.531).

Table 1. Patient characteristics.

| Patient characteristics (n=36) | Number of patients | |
|--------------------------------|--------------------|--|
| Age (years, SD) | 70.7 (7.0) | |
| Female | 14 | |
| Fontaine stage | | |
| 2a | 4 | |
| 2b | 19 | |
| 3 | 9 | |
| 4 | 4 | |
| Diabetes | 12 | |
| Hypertension | 28 | |
| Active smoking | 10 | |
| Kidney failure | 0 | |
| Intervention type | | |
| Endovascular | 21 | |
| Bypass surgery | 5 | |
| TEA | 7 | |
| Hybrid | 2 | |
| Intervention successful | 32 | |

NIR fluorescence imaging results

An example of the ICG NIR fluorescence imaging results of a patient pre- and postintervention following a femoro-crural bypass on the left side are displayed in Figure 4 and in supplementary Video 1 (available online via Vascular). The differences as seen on quantitative analyses of the NIR fluorescence intensity in this patient is seen in Figure 5. Collected data of the results for the maximum slope, AUC ingress and AUC egress for the three regions of interests in the revascularized limb group are shown in Table 2. For the maximum slope, a significant increase was seen for all three ROIs. The

increase in inflow was most significant for ROI 3, i.e. the hallux (3.7 to 6.6, p=0.000). The AUC ingress showed a significant increase in ROI 3, but no significant difference for ROIs 1 and 2. The AUC egress showed a significant decrease for all three ROIs. This decrease was most significant for ROI 3, i.e. the hallux (49.5 to 42.4, p=0.014). Results pre- and post-intervention were also analyzed for the non-revascularized limb. These results are depicted in Table 3. Besides the AUC ingress for ROI 3, no significant differences were seen for all parameters in all three ROIs.

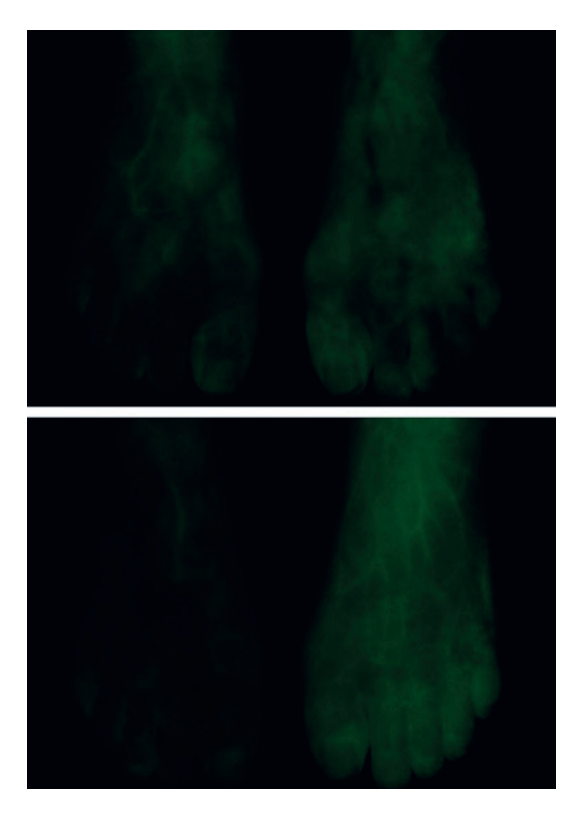


Figure 4. Near-infrared fluorescence intensity before (above) and after (below) bypass surgery on the left side.

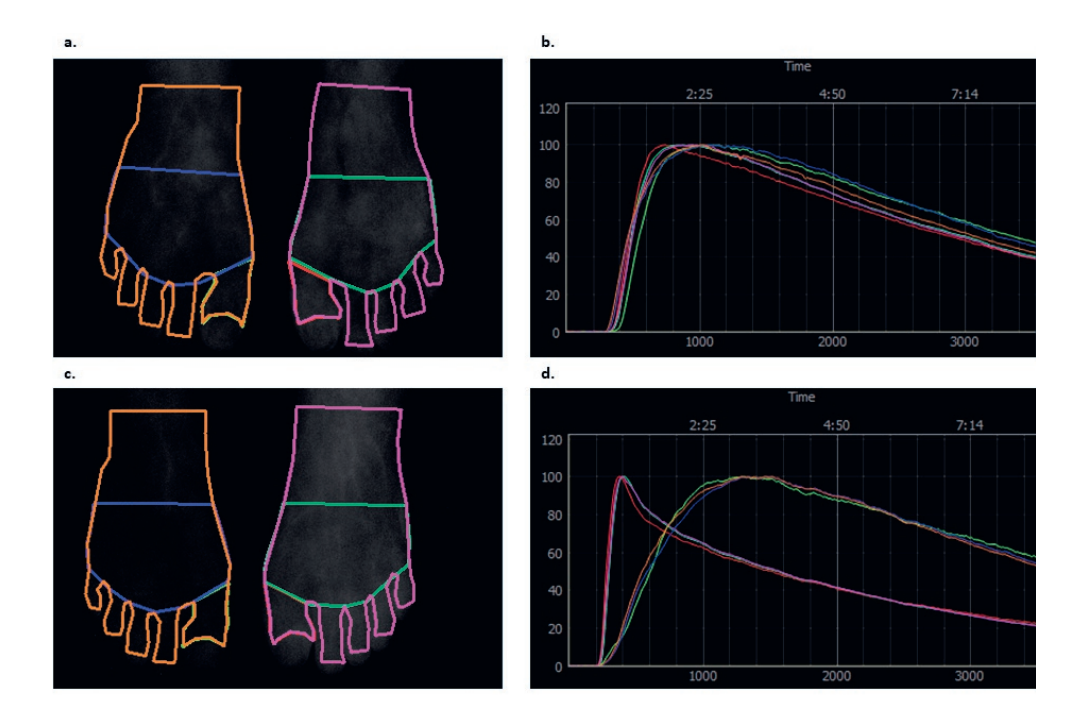


Figure 5. ICG NIR fluorescence imaging results in a patient undergoing femoro-crural bypass surgery on the left side:

- a. NIR fluorescence signal and ROI selection pre-revascularization.
- b. Normalized time-intensity curves pre-revascularization.
- c. NIR fluorescence signal and ROI selection post-revascularization.
- d. Normalized time-intensity curves post-revascularization.

Table 2. ICG NIR fluorescence imaging results pre- and post-revascularization in revascularized limb.

| Perfusion parameter | ROI 1 | | | ROI 2 | | | ROI 3 | | |
|------------------------|---------------|------------|-------|---------------|------------|-------|------------|------------|-------|
| | Pre | Post | p | Pre | Post | p | Pre | Post | p |
| Maximum slope (%/s) | 3.3 ± 2.0 | 5.6 ± 2.7 | 0.000 | 3.4 ± 2.1 | 5.6 ± 2.5 | 0.000 | 3.7 ± 2.2 | 6.6 ± 3.2 | 0.000 |
| AUC ingress (%) | 70.2 ± 6.3 | 67.9 ± 8.9 | 0.681 | 69.9 ± 6.2 | 66.2 ± 9.7 | 0.191 | 70.6 ± 6.3 | 64.0 ± 9.7 | 0.003 |
| AUC egress (%) | 52.6 ± 7.2 | 47.2 ± 9.1 | 0.004 | 52.2 ± 8.4 | 46.8 ± 9.3 | 0.002 | 49.2 ± 8.7 | 41.6 ± 9.8 | 0.007 |

| | | | 0 0 | | | | | C | |
|------------------------|---------------|----------------|-------|---------------|---------------|-------|------------|----------------|-------|
| Perfusion parameter | ROI 1 | | | ROI 2 | | | ROI 3 | | |
| | Pre | Post | p | Pre | Post | p | Pre | Post | p |
| Maximum slope (%/s) | 3.2 ± 1.9 | 3.6 ± 2.3 | 0.390 | 3.2 ± 1.9 | 3.5 ± 2.3 | 0.304 | 3.9 ± 2.4 | 4.6 ± 3.0 | 0.204 |
| AUC ingress (%) | 71.4 ± 5.1 | 70.4 ± 5.5 | 0.525 | 71.2 ± 5.6 | 69.4 ± 5.0 | 0.270 | 70.4 ± 5.5 | 66.3 ± 7.6 | 0.029 |
| AUC egress | 53.1 ± 5.9 | 52.4 ± 7.2 | 0.695 | 52.4 ± 6.1 | 52.1 ± 6.8 | 0.922 | 50.1 ± 8.2 | 47.7 ± 9.1 | 0.501 |

Table 3. ICG NIR fluorescence imaging results pre- and post-revascularization in control group.

The four patients for whom revascularization was unsuccessful all underwent endovascular procedures. No significant differences were seen for all three parameters in all three ROIs for both limbs.

Discussion

Currently, the medical field lacks a valid and reliable tool for quantification of changes in tissue perfusion following revascularization. This study emphasizes the potential of ICG NIR fluorescence imaging to fill this gap by showing a significant improvement for 2 out of the 3 parameters in patients undergoing a successful revascularization. No significant differences were seen for these parameters pre- and postintervention in patients with an unsuccessful revascularization, underlining the repeatability of ICG NIR fluorescence imaging for measurement of tissue perfusion. As opposed to the findings reported by Nakamura et al.(13), this study reported no changes for most parameters measured in the contralateral non-treated leg. Although there was a significant increase in AUC ingress in one region in the control group, it is unclear whether this parameter is reliable enough to report changes in foot perfusion. This is emphasized by the non-significant differences found for this parameter in the treated leg. A possible explanation for this finding is the fact that a faster increase will not automatically lead to a higher AUC. Earlier studies on the use of ICG NIR fluorescence imaging in patients with LEAD have shown that significant improvement following revascularization is most often seen in time-related parameters (14). This might be due to the variation in absolute fluorescence intensity, which is influenced by several factors, including camera distance and patientrelated factors, such as edema and skin temperature (15). To minimize the effect of these influencing factors, the intensity can be described as a percentage of the measured maximum intensity. The use of this normalization for maximum intensity was used by Kang et al., a study in which perfusion using ICG NIR fluorescence imaging was used in hindlimbs of mice (16). This is the first study to use this approach for analysis in clinical patients with LEAD and in the search for quantitative analysis of tissue perfusion, the use of these normalized parameters seems to be superior to intensity related parameters (17).

The three parameters used in this study were selected following a thorough examination of the time-intensity curves following successful revascularization. Most often, a faster inflow was seen followed by a sharper decline in intensity. To quantify these findings, the parameters were set at maximum slope, AUC ingress and AUC egress. The findings in this study show that the slope and AUC egress have the best potential in future studies on assessment of tissue perfusion with ICG NIR fluorescence imaging following revascularization. These studies should also incorporate data on clinical outcome, which is a limitation of this study. The predictive value of ICG NIR fluorescence imaging on clinical outcome following revascularization was reported earlier in a study by Colvard et al. (18). In this study, an increase in inflow- as well as outflow parameters was found in patients with a clinically successful outcome. Similar to this study, these measurements were performed postinterventional. For the intra-operative guidance of revascularization strategies, studies on the feasibility of the intra-operative use of this technique have to be performed. Furthermore, this study is limited by the heterogeneity and size of the study population. A larger cohort with information about follow-up will lead to better understanding of perfusion patterns and to what extent a patient will benefit from a revascularization procedure. This cohort should also include an analysis on the effect of impaired microcirculation on results found with ICG NIR fluorescence imaging. Earlier studies have reported contradictory results on the in- and outflow patterns between patients with- and without microvascular disease (19, 20). To provide cut-off values to guide treatment strategies, these differences in patient characteristics have to be incorporated.

Conclusion

This study shows the potential of ICG NIR fluorescence imaging in assessing changes in foot perfusion following successful revascularization. The perfusion of the non-treated leg does not appear to be influenced by a revascularization procedure on the contralateral side. Future studies should incorporate normalized parameters and focus on the potential of intra-operative ICG NIR fluorescence imaging in predicting favorable outcome following revascularization.

Reference list

- Aboyans V, Ricco JB, Bartelink MEL, Bjorck M, Brodmann M, Cohnert T, et al. 2017 ESC Guidelines on the Diagnosis and Treatment of Peripheral Arterial Diseases, in collaboration with the European Society for Vascular Surgery (ESVS). Rev Esp Cardiol (Engl Ed). 2018;71(2):111.
- Norgren L, Hiatt WR, Dormandy JA, Nehler MR, Harris KA, Fowkes FG, et al. Inter-Society Consensus for the Management of Peripheral Arterial Disease (TASC II). J Vasc Surg. 2007;45 Suppl S:S5-67.
- Misra S, Shishehbor MH, Takahashi EA, Aronow HD, Brewster LP, Bunte MC, et al. Perfusion
 Assessment in Critical Limb Ischemia: Principles for Understanding and the Development of
 Evidence and Evaluation of Devices: A Scientific Statement From the American Heart Association.
 Circulation. 2019;140(12):e657-e72.
- 4. Benitez E, Sumpio BJ, Chin J, Sumpio BE. Contemporary assessment of foot perfusion in patients with critical limb ischemia. Semin Vasc Surg. 2014;27(1):3-15.
- 5. Sumpio BE, Forsythe RO, Ziegler KR, van Baal JG, Lepantalo MJ, Hinchliffe RJ. Clinical implications of the angiosome model in peripheral vascular disease. J Vasc Surg. 2013;58(3):814-26.
- 6. van den Hoven P, Ooms S, van Manen L, van der Bogt KEA, van Schaik J, Hamming JF, et al. A systematic review of the use of near-infrared fluorescence imaging in patients with peripheral artery disease. J Vasc Surg. 2019;70(1):286-97 e1.
- 7. Schaafsma BE, Mieog JS, Hutteman M, van der Vorst JR, Kuppen PJ, Lowik CW, et al. The clinical use of indocyanine green as a near-infrared fluorescent contrast agent for image-guided oncologic surgery. J Surg Oncol. 2011;104(3):323-32.
- 8. Alander JT, Kaartinen I, Laakso A, Patila T, Spillmann T, Tuchin VV, et al. A review of indocyanine green fluorescent imaging in surgery. Int J Biomed Imaging. 2012;2012:940585.
- 9. Driessen C, Arnardottir TH, Lorenzo AR, Mani MR. How should indocyanine green dye angiography be assessed to best predict mastectomy skin flap necrosis? A systematic review. J Plast Reconstr Aesthet Surg. 2020;73(6):1031-42.
- Settembre N, Kauhanen P, Alback A, Spillerova K, Venermo M. Quality Control of the Foot Revascularization Using Indocyanine Green Fluorescence Imaging. World J Surg. 2017;41(7):1919-26.
- 11. Braun JD, Trinidad-Hernandez M, Perry D, Armstrong DG, Mills JL, Sr. Early quantitative evaluation of indocyanine green angiography in patients with critical limb ischemia. J Vasc Surg. 2013;57(5):1213-8.
- 12. Igari K, Kudo T, Toyofuku T, Jibiki M, Inoue Y, Kawano T. Quantitative evaluation of the outcomes of revascularization procedures for peripheral arterial disease using indocyanine green angiography. Eur J Vasc Endovasc Surg. 2013;46(4):460-5.
- 13. Nakamura M, Igari K, Toyofuku T, Kudo T, Inoue Y, Uetake H. The evaluation of contralateral foot circulation after unilateral revascularization procedures using indocyanine green angiography. Sci Rep. 2017;7(1):16171.
- 14. Igari K, Kudo T, Uchiyama H, Toyofuku T, Inoue Y. Indocyanine green angiography for the diagnosis of peripheral arterial disease with isolated infrapopliteal lesions. Ann Vasc Surg. 2014;28(6):1479-84.

- 15. Frangioni JV. In vivo near-infrared fluorescence imaging, Curr Opin Chem Biol. 2003;7(5):626-34.
- 16. Kang Y, Choi M, Lee J, Koh GY, Kwon K, Choi C. Quantitative analysis of peripheral tissue perfusion using spatiotemporal molecular dynamics. PLoS One. 2009;4(1):e4275.
- 17. Lutken CD, Achiam MP, Svendsen MB, Boni L, Nerup N. Optimizing quantitative fluorescence angiography for visceral perfusion assessment. Surg Endosc. 2020;34(12):5223-33.
- 18. Colvard B, Itoga NK, Hitchner E, Sun Q, Long B, Lee G, et al. SPY technology as an adjunctive measure for lower extremity perfusion. J Vasc Surg. 2016;64(1):195-201.
- 19. An Y, Kang Y, Lee J, Ahn C, Kwon K, Choi C. Blood flow characteristics of diabetic patients with complications detected by optical measurement. Biomed Eng Online. 2018;17(1):25.
- 20. Igari K, Kudo T, Uchiyama H, Toyofuku T, Inoue Y. Quantitative evaluation of microvascular dysfunction in peripheral neuropathy with diabetes by indocyanine green angiography. Diabetes Res Clin Pract. 2014;104(1):121-5.



Chapter 8

Assessment of tissue viability following amputation surgery using near-infrared fluorescence imaging with indocyanine green

P. van den Hoven ¹, S.D. van den Berg ¹, J.P. van der Valk ¹, H. van der Krogt ¹, L.P. van Doorn ¹, K.E.A. van der Bogt ¹, J. van Schaik ¹, A. Schepers ¹, A.L. Vahrmeijer ¹, J.F. Hamming ¹, J.R. van der Vorst ¹

1. Leiden University Medical Center, Leiden, The Netherlands

Published in Annals of Vascular Surgery, June 2021.

Abstract

Introduction

Patients with chronic limb threatening ischemia have a risk of undergoing a major amputation within 1 year of nearly 30% with a substantial risk of re-amputation since wound healing is often impaired. Quantitative assessment of regional tissue viability following amputation surgery can identify patients at risk for impaired wound healing. In quantification of regional tissue perfusion, near-infrared (NIR) fluorescence imaging using indocyanine green (ICG) seems promising.

Methods

This pilot study included adult patients undergoing lower extremity amputation surgery due to peripheral artery disease or diabetes mellitus. ICG NIR fluorescence imaging was performed within 5 days following amputation surgery using the Quest Spectrum Platform®. Following intravenous administration of ICG, the NIR fluorescence intensity of the amputation wound was recorded for 10 minutes. The NIR fluorescence intensity videos were analyzed and if a fluorescence deficit was observed, this region was marked as "low fluorescence". All other regions were marked as "normal fluorescence".

Results

Successful ICG NIR fluorescence imaging was performed in 10 patients undergoing a total of 15 amputations. No "low fluorescence" regions were observed in 11 out of 15 amputation wounds. In 10 out of these 11 amputations, no wound healing problems occurred during follow-up. Regions with "low fluorescence" were observed in 4 amputation wounds. Impaired wound healing corresponding to these regions was observed in all wounds and a re-amputation was necessary in 3 out of 4. When observing time-related parameters, regions with low fluorescence had a significantly longer time to maximum intensity (113 seconds versus 32 seconds, p=0.003) and a significantly lesser decline in outflow after five minutes (80.3% versus 57.0%, p=0.003).

Conclusions

ICG NIR fluorescence imaging was able to predict postoperative skin necrosis in all four cases. Quantitative assessment of regional perfusion remains challenging due to influencing factors on the NIR fluorescence intensity signal, including camera angle, camera distance and ICG dosage. This was also observed in this study, contributing to a large variety in fluorescence intensity parameters among patients. To provide surgeons with reliable NIR fluorescence cut-off values for prediction of wound healing, prospective studies on the intra-operative use of this technique are required. The potential prediction of wound healing using ICG NIR fluorescence imaging will have a huge impact on patient mortality, morbidity as well as the burden of amputation surgery on health care.

Introduction

Peripheral artery disease (PAD) affects more than 200 million people and the burden of PAD is increasing due to a rise in known risk factors such as increased age and diabetes mellitus (1, 2). Patients with PAD present with a variety of symptoms with chronic limb threatening ischemia (CLTI) being the most severe form. It is estimated that the prevalence of CLTI in patients with PAD is between 3 and 10% (3, 4). These patients have a risk of undergoing a major amputation within 1 year of nearly 30% (5). Furthermore, there is a substantial risk of re-amputation since wound healing is often impaired due to the compromised vascular status and concomitant comorbidities, including diabetes mellitus (6). Although wound healing depends on several factors, adequate blood supply to the wound site is most important (7). Therefore, in prediction of wound healing and assessing the level of amputation, quantification of regional tissue perfusion is crucial. Several modalities including transcutaneous oxygen pressure measurement and hyperspectral imaging have been examined for the purpose of quantifying perfusion, however evidence on prediction of wound healing is limited (7, 8). For quantification of regional perfusion, near-infrared (NIR) fluorescence imaging using indocyanine green (ICG) has shown promising results (9, 10). This technique is based on the visualization of a fluorescent dye, ICG, in the NIR light spectrum. Upon intravenous administration of ICG, a camera creates a time-intensity curve of the region of interest (ROI) (Figure 1). Quantification of perfusion is achieved by extraction of parameters from these curves. The use of this technique following amputation surgery in patients with PAD has been described in several case studies (10-14). In a retrospective cohort study of 13 patients undergoing a lower extremity amputation, Yang et al. (14) found a relative perfusion value lower than 32% to have a sensitivity of 100% in identifying necrotic tissue. Prospective studies on the predictive value of ICG NIR fluorescence imaging in healing of amputation wounds have yet to be performed.

Methods

This prospective cohort study was approved by the Medical Research and Ethics Committee and registered in the Dutch Trial Register with number NL7531. Adult patients undergoing minor and major lower extremity amputation surgery due to PAD or diabetes mellitus were included in this study. Patients were included from October 2019 until March 2021 in a single academic hospital in the Netherlands. Exclusion criteria were allergy or hypersensitivity to sodium iodide, iodide, or ICG; hyperthyroidism or autonomous thyroid adenoma; pregnancy; kidney failure (eGFR <45) or severe liver failure. All patients were required to provide informed consent. The patients' sex, age, weight, length, Fontaine classification and previous medical history

were obtained. All patients were treated according to Dutch clinical guidelines (15). To prevent postoperative edema, a soft dressing was used. Patients undergoing transtibial amputation were treated with a rigid dressing (Össur, Reykjavik, Iceland).

ICG NIR fluorescence imaging measurement

The Quest Spectrum Platform® (Quest Medical Imaging, Middenmeer, The Netherlands) was used to perform ICG NIR fluorescence imaging. This imaging system is capable of measuring both visible light as well as the NIR signal of ICG. Measurements were performed within 5 days following amputation surgery. Each patient was administered an intravenous bolus injection of 0.1 mg/kg ICG (VERDYE 25 mg, Diagnostic Green GmbH, Aschheim-Dornach, Germany), using a peripheral venous line. Following administration of ICG, fluorescence intensity of the amputation wound was recorded for 10 minutes. Measurements were performed on patients in a supine position in a room cleared of ambient light.

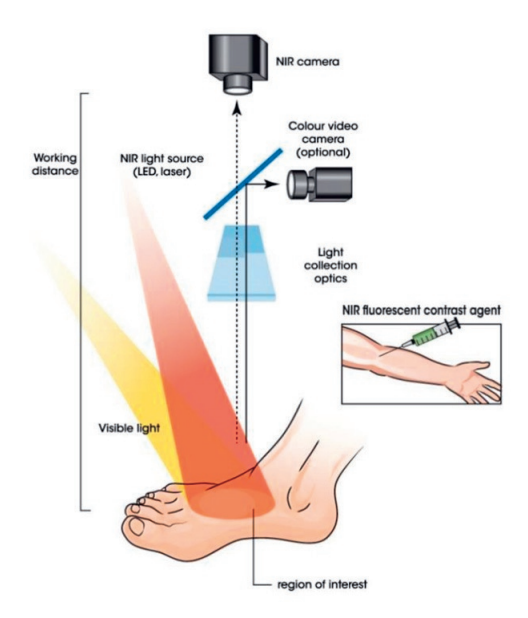


Figure 1. ICG NIR fluorescence imaging setup.

Data interpretation

The NIR fluorescence intensity videos of the amputation wound were interpreted without knowledge of the clinical follow-up. If an area with diminished fluorescence intensity was observed, this region was marked as "low fluorescence". All other regions were marked as "normal fluorescence". The time-intensity curves of these regions were analyzed in the recorded videos using the Quest Research Framework® (Quest Medical Imaging, Middenmeer, the Netherlands). A tracker was used to ensure the region was

synchronized with movement. Parameters extracted from the time intensity curves were: the ingress rate, maximum intensity, time to maximum intensity and the area under the curve for the egress after 5 minutes. Means of measured parameters were compared using an independent samples t-test. Data was analyzed using IBM SPSS Statistics 25 (IBM Corp. Released 2017. IBM SPSS Statistics for Windows, Version 25.0. Armonk, NY, USA: IBM Corp.).

Results

During the study period, successful ICG NIR fluorescence imaging was performed in 10 patients undergoing a total of 15 amputations. A summary of the patient characteristics is given in Table I. Three patients underwent multiple amputations.

Table I. Patient characteristics.

| Characteristics | Number of patients (n=10) | |
|-------------------------|---------------------------|--|
| Age (years, SD) | 70.7 (7.0) | |
| Female | 4 | |
| Diabetes | 7 | |
| Hypertension | 5 | |
| Active smoking | 0 | |
| History of smoking | 5 | |
| Type amputation surgery | | |
| Transfemoral | 2 | |
| Transtibial | 6 | |
| Partial foot | 1 | |
| Digit(s) | 6 | |

One patient underwent a transtibial amputation after impaired wound healing following a digit amputation and a subsequent partial foot amputation. In this patient, a transfemoral amputation of the contralateral leg was performed six months later. Another patient underwent a right transtibial amputation during follow-up following initial transtibial amputation on the left side. A third patient underwent a transfemoral amputation following a non-healing transtibial amputation wound. No fluorescence intensity deficits were observed in 11 out of 15 amputation wounds. In 10 out of these 11 amputations, no wound healing problems occurred during follow-up. An example of a patient with a normal fluorescence intensity is shown in Figure 2. This patient

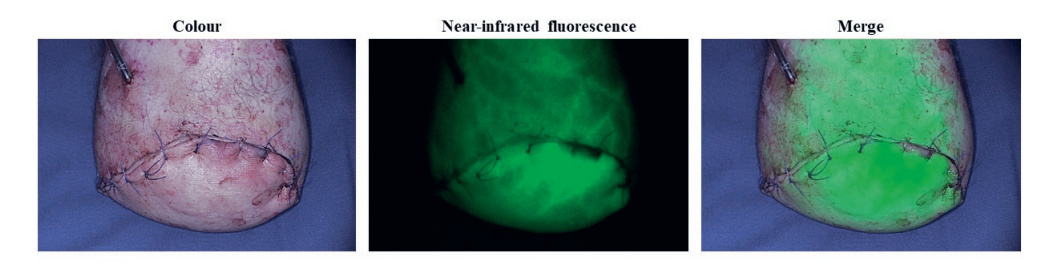


Figure 2. ICG NIR fluorescence imaging in a 60-year old male patient following transtibial amputation on the left side, showing the visual output (left), the NIR fluorescence signal (middle) and the merged image (right). No fluorescence intensity deficits were observed.

underwent a transtibial amputation on the left side. The merged image combines the visual and NIR fluorescence output. In one patient where no fluorescence intensity deficits were observed, a re-operation was necessary. This was a 69-year old male with a history of diabetes mellitus undergoing a hallux amputation on the left side because of osteomyelitis. A re-operation was performed during follow-up because of ongoing bone infection. However, no skin necrosis was observed following the initial amputation and neither was debridement of the skin necessary. Regions with "low fluorescence" were observed in 4 amputation wounds. One patient, an 82-year old female, underwent a fourth digit amputation on the right side due to a non-healing diabetic ulcer (Figure 3).

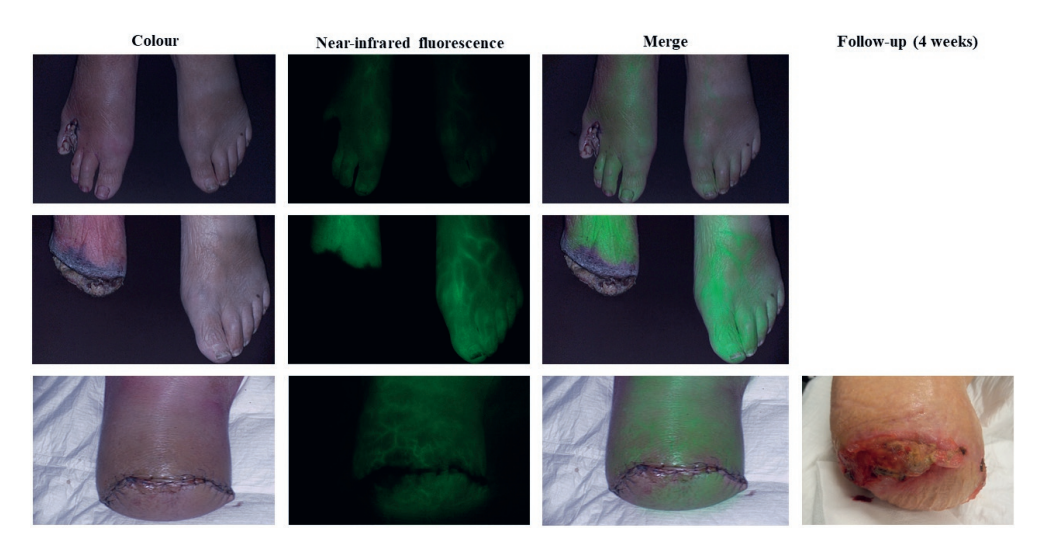


Figure 3. ICG NIR fluorescence imaging in an 82-year old female patient showing the visual (left), NIR fluorescence (lower) and merged image (right) following multiple amputations on the right side. A region of "low fluorescence" was seen in all wound edges. The region of low fluorescence of the transtibial amputation corresponded with the area where postoperative necrosectomy was necessary.

ICG NIR fluorescence imaging showed a region of low fluorescence in the skin surrounding the amputation wound as well as the fifth digit. A partial foot amputation was performed six days later. ICG NIR fluorescence imaging showed an area of low fluorescence intensity following this amputation. A transtibial amputation was performed 5 days later, due to ischemia of the wound edges corresponding with the low fluorescence region. ICG NIR fluorescence imaging of the transtibial amputation wound showed a fluorescence deficit in the caudolateral wound edge. One month postoperatively, a necrosectomy was performed in this region of low fluorescence.

The fourth region of low fluorescence was observed in a 76-year old male patient undergoing transtibial amputation on the right side due to Fontaine stage 4 PAD. This patient was discharged 9 days postoperatively without signs of impaired wound healing. However, three weeks postoperatively, necrosis of the wound occurred in the area corresponding with the low fluorescence region on NIR fluorescence imaging and a transfemoral amputation was necessary (Figure 4). No fluorescence intensity deficits were observed on ICG NIR fluorescence imaging of the transfemoral amputation wound. No complications occurred during follow-up regarding wound healing.

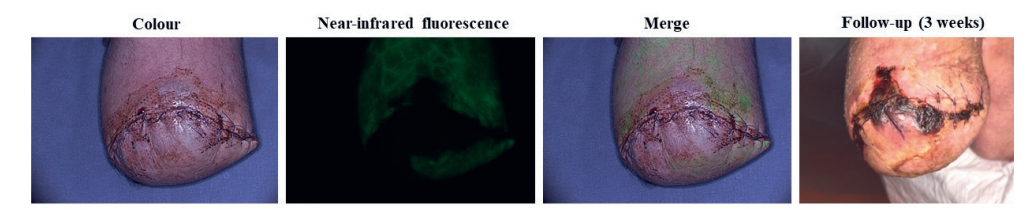


Figure 4. ICG NIR fluorescence imaging in a 76-year old male patient showing the visual (left), NIR fluorescence (lower) and merged imaged (right) following transtibial amputation on the right side. A region of low fluorescence is seen in the middle and lateral wound region. The demarcation of the skin was clearly visible 3 weeks postoperatively and corresponded with the area of low fluorescence.

Quantitative analysis of ICG NIR fluorescence imaging

The time-intensity curves for the regions with "normal fluorescence" and "low fluorescence" were compared. An overview of these time-intensity curves is shown in Figure 5. Regions marked as normal fluorescence generally show a higher absolute intensity value compared with low fluorescence regions. Furthermore, an incline in inflow of fluorescence intensity can be observed. With regards to the outflow, regions with low fluorescence tend to have a more gradual egress. The extracted fluorescence parameters are displayed in Table II. An increased maximum fluorescence intensity was observed in normal fluorescence intensity regions. Furthermore, there was a 15-fold increase in ingress rate in this group. When observing time-related parameters, regions

with low fluorescence had a longer time to maximum intensity (113 seconds versus 32 seconds, p=0.003) and a lesser decline in outflow after five minutes (80.3% versus 57.0%, p=0.003). All reported fluorescence parameters were statistically significant between groups.

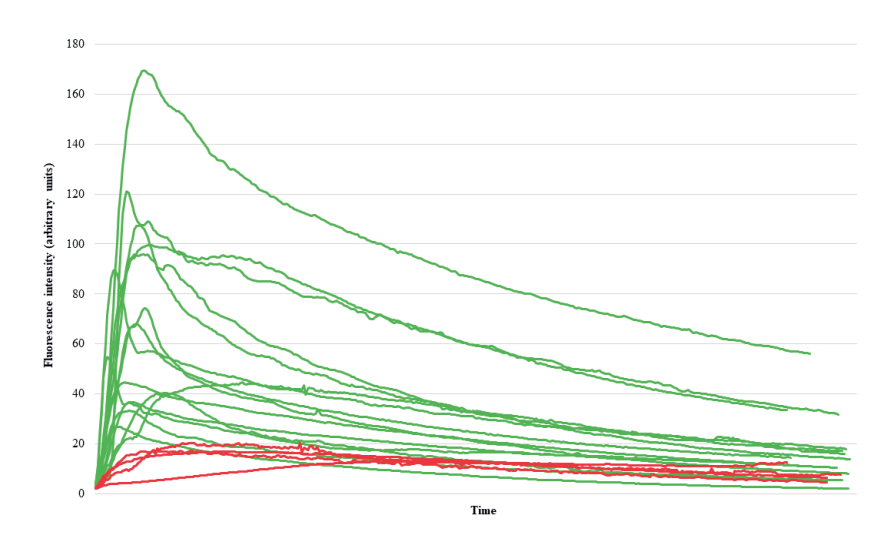


Figure 5. Time-intensity curves in regions with normal (green) and low (red) NIR fluorescence intensity.

Table II. ICG NIR fluorescence imaging parameters of "normal fluorescence" and "low fluorescence" regions.

| Parameter | Normal fluorescence | Low fluorescence | p-value |
|--------------------------|---------------------|------------------|---------|
| Maximum intensity (a.u.) | 73.8 ± 10.4 | 16.6 ± 1.3 | 0.013 |
| Ingress rate (a.u./s) | 3.0 ± 0.6 | 0.2 ± 0.1 | 0.039 |
| Tmax (s) | 32.0 ± 6.1 | 113.0 ± 42 | 0.003 |
| Egress AUC 300 (%) | 57.0 ± 3.2 | 80.3 ± 4.4 | 0.003 |

Abbreviations: a.u., arbitrary unit; s, second.

Discussion

Wound healing problems occurred in 5 amputation wounds described in this cohort study. In 4 out of these 5 wounds, healing problems occurred due to non-viability of the surrounding skin. ICG NIR fluorescence imaging was able to predict this postoperative skin necrosis in all cases. Of the 11 amputation wounds classified as normal fluorescence on ICG NIR fluorescence imaging, 10 healed without complications. Impaired healing

in the wound classified as normal fluorescence was not the result of skin necrosis, but ongoing osteomyelitis. Similar findings were observed in a study by Zimmerman et al. (10). In this case series, ICG NIR fluorescence imaging was able to predict tissue necrosis of transtibial amputation wounds in 3 patients based on fluorescence deficits. A re-operation was needed in all these patients. The value of ICG NIR fluorescence imaging in predicting tissue necrosis in patients with PAD was also described in a retrospective cohort study of 17 amputation wounds (14). This study found a relative fluorescence intensity of <32% to be able to detect tissue necrosis. Whether this cutoff value is applicable for use in clinical practice has yet to be examined in prospective cohort studies. More extensive research on the quantitative assessment of tissue viability was conducted in reconstructive breast surgery (16, 17). These studies show that the intra-operative use of ICG NIR fluorescence imaging has potential beneficial effects on the prediction of flap viability and clinical outcome, however, quantification of perfusion remains challenging. This is mainly the result of factors influencing the NIR fluorescence intensity signal, including camera angle, camera distance and ICG dosage (18). This was also observed in this study, contributing to a large variety in fluorescence intensity parameters among patients. Although a large inter-patient variety was observed, three parameters show a clear significant difference between "normal" and "low" fluorescence regions: the maximum intensity, the time to maximum intensity and the egress after 5 minutes. Since relative and time-related parameters are less susceptible to camera settings and ICG dosage, it seems reasonable to explore these parameters in future studies on quantification of tissue perfusion. The same conclusion was stated in a recent systematic review on the quantification of ICG NIR fluorescence imaging in visceral perfusion (19). Although reliable quantification still faces several challenges, the potential prediction of ICG NIR fluorescence imaging on wound healing is promising. In this study, clinical judgement raised no concerns in 3 out of the 4 wounds where a low fluorescence signal was observed. In the first patient, described in Figure 3, these findings could have led to an earlier, more proximal initial amputation. The second patient, described in Figure 4, was admitted to the hospital 3 weeks postoperatively and underwent a transfemoral amputation on admission. More proximal amputation would possibly have resulted in prevention of re-admission, re-amputation and earlier recovery. However, this study is limited by a small set of patients and to incorporate ICG NIR fluorescence imaging for intra-operative decision making in amputation surgery, larger prospective studies with focus on quantification are needed. Providing vascular surgeons with an imaging technique able to reliably predict tissue necrosis intra-operatively will have a huge impact on patient mortality, morbidity as well as the burden of amputation surgery on health care.

Conclusion

This study emphasizes the potential of ICG NIR fluorescence imaging in predicting wound healing following amputation surgery. To provide surgeons with reliable NIR fluorescence cut-off values for prediction of wound healing, prospective studies on the intra-operative use of this technique are required. This includes further research on the quantification of the measured NIR fluorescence intensity.

Reference list

- 1. Fowkes FG, Rudan D, Rudan I, Aboyans V, Denenberg JO, McDermott MM, et al. Comparison of global estimates of prevalence and risk factors for peripheral artery disease in 2000 and 2010: a systematic review and analysis. Lancet. 2013;382(9901):1329-40.
- 2. Criqui MH, Aboyans V. Epidemiology of peripheral artery disease. Circ Res. 2015;116(9):1509-26.
- Norgren L, Hiatt WR, Dormandy JA, Nehler MR, Harris KA, Fowkes FG, et al. Inter-Society Consensus for the Management of Peripheral Arterial Disease (TASC II). J Vasc Surg. 2007;45 Suppl S:S5-67.
- 4. Nehler MR, Duval S, Diao L, Annex BH, Hiatt WR, Rogers K, et al. Epidemiology of peripheral arterial disease and critical limb ischemia in an insured national population. J Vasc Surg. 2014;60(3):686-95 e2.
- 5. Mustapha JA, Katzen BT, Neville RF, Lookstein RA, Zeller T, Miller LE, et al. Disease Burden and Clinical Outcomes Following Initial Diagnosis of Critical Limb Ischemia in the Medicare Population. JACC Cardiovasc Interv. 2018;11(10):1011-2.
- Czerniecki JM, Thompson ML, Littman AJ, Boyko EJ, Landry GJ, Henderson WG, et al. Predicting reamputation risk in patients undergoing lower extremity amputation due to the complications of peripheral artery disease and/or diabetes. Br J Surg. 2019;106(8):1026-34.
- 7. Benitez E, Sumpio BJ, Chin J, Sumpio BE. Contemporary assessment of foot perfusion in patients with critical limb ischemia. Semin Vasc Surg. 2014;27(1):3-15.
- 8. Wang Z, Hasan R, Firwana B, Elraiyah T, Tsapas A, Prokop L, et al. A systematic review and metaanalysis of tests to predict wound healing in diabetic foot. J Vasc Surg. 2016;63(2 Suppl):29S-36S e1-2.
- 9. van den Hoven P, Ooms S, van Manen L, van der Bogt KEA, van Schaik J, Hamming JF, et al. A systematic review of the use of near-infrared fluorescence imaging in patients with peripheral artery disease. J Vasc Surg. 2019;70(1):286-97 e1.
- 10. Zimmermann A, Roenneberg C, Wendorff H, Holzbach T, Giunta RE, Eckstein HH. Early postoperative detection of tissue necrosis in amputation stumps with indocyanine green fluorescence angiography. Vasc Endovascular Surg. 2010;44(4):269-73.
- 11. Sumpio BE, Forsythe RO, Ziegler KR, van Baal JG, Lepantalo MJ, Hinchliffe RJ. Clinical implications of the angiosome model in peripheral vascular disease. J Vasc Surg. 2013;58(3):814-26.
- 12. Samies JH, Gehling M, Serena TE, Yaakov RA. Use of a fluorescence angiography system in assessment of lower extremity ulcers in patients with peripheral arterial disease: A review and a look forward. Semin Vasc Surg. 2015;28(3-4):190-4.
- 13. Joh JH, Park HC, Han SA, Ahn HJ. Intraoperative indocyanine green angiography for the objective measurement of blood flow. Ann Surg Treat Res. 2016;90(5):279-86.
- 14. Yang AE, Hartranft CA, Reiss A, Holden CR. Improving Outcomes for Lower Extremity Amputations Using Intraoperative Fluorescent Angiography to Predict Flap Viability. Vasc Endovascular Surg. 2018;52(1):16-21.
- 15. Revalidatieartsen NVv. Amputatie en prothesiologie onderste extremiteit 2018 [Available from: https://richtlijnendatabase.nl/richtlijn/amputatie_prothesiologie_onderste_extremiteit/startpagina amputatie en prothesiologie_onderste_extremiteit.html.

- Parmeshwar N, Sultan SM, Kim EA, Piper ML. A Systematic Review of the Utility of Indocyanine Angiography in Autologous Breast Reconstruction. Ann Plast Surg. 2020; Publish Ahead of Print.
- 17. Driessen C, Arnardottir TH, Lorenzo AR, Mani MR. How should indocyanine green dye angiography be assessed to best predict mastectomy skin flap necrosis? A systematic review. J Plast Reconstr Aesthet Surg. 2020;73(6):1031-42.
- 18. Pruimboom T, van Kuijk SMJ, Qiu SS, van den Bos J, Wieringa FP, van der Hulst R, et al. Optimizing Indocyanine Green Fluorescence Angiography in Reconstructive Flap Surgery: A Systematic Review and Ex Vivo Experiments. Surg Innov. 2020;27(1):103-19.
- 19. Lutken CD, Achiam MP, Svendsen MB, Boni L, Nerup N. Optimizing quantitative fluorescence angiography for visceral perfusion assessment. Surg Endosc. 2020;34(12):5223-33.



Part III

Summary, discussion and appendices



Chapter 9

Summary

Discussion and future perspectives

Summary

For the assessment of skin circulation in patients with lower extremity arterial disease (LEAD), vascular surgeons rely on physical examination, supported by diagnostic methods providing information about the macrovascular status of the leg. Amongst these methods are the ankle-brachial index, toe pressure measurement and duplex ultrasonography. However, the field of vascular surgery lacks a diagnostic tool for the valid and reliable quantification of tissue perfusion. Near-infrared (NIR) fluorescence imaging using indocyanine green (ICG) is currently used for assessment of tissue perfusion in other surgical fields and could possibly have huge potential in patients with LEAD. This is outlined in **Chapter 1**. With the aim to move the field of vascular surgery forward, this thesis describes the quest for valid and reliable quantitative assessment of skin perfusion using NIR fluorescence imaging with ICG, predominantly in patients with LEAD.

Part I - Quantification of tissue perfusion using near-infrared fluorescence imaging with indocyanine green

This part provides an overview of the past use of ICG NIR fluorescence imaging in tissue perfusion assessment by means of two systematic reviews. Furthermore, the quantification of skin perfusion is explored in three clinical studies of patients with LEAD and patients undergoing reconstructive breast surgery. Chapter 2 describes a systematic review on the use of ICG NIR fluorescence imaging in patients with peripheral artery disease, more specifically LEAD. This technique was used in these patients for either diagnosis, quality control following revascularization, assessment of tissue viability and angiography. Studies were performed in small cohorts and quantitative analyses showed large variety in used – and appropriate parameters for various indications. In diagnosing LEAD, time-related parameters seemed most appropriate, with a sensitivity between 67% and 100%. In describing the difference in perfusion following successful revascularization, both intensity – and time-related parameters improved significantly in most studies. Although these results seem promising, there is a widespread variation amongst measurement settings and quantification methods. This is further emphasized in Chapter 3, which describes the application of quantitative perfusion analysis with ICG NIR fluorescence imaging in all surgical fields in a systematic review on perfusion parameters. Quantitative assessment using this technique has been described in various fields including gastro-intestinal surgery, neurosurgery, reconstructive surgery, transplantation surgery and thyroid surgery. In this systematic review, relative - and time-related parameters seemed most useful in adequately describing tissue perfusion. Comparable to the earlier systematic review, measurement protocols differed amongst studies, including camera settings and ICG dosage. To provide a first step towards the standardization of quantification of tissue perfusion with ICG NIR fluorescence imaging using the Quest Spectrum Platform[®], three clinical studies were performed, described in Chapter 4 to 6. In Chapter 4, the ICG NIR fluorescence perfusion patterns in patients with chronic limb-threatening ischemia (CLTI) were compared to non-LEAD control patients. Following intravenous bolus administration of ICG, the fluorescence intensity in the feet was recorded for 10 minutes. Following quantitative assessment of the fluorescence intensity over time on the dorsum of the foot, an increased inflow of ICG was seen for patients with CLTI. This can possible be explained by damage to the regulatory mechanisms of the microcirculation, arterial stiffness and transcapillary leakage. The reliable quantification of tissue perfusion using ICG NIR fluorescence imaging is further explored in Chapter 5, in which normalization of the fluorescence intensity was applied. This analyzing method describes the fluorescence intensity change over time as a percentage of the maximum intensity. This resulted in increased reliability for repeated measurements in patients with LEAD. In non-LEAD control patients, this method resulted in a more homogenous perfusion pattern in the foot. To explore the perfusion patterns displayed with ICG NIR fluorescence imaging in reconstructive breast surgery, quantitative assessment of free flaps was performed in Chapter 6. On quantitative assessment, the site with the perforator and regions marked as high fluorescence showed superior inflow compared to regions with low fluorescence. Furthermore, within the 3 minute time frame of ICG NIR fluorescence measurement, no outflow was observed for regions marked as low fluorescence.

Part II - Clinical translation of quantitative tissue perfusion assessment using near-infrared fluorescence imaging with indocyanine green in lower extremity arterial disease

Two indications for which ICG NIR fluorescence imaging could have huge potential are the effect of revascularization procedures on regional foot perfusion and the assessment of tissue viability in patients with wounds. Therefore, this part describes two clinical studies exploring these indications.

In **Chapter 7**, ICG NIR fluorescence imaging was performed pre- and postprocedural in patients undergoing unilateral revascularization. Quantitative perfusion assessment within three regions of the foot demonstrated a significant improvement of in- and outflow following revascularization in the treated limb. The same parameters showed no difference in the contralateral, non-treated limb. Analysis of the ICG NIR fluorescence parameters in patients where revascularization was unsuccessful displayed no differences. To examine the prediction of tissue viability, **Chapter 8** includes a pilot study of patients undergoing amputation surgery and postprocedural ICG NIR fluorescence imaging. This technique was able to predict postoperative skin necrosis in all four cases. Quantitative assessment of the areas with diminished fluorescence displayed a decreased in- as well as outflow of ICG.

Discussion and future perspectives

Reliable assessment of tissue perfusion can have huge consequences for patient outcome within many surgical fields. Therefore, the search for a technique capable of assessing tissue perfusion has been the subject to multiple studies for various indications (1-10). For patients with lower-extremity arterial disease (LEAD), studies have been performed on transcutaneous oxygen pressure measurement, laser speckle imaging and dynamic volume computed tomography (11-14). Although studies on perfusion assessment in patients with LEAD have provided clinical relevance, including cut-off values for wound healing, no single technique has shown to be capable of perfusion assessment. This thesis explored the possible application of near-infrared (NIR) fluorescence imaging using indocyanine green (ICG) for tissue perfusion assessment, an imaging technique with seemingly appropriate features.

First of all, the past use of ICG NIR fluorescence imaging within various surgical fields and vascular surgery in particular is characterized by a large variety in measurement protocols, including camera type, camera settings and ICG dosage. Concerning the camera type, several systems have been used, limiting comparability of fluorescence parameters between studies (15). Furthermore, the camera settings, including camera distance and angle to the camera, vary amongst studies. It is known that these settings influence the signal and therefore should be standardized in order to allow for reliable comparison (16). Thirdly, variations in ICG dosage influence the measured fluorescence intensity, making comparability even more difficult (17). The two systematic reviews in this thesis underline these factors and encourage the use of standardized protocols for the assessment of tissue perfusion using ICG NIR fluorescence imaging. Furthermore, comparability studies between these camera systems are a vital step towards reliable perfusion assessment.

The three studies in this thesis describing the quantification of tissue perfusion in patients with LEAD have provided interesting insights in perfusion patterns of the foot. First of all, it was demonstrated that patients with chronic limb-threatening ischemia had increased inflow of ICG, compared to non-LEAD control patients. This is in contrast to an earlier study by Igari et al. on perfusion assessment with ICG in healthy control patients (18). However, Terasaki et al. did demonstrate faster inflow in patients with advanced stage LEAD (19). Although the superior inflow in this thesis was significant, there is still a large distribution within each group, precluding fierce statements on cutoff values for adequate perfusion. Possibly contributing to this distribution is the high presence of patients with diabetes mellitus, a group often presenting with microvascular – rather than macrovascular disease. Therefore, future studies on perfusion patterns should take this subgroup into account.

To minimize the effect of influencing factors in the measured fluorescence intensity, this thesis describes the application of normalization of time-intensity curves. This was described earlier in studies on gastro-intestinal perfusion (5, 20, 21). It was hypothesized that describing the fluorescence intensity as a percentual change of the maximum intensity, this would enhance the validity and reliability. Concerning repeatability, this method indeed provided good comparability between repeated measurements on the non-treated side of patients undergoing unilateral revascularization. Furthermore, normalized time-intensity curves were comparable amongst various regions of the foot in non-LEAD control patients, in contrary to absolute time-intensity curves. Although normalization enhances the validity and reliability, intensity-related parameters are depleted, which could be useful in the assessment of tissue viability, as shown in the study on clinical translation. Furthermore, normalization of time-intensity curves in areas with diminished fluorescence intensity leads to fluttering of the curves, making them non-interpretable. Therefore, applying normalization to time-intensity curves should be considered depending on the indication.

Concerning the clinical implementation, this thesis has provided two fields within vascular surgery in which ICG NIR fluorescence imaging could make an impact. First of all, this technique was able to quantify changes in foot perfusion following successful revascularization. Although these results are encouraging, studies on correlation with clinical outcome have to be performed in order to define clinical relevance. These studies should also incorporate the analysis of angiosome targeted revascularization, a field within vascular surgery that is still subject to debate (22, 23). The possible prediction of favorable outcome following revascularization using ICG NIR fluorescence imaging can provide guidance in choice and timing of treatment. Secondly, this thesis has made a first step towards the prediction of tissue viability following amputation surgery. Patients with LEAD undergoing amputation surgery are at a disturbingly high risk of re-interventions (24). Although this study has shown a rate of 100% in predicting skin necrosis, this study was performed in only a small cohort of patients. Therefore, studies are already designed to perform ICG NIR fluorescence imaging intra-operatively in larger cohorts. A third possible application in clinical practice includes the prediction of ulcer healing. Although the ethiology of ulcers is multifactorial, adequate perfusion is essential. Although ICG NIR fluorescence imaging shows potential in describing foot circulation, cut-off values to predict ulcer healing have yet to be found. The consequences of adequate prediction of ulcer healing on patient outcome as well as healthcare costs would be enormous.

Alongside the future study of ICG NIR fluorescence imaging for perfusion assessment for the aforementioned applications, there are several other imaging modalities with high potential as well. These include hyperspectral imaging, multispectral imaging and optoacoustic imaging. Optoacoustic imaging for example, has shown significant differences in microvasculature architecture in patients with diabetes compared to healthy volunteers (25). Hyperspectral imaging, which measures the amount of light at several wavelengths within both the visible and near-infrared light spectrum, has proven to distinct patients with- and without lower-extremity arterial disease (26). With the ultimate goal of reliable quantification of tissue perfusion to improve patient outcome, these potential modalities should be examined in future studies as well.

Traversing all recommendations in this thesis for future studies on the reliable assessment of tissue perfusion using ICG NIR fluorescence imaging, is the call for collaboration. Cooperations between surgical disciplines, both national and international, together with experts in the field of perfusion imaging are needed to bridge the current gaps. Besides the impact reliable perfusion assessment can have on patients with LEAD, this technique has the potential to improve the outcome of patients in many other surgical fields as well.

Reference list

- Misra S, Shishehbor MH, Takahashi EA, Aronow HD, Brewster LP, Bunte MC, et al. Perfusion
 Assessment in Critical Limb Ischemia: Principles for Understanding and the Development of
 Evidence and Evaluation of Devices: A Scientific Statement From the American Heart Association.
 Circulation. 2019;140(12):e657-e72.
- 2. Benitez E, Sumpio BJ, Chin J, Sumpio BE. Contemporary assessment of foot perfusion in patients with critical limb ischemia. Semin Vasc Surg. 2014;27(1):3-15.
- 3. Forsythe RO, Hinchliffe RJ. Assessment of foot perfusion in patients with a diabetic foot ulcer. Diabetes Metab Res Rev. 2016;32 Suppl 1:232-8.
- 4. Lutken CD, Achiam MP, Svendsen MB, Boni L, Nerup N. Optimizing quantitative fluorescence angiography for visceral perfusion assessment. Surg Endosc. 2020;34(12):5223-33.
- 5. Osterkamp J, Strandby R, Nerup N, Svendsen M, Svendsen L, Achiam M. Quantitative fluorescence angiography detects dynamic changes in gastric perfusion. Surg Endosc. 2020.
- Parmeshwar N, Sultan SM, Kim EA, Piper ML. A Systematic Review of the Utility of Indocyanine Angiography in Autologous Breast Reconstruction. Ann Plast Surg. 2020; Publish Ahead of Print.
- 7. Wang Z, Hasan R, Firwana B, Elraiyah T, Tsapas A, Prokop L, et al. A systematic review and metaanalysis of tests to predict wound healing in diabetic foot. J Vasc Surg. 2016;63(2 Suppl):29S-36S e1-2.
- 8. Lang BHH, Wong CKH, Hung HT, Wong KP, Mak KL, Au KB. Indocyanine green fluorescence angiography for quantitative evaluation of in situ parathyroid gland perfusion and function after total thyroidectomy. Surgery (United States). 2017;161(1):87-95.
- 9. Driessen C, Arnardottir TH, Lorenzo AR, Mani MR. How should indocyanine green dye angiography be assessed to best predict mastectomy skin flap necrosis? A systematic review. J Plast Reconstr Aesthet Surg. 2020;73(6):1031-42.
- 10. Uchino H, Nakamura T, Houkin K, Murata JI, Saito H, Kuroda S. Semiquantitative analysis of indocyanine green videoangiography for cortical perfusion assessment in superficial temporal artery to middle cerebral artery anastomosis. Acta Neurochirurgica. 2013;155(4):599-605.
- 11. Arsenault KA, Al-Otaibi A, Devereaux PJ, Thorlund K, Tittley JG, Whitlock RP. The use of transcutaneous oximetry to predict healing complications of lower limb amputations: a systematic review and meta-analysis. Eur J Vasc Endovasc Surg. 2012;43(3):329-36.
- 12. Ronn JH, Nerup N, Strandby RB, Svendsen MBS, Ambrus R, Svendsen LB, et al. Laser speckle contrast imaging and quantitative fluorescence angiography for perfusion assessment. Langenbecks Arch Surg. 2019;404(4):505-15.
- Mennes OA, van Netten JJ, van Baal JG, Slart R, Steenbergen W. The Association between Foot and Ulcer Microcirculation Measured with Laser Speckle Contrast Imaging and Healing of Diabetic Foot Ulcers. J Clin Med. 2021;10(17).
- Cindil E, Erbas G, Akkan K, Cerit MN, Sendur HN, Zor MH, et al. Dynamic Volume Perfusion CT of the Foot in Critical Limb Ischemia: Response to Percutaneous Revascularization. AJR Am J Roentgenol. 2020;214(6):1398-408.

- 15. AV DS, Lin H, Henderson ER, Samkoe KS, Pogue BW. Review of fluorescence guided surgery systems: identification of key performance capabilities beyond indocyanine green imaging. J Biomed Opt. 2016;21(8):80901.
- 16. Pruimboom T, van Kuijk SMJ, Qiu SS, van den Bos J, Wieringa FP, van der Hulst R, et al. Optimizing Indocyanine Green Fluorescence Angiography in Reconstructive Flap Surgery: A Systematic Review and Ex Vivo Experiments. Surg Innov. 2020;27(1):103-19.
- 17. Desmettre T, Devoisselle JM, Mordon S. Fluorescence properties and metabolic features of indocyanine green (ICG) as related to angiography. Surv Ophthalmol. 2000;45(1):15-27.
- 18. Igari K, Kudo T, Uchiyama H, Toyofuku T, Inoue Y. Indocyanine green angiography for the diagnosis of peripheral arterial disease with isolated infrapopliteal lesions. Ann Vasc Surg. 2014;28(6):1479-84.
- 19. Terasaki H, Inoue Y, Sugano N, Jibiki M, Kudo T, Lepantalo M, et al. A quantitative method for evaluating local perfusion using indocyanine green fluorescence imaging. Ann Vasc Surg. 2013;27(8):1154-61.
- Lutken CD, Achiam MP, Osterkamp J, Svendsen MB, Nerup N. Quantification of fluorescence angiography: Toward a reliable intraoperative assessment of tissue perfusion - A narrative review. Langenbecks Archives of Surgery. 2020;21:21.
- 21. Nerup N, Andersen HS, Ambrus R, Strandby RB, Svendsen MBS, Madsen MH, et al. Quantification of fluorescence angiography in a porcine model. Langenbecks Arch Surg. 2017;402(4):655-62.
- 22. Sumpio BE, Forsythe RO, Ziegler KR, van Baal JG, Lepantalo MJ, Hinchliffe RJ. Clinical implications of the angiosome model in peripheral vascular disease. J Vasc Surg. 2013;58(3):814-26.
- 23. van den Berg JC. Angiosome perfusion of the foot: An old theory or a new issue? Semin Vasc Surg. 2018;31(2-4):56-65.
- Mustapha JA, Katzen BT, Neville RF, Lookstein RA, Zeller T, Miller LE, et al. Disease Burden and Clinical Outcomes Following Initial Diagnosis of Critical Limb Ischemia in the Medicare Population. JACC Cardiovasc Interv. 2018;11(10):1011-2.
- 25. Karlas A, Kallmayer M, Fasoula NA, Liapis E, Bariotakis M, Kronke M, et al. Multispectral optoacoustic tomography of muscle perfusion and oxygenation under arterial and venous occlusion: A human pilot study. J Biophotonics. 2020;13(6):e201960169.
- 26. Chin JA, Wang EC, Kibbe MR. Evaluation of hyperspectral technology for assessing the presence and severity of peripheral artery disease. J Vasc Surg. 2011;54(6):1679-88.



Chapter 10

Dutch summary (Nederlandse samenvatting)

Curriculum Vitae

List of publications

Dutch summary (Nederlandse samenvatting)

Binnen de chirurgie wordt voor de beoordeling van weefselperfusie voornamelijk vertrouwd op de klinische blik. Onder meer binnen de vaatchirurgie, gastroenterologische chirurgie en reconstructieve chirurgie is een betrouwbare beoordeling van weefselperfusie uitermate belangrijk. Het ontbreekt ons echter aan diagnostische technieken die de klinische blik van een chirurg hierin kunnen ondersteunen. Een techniek met potentie die reeds langere tijd binnen de chirurgie wordt toegepast is nabijinfrarood (NIR) fluorescentie met indocyanine groen (ICG). Dit staat beschreven in **Hoofdstuk 1**. Met het doel de chirurgie verder te helpen beschrijft dit proefschrift de zoektocht naar betrouwbare kwantificatie van weefselperfusie middels ICG NIR fluorescentie beeldvorming. De klinische studies hierin beschreven concentreren zich met name op het gebruik van deze techniek bij patiënten met perifeer arterieel vaatlijden (PAV).

Deel I – Kwantificatie van weefselperfusie middels nabij-infrarood fluorescentie beeldvorming met indocyanine groen

Dit deel geeft een overzicht van de reeds opgedane ervaringen met kwantificatie van weefselperfusie middels ICG NIR fluorescentiebeeldvorming in twee systematische reviews. Daarnaast wordt in drie klinische studies de kwantificatie van huiddoorbloeding beschreven in patiënten met PAV en patiënten die een autologe borstreconstructie hebben ondergaan. Hoofdstuk 2 beschrijft een systematische review naar het gebruik van ICG NIR fluorescentie beeldvorming bij patiënten met PAV. Deze techniek is bij deze groep patiënten toegepast als diagnosticum, controle na revascularisatie, beoordeling van weefselperfusie na amputatiechirurgie en als angiografie. Eerdere studies werden voornamelijk verricht in kleine cohorten en er werd een grote spreiding gezien in de gebruikte kwantificatiemethoden. Om PAV te diagnosticeren lijken tijdgerelateerde parameters het meest geschikt, waarbij een sensitiviteit tussen de 67% en 100% werd beschreven. Voor de kwantificatie van verschil in voetdoorbloeding na revascularisatie bleken zowel tijd-gerelateerde als intensiteit-gerelateerde parameters van toepassing. Hoewel deze resultaten veelbelovend zijn werd een grote variatie gezien in de meetmethoden. Dit wordt benadrukt in Hoofdstuk 3, waarin een systematische review de gebruikte parameters voor kwantificatie van weefselperfusie met ICG NIR fluorescentiebeeldvorming binnen verschillende chirurgische disciplines weergeeft. Deze techniek is toegepast in onder andere gastro-enterologische chirurgie, neurochirurgie, reconstructieve chirurgie, transplantatiechirurgie en endocriene chirurgie. Deze studie laat zien dat relatieve en tijd-gerelateerde parameters het meest geschikt lijken voor adequate beoordeling van weefselperfusie met ICG NIR fluorescentie beeldvorming. Vergelijkbaar met de eerdere systematische review werd ook in deze studie een grote verscheidenheid gezien in meetmethoden. Om een eerste aanzet te doen naar een systematische methode voor kwantificatie van weefselperfusie met ICG NIR fluorescentiebeeldvorming worden in Hoofdstuk 4 tot en met 6 drie klinische studies beschreven. In **Hoofdstuk 4** worden de verschillende ICG NIR fluorescentiepatronen vergeleken tussen patiënten met kritieke ischemie en patiënten zonder PAV. Na intraveneuze bolusinjectie van ICG werd de fluorescentie intensiteit in de voeten gemeten gedurende tien minuten. Patiënten met kritieke ischemie bleken een verhoogde inflow van ICG te hebben, hetgeen mogelijk wordt verklaard door gestoorde autoregulatie, stijfheid van de grote vaten en lekkage van ICG door vaatschade. In de zoektocht naar betrouwbare kwantificatie van weefselperfusie met ICG NIR fluorescentie beeldvorming is in Hoofdstuk 5 het effect van normalisatie van het fluorescentiesignaal onderzocht. Deze methode beschrijft de fluorescentie intensiteitsverandering over de tijd als een percentage van de maximale intensiteit. Dit resulteerde in een verhoogde betrouwbaarheid van herhaalde metingen bij patiënten met PAV. Bij non-PAV controle patiënten zorgde deze methode voor een homogener perfusiepatroon van de voet. Deze perfusiepatronen worden verder onderzocht in Hoofdstuk 6, waarin een studie staat beschreven naar de ICG NIR fluorescentie perfusiepatronen bij vrije lappen van patiënten die een reconstructie van de mamma(e) ondergingen. In de regio van de perforator, alsmede gebieden met een hoge intensiteit werden verhoogde instroomwaarden gevonden bij kwantitatieve analyse vergeleken met gebieden met een lagere intensiteit. De gebieden met een lage intensiteit toonden eveneens geen outflow gedurende de drie minuten durende opname.

Deel II – Klinische translatie van kwantitatieve perfusie analyse middels nabij-infrarood fluorescentie met indocyanine groen bij patiënten met perifeer arterieel vaatlijden

Een betrouwbare beoordeling van huiddoorbloeding bij patiënten met PAV heeft grote potentie voor meerdere indicaties, waaronder het beoordeling van het effect op weefseldoorbloeding na revascularisatie en de inschatting van vitaliteit van de huid bij wonden. In dit deel staat de klinische translatie van kwantificatie van weefselperfusie met ICG NIR fluorescentiebeeldvorming voor deze twee indicaties beschreven. In **Hoofdstuk** 7 zijn bij patiënten die een unilaterale revascularisatieprocedure ondergaan ICG NIR fluorescentiemetingen verricht. Kwantitatieve analyse van het fluorescentiesignaal voor - en na de procedure liet een significante toename van de in- en uitstroom zien in het behandelde been. Dezelfde parameters bleven in het contralaterale onbehandelde been onveranderd. Bij patiënten voor wie de revascularisatieprocedure niet succesvol was werd geen verschil in parameters gezien voor- en na de procedure. Om de vitaliteit van de huid te voorspellen staat in Hoofdstuk 8 een pilot studie beschreven van een cohort patiënten, waarbij ICG NIR fluorescentie beeldvorming van de wond is verricht na amputatiechirurgie. De techniek bleek in staat alle gevallen van huidnecrose te voorspellen. Kwantitatieve analyse van de gebieden met een lage fluorescentie toonde zowel een vertraagde in- als uitstroom van ICG.

Deel III - Discussie en toekomstperspectieven

Het huidig gebruik van ICG NIR fluorescentiebeeldvorming voor de kwantitatieve beoordeling van weefselperfusie wordt gekenmerkt door een grote verscheidenheid aan meetmethoden. Voor patiënten met PAV laat dit proefschrift zien dat ICG NIR fluorescentiebeeldvorming in staat is veranderingen in weefseldoorbloeding te detecteren na een revascularisatie en in staat is vitaliteit van de huid te voorspellen. Normalisatie van de tijd-intensiteitcurves vergroot hierbij de betrouwbaarheid. Voordat ICG NIR fluorescentiebeeldvorming kan worden geïmplementeerd in de dagelijkse praktijk is meer onderzoek nodig naar de klinische relevantie. Dit kan aantonen dat ICG NIR fluorescentiebeeldvorming in staat is succes van revascularisatieprocedures te voorspellen of de aannemelijkheid van wondgenezing inzichtelijk kan maken. Voor dit ultieme doel is samenwerking binnen zowel chirurgische – als niet-chirurgische disciplines essentieel.

Curriculum Vitae

Pim van den Hoven is op 23 maart 1990 geboren in Hengelo, Twente. In 2008 behaalde hij zijn VWO diploma aan het Scholengemeenschap Twickel College te Hengelo, waarna hij voor een half jaar de studie Advanced Technology aan de Universiteit Twente heeft gevolgd. In 2009 is hij begonnen met zijn Studie Geneeskunde aan de Universiteit Leiden. Tijdens deze studie heeft hij onder leiding van prof. dr. Menno Huisman en dr. P.L. den Exter klinisch onderzoek verricht naar de behandeling van veneuze trombo-embolieën. Als onderdeel van zijn coschappen heeft hij ervaring opgedaan op de Spoedeisende Hulp in het Academisch Ziekenhuis Paramaribo te Suriname en bij de Medische Zending in de binnenlanden van Suriname. Na het behalen van zijn artsendiploma in 2016 is hij achtereenvolgens als arts-assistent chirurgie werkzaam geweest in het Groene Hart Ziekenhuis te Gouda en het Leids Universitair Medisch Centrum. In 2018 werd hij aangenomen voor de opleiding tot chirurg in regio Leiden. Zijn opleiding volgt hij sindsdien in het Alrijne Ziekenhuis te Leiderdorp onder supervisie van dr. Zeillemaker en dr. Schepers. In 2021 heeft hij zijn opleiding voor een jaar in deeltijd verricht om zijn promotieonderzoek in het Leids Universitair Medisch Centrum af te ronden. Onder supervisie van promotor prof. dr. J.F. Hamming en copromotoren dr. J.R. van der Vorst en dr. A.L. Vahrmeijer heeft hij onderzoek verricht naar het gebruik van nabijinfrarood fluorescentie met indocyanine groen voor de kwantificatie van weefselperfusie bij patiënten met perifeer arterieel vaatlijden. In deze periode heeft hij een research fellowship in het Rigshospitalet te Kopenhagen gedaan onder leiding van dr. M.P. Achiam en dr. N.A. Nerup. Naast zijn werk is hij betrokken bij de Stichting ZGT over Zee met als doel een cardiovasculair centrum te helpen ontwikkelen in het Kilimanjaro Christian Medical Center te Moshi, Tanzania.

List of publications

van den Hoven P, Tange F, Van Der Valk J, Nerup N, Putter H, Van Rijswijk C, Van Schaik J, Schepers A, Vahrmeijer A, Hamming J, Van Der Vorst J. Normalization of Time-Intensity Curves for Quantification of Foot Perfusion Using Near-Infrared Fluorescence Imaging With Indocyanine Green. J Endovasc Ther. 2022 Mar 3:15266028221081085.

van den Hoven P, Verduijn PS, van Capelle L, Tange FP, Michi M, Corion LUM, Sibinga Mulder BG, Mureau MAM, Vahrmeijer AL, van der Vorst JR. Quantification of near-infrared fluorescence imaging with indocyanine green in free flap breast reconstruction. J Plast Reconstr Aesthet Surg. 2022 Jan 14:S1748-6815(22)00003-1.

van den Hoven P, Goncalves LN, Quax PHA, van Rijswijk CSP, van Schaik J, Schepers A, Vahrmeijer AL, Hamming JF, van der Vorst JR. Perfusion patterns in patients with chronic limb-threatening ischemia versus control patients using near-infrared fluorescence imaging with indocyanine green. Biomedicines. 2021 Oct 9;9(10):1417.

van den Hoven P, Weller FS, van de Bent M, Goncalves LN, Ruig M, van den Berg SD, Ooms S, Mieog JSD, van de Bogt KEA, Van Schaik J, Schepers A, Vahrmeijer AL, Hamming JF, van der Vorst JR. Near-infrared fluorescence imaging with indocyanine green for quantification of changes in tissue perfusion following revascularization. Vascular. 2021 Jul 28:17085381211032826.

van den Hoven P, van den Berg SD, van der Valk JP, van der Krogt H, van Doorn LP, van de Bogt KEA, Van Schaik J, Schepers A, Vahrmeijer AL, Hamming JF, Van Der Vorst JR. Assessment of tissue viability following amputation surgery using near-infrared fluorescence imaging with indocyanine green. Ann Vasc Surg. 2022 Jan;78:281-287

van den Hoven P*, Goncalves LN*, van Schaik J, Leeuwenburgh L, Hendricks CHF, Verduijn PS, van der Bogt KEA, van Rijswijk CSP, Schepers A, Vahrmeijer AL, Hamming JF, van der Vorst JR. perfusion parameters in near-infrared fluorescence imaging with indocyanine green: A systematic review of the literature. Life (Basel). 2021 May 11;11(5):433.

van den Hoven P, Ooms S, van Manen L, van der Bogt KEA, van Schaik J, Hamming JF, Vahrmeijer AL, van der Vorst JR, Mieog JSD. A systematic review of the use of near-infrared fluorescence imaging in patients with peripheral artery disease. J Vasc Surg. 2019 Jul;70(1):286-297.e1

van der Hulle T, den Exter PL, **van den Hoven P**, van der Hoeven JJ, van der Meer FJ, Eikenboom J, Huisman MV, Klok FA. Cohort study on the management of cancer-associated venous thromboembolism aimed at the safety of stopping anticoagulant therapy in patients cured from cancer. Chest. 2016 May;149(5):1245-5.

van den Hoven P*, den Exter PL*, van der Hulle T, Mos IC, Douma RA, van Es J, Huisman MV, Klok FA. Performance of the revised Geneva score in patients with a delayed suspicion of pulmonary embolism. Eur Respir J. 2014 Jun;43(6):1801-4.

den Exter PL, van Es J, Erkens PM, van Roosmalen MJ, **van den Hoven P**, Hovens MM, Kamphuisen PW, Klok FA, Huisman MV. Impact of delay in clinical presentation on the diagnostic management and prognosis of patients with suspected pulmonary embolism. American Journal of Respiratory and Critical Care Medicine. 2013 Jun;187(12):1369-73.

den Exter PL, van Roosmalen MJ, **van den Hoven P**, Klok FA, Monreal M, Jiménez D, Huisman MV. Physicians' management approach to an incidental pulmonary embolism: an international survey. Journal of Thrombosis and Haemostasis.2013 Jan;11(1):208-13.

^{*} Authors contributed equally and share first authorship.

Dankwoord

Dit proefschrift heb ik slechts kunnen schrijven door de hulp en steun van velen. Deze woorden zijn voor jullie.

Allereerst wil ik alle patiënten bedanken die zich hebben ingezet voor ons onderzoek. Jullie onbaatzuchtige medewerking aan onze metingen was van onschatbare waarde voor het team. Voor jullie doen we het.

Prof. dr. Hamming, promotor, beste Jaap, dank voor je wijsheid tijdens mijn promotietraject en daarbuiten. Je visie, rust en betrokkenheid zijn bijzonder waardevol voor me.

Dr. Van Der Vorst, beste Joost, copromotor en boven alles mijn mentor. Zonder jouw rotsvaste vertrouwen in mij en ons onderzoek was dit proefschrift er niet geweest. Je hebt de gave een team te inspireren en dat was ook in mijn promotie essentieel. Dank voor alles.

Dr. Vahrmeijer, beste Alex, copromotor en degene die mijn promotietraject mogelijk heeft gemaakt. Daar ben ik je ontzettend dankbaar voor. Dank voor je inzicht, ervaring en positiviteit.

Een diepe buiging wil ik maken voor alle wetenschapsstudenten: Floris, Merel, Simen, Melissa, Lauren, Laura, Cas, Jesse, Thijs, Lisette, Jurrian en Chris. Jullie vormen samen de stille kracht achter dit proefschrift.

Aan de vaste krachten binnen mijn onderzoeksteam: dr. Van Schaik, beste Jan, dank voor je enthousiasme en betrokkenheid. Dr. Schepers, beste Abbey, dank voor al je inzet voor zowel ons onderzoek als mijn opleiding.

Floris, aan jou de eer het verhaal een mooi vervolg te geven. Jouw bravoure en frisse energie tijdens mijn promotie was verademend.

Aan alle promovendi met wie ik het afgelopen jaar heb mogen samenwerken, dank voor jullie onmisbare afleiding. Het was een voorrecht. Aan de promovendi van het Green Light Leiden team, kamergenoten Okker en Robin in het bijzonder, dank voor de samenwerking in deze mooie groep.

Chirurgen van het Alrijne Ziekenhuis, zowel in mijn opleiding tot chirurg als tijdens mijn promotietraject creëren jullie de ideale omstandigheden om het beste uit mezelf

te halen. Daar ben ik jullie ongelooflijk dankbaar voor. Dr. Zeillemaker, beste Anneke, dank dat je als opleider alles mogelijk maakt. Dr. Hoencamp, beste Rigo, dank voor al je support.

Dr. Verduijn, beste Pieter, er is natuurlijk ook een wereld buiten de vaatchirugie, dank voor onze mooie samenwerking.

Aan allen die hebben bijgedragen aan de totstandkoming van de onderzoeken in mijn proefschrift: Sven, Sophie, Koen, Paul, Hein, Jan, Carla en Labrinus, dank jullie wel.

Medewerkers van Quest, Richelle in het bijzonder, dank voor jullie hulp en geduld.

Arts-assistenten en verpleegkundigen van het Leids Universitair Medisch Centrum, bedankt voor jullie inzet.

Loes, dankjewel voor alles in de lange tijd dat je naast me hebt gestaan. Dat koester ik.

To Dr. Achiam and dr. Nerup, dear Michael and Nikolaj, mange tak. My research fellowship at the Rigshospitalet in Copenhagen felt like home because of you. Together, we can hopefully bridge the gap towards reliable perfusion assessment. To dr. Hillingsø, dr. De Heer, prof. Eiberg, prof. Resch, Jens, August, Charlotte and Trygve, thanks for showing me Danish hospitality.

Mannen van de Amsterdamse soldaten, mijn Twentse vrienden, dank voor onze vriendschap. Het blijft bijzonder om te zien hoe iedereen elkaar steunt en het beste in elkaar naar boven haalt. Aan Reinier, dank dat je er altijd bent als ik je nodig heb. Aan Ruud, dank dat je mijn wingman bent.

Vrienden van de Rijnstraat, Bas, Joep en Mathijs, dank dat jullie er altijd zijn om mij op te vangen. Aan Bas, dit dank ik uiteindelijk allemaal aan jou.

Tolga, je bent als een broer voor me. Dat jouw deur altijd open staat is een grote steun voor me.

Hero, paranimf, broeder. Sinds Paramaribo lezen en schrijven we met elkaar. Het maakt me trots dat jij aan mijn zijde staat.

Lieve oma, altijd wanneer ik je zie straal je uit hoe trots je op me bent. Dankjewel voor alles.

Loes, grote zus, hoe jij samen met Rutger een thuis bouwt voor jullie en je kinderen is uitzonderlijk. Je liefde, kracht en doorzettingsvermogen zijn een inspiratie voor me. Aan Rutger, dank dat je me altijd aanmoedigt.

Anna, wat heb ik geluk met jou als mijn zusje. De energie en levenslust die jij uitstraalt is bijzonder, dat elke dag telt. Dank dat je er altijd voor me bent.

Dirk, broer, paranimf, natuurlijk sta jij naast me, zoals altijd. Ik hoef niet achterom te kijken om te weten dat jij me rugdekking geeft. Dankjewel dat je in alles mijn broer bent.

Pap en mam, jullie noem ik samen, omdat ik niet anders ken. Ik wil jullie uit het diepst van mijn hart bedanken voor het thuis wat ik door jullie voel. Door jullie onvoorwaardelijke liefde kan ik mijn vleugels uitslaan.

Lieve Kim, jou kan ik nooit genoeg bedanken. Ik kan het alleen maar samen met jou. Jouw liefde geeft me rust. Jij laat mij inzien dat alles mogelijk is, omdat we elkaar hebben. Dankjewel voor de betekenis die jij mijn leven geeft.

